CONTROL OF ION MOTION IN ROTATING MAGNETIC FIELD CURRENT DRIVE

by

Denis C. Visentin B.Sc. (Hons)

Submitted in fulfilment of the requirements for the Degree of Doctor of Philosophy

University of Tasmania

March 2007

DECLARATION

I hereby declare that this thesis contains no material which has been accepted for the award of any other degree or diploma in any tertiary institution, and that, to the best of knowledge and belief, it contains no material published or written by any other person except where due acknowledgement is made in the text of the thesis.

_____ Denis Visentin, 9th March 2007

AUTHORITY OF ACCESS

This thesis may be made available for loan and limited copying in accordance with the *Copyright Act 1968*.

_____ Denis Visentin, 9th March 2007

ABSTRACT

This thesis presents theoretical results, a numerical model and simulation results for the control of the ion motion for a pre-formed field-reversed-configuration (FRC) using two counter-rotating magnetic fields (RMFs). One RMF (denoted the (-) RMF) is applied first to entrain the electron fluid and maintain the plasma current. In the absence of a mechanism for controlling the ion motion, if the confinement time is sufficiently large, the rotation of the ion fluid due to collisions with the electron fluid would diminish the plasma current and thus destroy the FRC equilibrium. A second RMF (denoted the (+) RMF) is applied after the (-) RMF has penetrated the plasma, to entrain the ion fluid and maintain the equilibrium.

It is shown that there exists a true steady state (the Clemente steady state), where the electron fluid rotates almost synchronously with the (-) RMF and the ion fluid rotates almost synchronously with the (+) RMF. This allows the equilibrium to be maintained indefinitely. Both RMFs penetrate much farther than a classical skin depth. The accessibility of the Clemente steady states are examined theoretically and by simulation.

A 1-D numerical model is developed to simulate the application of the RMF for two cases:

1. A constant density model where the radial motion is constrained.
2. A preformed FRC model with radial motion.

For both cases it is demonstrated that the Clemente steady states are accessible from a small class of initial conditions. The class of initial conditions may be broadened by allowing the frequency of the (+) RMF to vary. The penetration and entrainment of the (+) RMF is shown to be highly non-linear (as is well known for the (-) RMF) and hence the magnitude of the (+) RMF required for accessibility of the steady state

is much greater than that required to maintain the steady state. It is also demonstrated that it is possible to increase the closed flux of the FRC by increasing the frequency of either RMF.

ACKNOWLEDGEMENTS

I wish to express my thanks to the many people who have assisted in making this thesis possible. Firstly to my supervisor Dr. Waheed Hugrass, whose introduction to the field and guidance through the research has been superb. One of the great pleasures arising from this period has been to work with a person who embodied the oft-used expression, “a scholar and a gentleman”. Although I have gone to great lengths to irritate him over the years as a postgraduate student and a colleague, my efforts have borne no fruit.

Many thanks to the staff and postgraduate students at the School of Computing in Launceston. With the transfer of Dr. Hugrass and myself to the school, they have been very accepting and accommodating of the physicists in their midst. Thanks especially to the technical and administrative staff who have facilitated almost every whim. My appreciation also to staff in other departments who have helped me juggle teaching commitments and research during the course of my candidature, in the School of Human Life Sciences, especially Marie-Louise Bird, and at the Australian Maritime College. My thanks also go to the staff from the now defunct School of Applied Science, particularly Roger Taylor.

Finally I would like to thank family and friends who have supported me, especially my mother Carlene and my wonderful children Gianni and Antonina. Watching my children grow, learning to draw and write on thesis drafts has been a pure pleasure and a most welcome distraction. To Susannah for her care and aid in proofing the thesis, Paul Semmens and the other members of ‘Hoof Hearted’, and everyone who has at least had a drink and been polite enough to not ask me how my research was going.

A Tasmanian Postgraduate Scholarship was held during the course of this research.

TABLE OF CONTENTS

LIST OF FIGURES

AUTHOR'S PUBLICATIONS

Visentin, D.C. (2003). Ion motion control in RMF current drive by means of a frequency modulated counter-RMF. *Plasma Physics and Controlled Fusion,* **45,** 1027-35.

Visentin, D.C., & Hugrass, W.N. (2003). Control of the motion of the ions in rotating magnetic field current drive. 2. Transient analysis. *Plasma Physics and Controlled Fusion,* **45** 209-19.

Visentin, D.C. & Hugrass, W.N. (2005). *Maintaining an FRC by two Counter-Rotating Magnetic Fields*. Australian Institute of Physics 16th National Congress, Canberra.

Visentin, D.C. & Hugrass, W.N. A Field Reversed Configuration Maintained by Two Counter-RMFs. To be submitted for publication to *Plasma Physics and Controlled Fusion.*

CHAPTER 1 INTRODUCTION

1.1 Controlled Nuclear Fusion

Controlled nuclear fusion requires heating a gas of low atomic number elements to high temperature and confining the plasma long enough for nuclear reactions to produce more energy than is consumed. Conventional fusion approaches require the production of large driven plasma currents which both heat the plasma and provide containment. The current produces a magnetic field around the plasma, thermally insulating the hot plasma from the wall. The current also exerts a force radially inward, which opposes the plasma pressure. The plasma is heated by Ohmic heating, resulting from an interaction between the current and the plasma resistivity.

The main focus of controlled nuclear fusion research is the "tokamak" reactor, a toroidal vessel in which an electric current is made to flow in a contained closed plasma ring. External magnetic fields confine and stabilise the plasma by interaction with the current, which is induced by transformer action. While the tokamak remains the most likely fusion reactor, inherent problems have been identified which suggest the benefit of alternative fusion research directions. The tokamak has a low engineering β value (the ratio of plasma pressure to magnetic pressure) which gives a low power density. The tokamak also has a large minimum size and is geometrically complex which means that the tokamak has a high capital cost.

The efficiency of the tokamak can be maximised by decreasing the toroidal aspect ratio (thereby increasing the average plasma beta value). In the limit this results in a

"compact torus" where the central hole is shrunk to zero and there are no internal material structures. The production of compact torus configurations requires techniques where the coils do not link the plasma. A compact torus consists of open and closed magnetic field lines, and may also have a toroidal field. The separatrix may be spherical, oblate or prolate.

1.2 Field-Reversed Configuration

A field-reversed configuration (FRC) is a prolate compact torus with no appreciable toroidal field (Tuszewski, 1988). A sketch of an FRC geometry is shown in Figure 1.1 (Steinhauer, 1996)

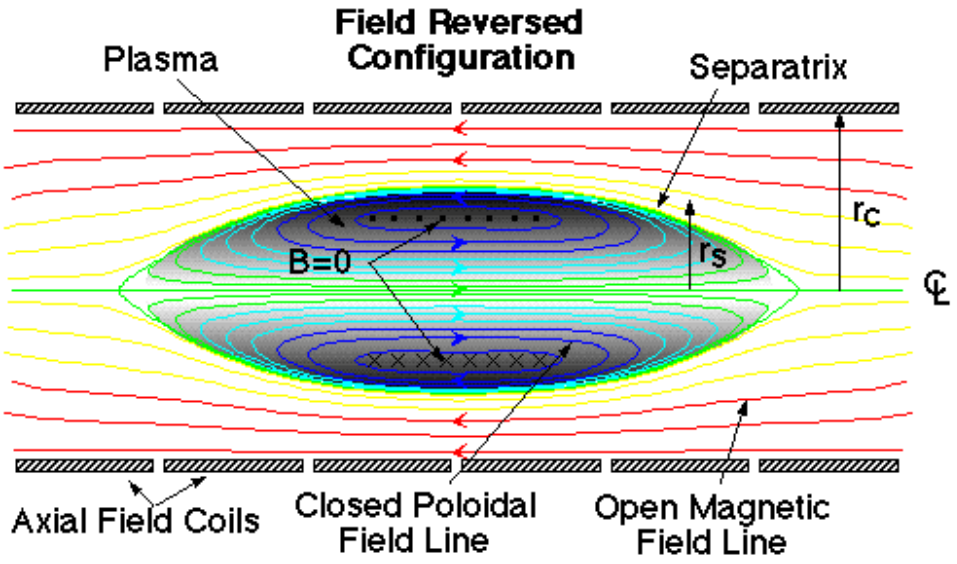

Figure 1.1. FRC Geometry

A highly prolate FRC has an average β value determined by the ratio of the separatrix radius r_s and the flux conserver radius r_c,

$$\langle \beta \rangle = 1 - \frac{1}{2}\left(\frac{r_s}{r_c}\right)^2 .$$

Hence $<\beta>$ has a minimum value of 0.5, and is typically greater than 0.8 (Steinhauer, 1996).

FRCs have several benefits that make them attractive for reactor design. An FRC can be produced in a cylindrical vessel, making the engineering of a reactor simpler than a tokamak, as it has a natural exhaust channel. This geometry also allows for the FRC to be easily translated to a separate burn chamber. FRCs have a high power density, giving a high engineering beta value (near unity), and the low internal magnetic field of FRCs may also make possible the use of advanced fuels. The minimum FRC reactor size would be significantly smaller than an advanced fuel tokamak reactor (Hoffman, 1995).

The standard method of producing field reversal is the Field-Reversed Theta-Pinch (FRTP) (Slough & Hoffman, 1990). A discharge tube is filled with neutral gas in the presence of an axial bias magnetic field. The gas is ionised, freezing the bias field into the plasma. The current in the theta-pinch coil is quickly reversed, producing a large inductive electric field, causing the plasma (and frozen bias field) to implode radially. The oppositely directed magnetic field lines connect near the ends of the theta-pinch coil, and magnetic tension at the ends of the FRC causes axial contraction to an equilibrium state. An FRC can also be formed using counter-helicity merging of spheromaks (Ono et al, 1997), or by rotating magnetic fields (Jones and Knight, 1985).

1.3 RMF Current Generation – The Rotamak

A branch of fusion research investigates continuously driven plasma currents, which overcome the problems associated with the pulsed operation of an FRC. A continuous current may be produced be means of a rotating magnetic field, allowing a steady state operation. This idea was originally expressed by Blevin & Thonemann (1962), and has been a focus of research from 1977 at Flinders University. The Rotamak is a compact torus device where the toroidal plasma current is generated and maintained by a rotating magnetic field (Jones, 1986a).

The physics of RMF current drive are greatly simplified if we consider an azimuthal current driven in an infinitely long plasma cylinder. A plasma column is contained in a cylindrical discharge tube of radius a, in the presence of a steady axial field B_a, produced by an external solenoid (Figure 1.2). A rotating magnetic field, of amplitude B_ω, angular frequency ω, is applied by means of two perpendicular longitudinal loops carrying RF current. A series of conducting rings is located exterior to the RF loops, and acts as an azimuthal conducting shell.

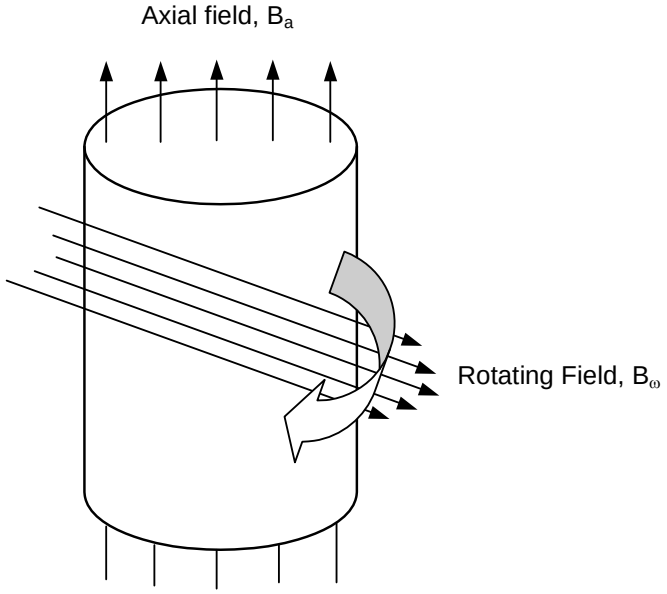

Figure 1.2. Schematic of the magnetic fields associated with the Rotamak, showing the transverse RMF and axial bias field applied to a cylindrical plasma column.

If the angular frequency of the RMF is between the electron and ion cyclotron frequencies (with respect to the RMF), and the electron cyclotron frequency is greater than the electron-ion collision frequency ν_{ei},

$$\text{i.e.} \qquad \frac{eB_\omega}{m_i} << \omega << \frac{eB_\omega}{m_e} \qquad \text{and} \qquad \nu_{ei} << \frac{eB_\omega}{m_e} \tag{1.1}$$

where m_e and m_i are the electron and ion masses, then the electrons are tied to the field lines of the RMF. The electrons will thus rotate synchronously with the RMF (Jones,

1979a). The presence of the externally applied bias field B_a does not affect the generation of azimuthal current.

In order to produce a significant steady current in the plasma requires that the RMF to fully penetrate the plasma column. An external time-varying magnetic field applied to the surface of a conducting medium has an amplitude which decreases exponentially with depth into the medium. This is the classical skin effect, where the the $1/e$ depth in the medium is the skin depth, δ,

$$\delta = \sqrt{\frac{2\eta}{\mu\omega}}, \tag{1.2}$$

where η is the resistivity of the medium (Jackson, 1999).

For the Rotamak concept to be viable requires that the RMF penetrate much farther than the classical skin depth. In the fixed ion model where the plasma ions form a uniformly distributed immobile background, and electron inertia and pressure are neglected, the appropriate Ohm's law for the electron fluid is,

$$\mathbf{E} = \eta\mathbf{J} + \frac{1}{ne}(\mathbf{J} \times \mathbf{B}). \tag{1.3}$$

The first term is the resistive term and the second is the Hall term. The relative dominance of the Hall term with respect to the resistive term is determined by the ratio

$$\frac{\omega_{ce}}{\nu_{ei}}, \tag{1.4}$$

where ω_{ce} is the electron cyclotron frequency (with respect to the RMF) and ν_{ei} is the electron-ion collision frequency. The response of the plasma to the applied RMF is highly dependent on the relative influence of these terms (Jones and Hugrass, 1981).

The RMF induces a time-varying axial electric field, E_z, in the plasma. The resistive term hence produces an associated AC current density J_z, which acts as screening current reducing further penetration of the RMF into the plasma column. The penetration of the RMF into the plasma for the case $\nu_{ei} >> \omega$ is determined by the classical skin effect.

For plasmas in which the resistive term in equation (1.2) dominates, there will be no significant penetration of the RMF.

The effect of the Hall term is to produce an azimuthal force with steady part,

$$\left(\mathbf{J}\times\mathbf{B}\right)_{\theta} = \left\langle J_z B_r \right\rangle, \tag{1.5}$$

which acts on the electrons. This provides a steady torque on the electron fluid, and hence produces a steady azimuthal current, J_θ. The electron fluid has a steady value of the azimuthal velocity $v_{e\theta}$, where the accelerating force in equation (1.4) is opposed by the retarding force due to collisions with the ion fluid. Due to the azimuthal symmetry of the plasma column (or sphere) this Hall current does not produce charge separation and can thus be maintained (Jones, 1986b).

The Hall term also provides an increased penetration of the RMF into the plasma column. In the steady-state, the z-component of Ohm's law can be rewritten in terms of an effective resistivity

$$E_z = \eta^* J_z, \tag{1.6}$$

$$\text{where } \eta^* = \frac{\eta}{1-\frac{v_{e\theta}}{\omega r}}. \tag{1.7}$$

The effective resistivity is increased as the RMF amplitude is increased, hence allowing further penetration of the RMF since the screening current J_z is reduced. The form of equation (1.6) suggests that when the electron fluid is rotating close to the RMF frequency, it is the Doppler shifted frequency of the RMF in the reference frame of the electron fluid that determines the screening current and hence the penetration of the RMF into the plasma. The magnetic field penetration can be expressed in terms of an effective (Doppler shifted) skin depth (Hugrass, 1998)

$$\delta^* = \sqrt{\frac{2\eta}{\mu_0 \omega \left(1 - \frac{v_{e\theta}}{\omega r}\right)}}. \tag{1.8}$$

For metallic conductors, the electron-ion collision frequency is very high (~10^{14} sec^{-1}) and hence the Hall term can usually be neglected. However, this value can be relatively small in plasma conductors suitable for fusion experiments (Jones, 1999), allowing the Hall term to dominate for significant RMF magnitudes. As the magnitude of the RMF is increased, the effective skin depth also increases. When the effective skin depth is greater than the plasma radius, there is complete penetration of the RMF, and a large azimuthal current may be generated (Hugrass and Grimm, 1981).

Experimental (Jones, 1999) and numerical (Milroy, 2000) studies have shown that when the magnitude of the RMF is increased beyond a threshold value, there is increased penetration of the RMF into the plasma column and an increased azimuthal current for plasmas where the Hall term is large with respect to the resistive term. Numerical simulations show that if the ion mass is infinite, a steady state is achieved where the electron fluid rotates almost synchronously with the applied RMF, with a maximum driven current given by

$$J_\theta = -n_e e \omega r \tag{1.9}$$

While the ions are unaffected by the applied RMF if the conditions in equation (1.1) are satisfied, they will undergo momentum transfer collisions with the electron fluid. This suggests that in the steady state, the ion fluid will rotate synchronously with the electron fluid unless a mechanism exists allowing the ion momentum to be relaxed to the surrounding environment. For experiments with lifetimes longer than the relaxation time of the ion fluid requires an effective collision frequency, ν^* exists to oppose the ion relaxation under collisions (Jones, 1986a) such that

$$\nu^* >> \frac{m_e}{m_i}\nu_{ei} \quad . \tag{1.10}$$

If ion motion is introduced, the current will decrease with time unless a torque on the ions opposes the torque due to collisions with the electron fluid. This torque may perhaps be provided by ion-neutral collisions, charge exchange or viscous effects (Hoffman, 2003). If there is not a mechanism to overcome ion relaxation, the current will decay with the ion relaxation time. The problem of current loss due to ion relaxation has not currently been observed (Jones,1999), possibly because the duration of the discharge was not long enough.

1.4 RMF FRC Generation

An FRC may be generated and sustained by using an RMF. The steady driven azimuthal current generates an axial magnetic field component $B_z(r)$, whose direction is determined by the sense of rotation of the RMF. If the sense of rotation is chosen so that $B_z(r)$ is in opposite direction to B_a, a sufficiently large driven current will produce a field-reversed configuration, where the steady part of the field has closed field lines (Hoffman et al, 2006). The RMF method generates an FRC which is sustainable over a long time period. RMFs can also be used to maintain an FRC formed by another method. RMFs are being utilized to maintain FRC equilibria in the TCS (Translation, Confinement and Sustainment) experiment (Hoffman et al, 2005).

The Rotamak experiments at Flinders University produced FRCs sustained for 40 ms using 200 kW of RMF power (Knight & Jones, 1990). Continuous driven currents were produced, limited only by the applied RMF power. RMF generation of FRCs provides a path to steady state reactor design, since the RMF can not only generate an FRC, but may sustain it in the steady state (Ohnishi & Ishida, 1996).

The Translation, Confinement and Sustainment experiment (TCS) begun in 1996 extended the LSX (Large s Experiment) at the University of Washington (Hoffmann et al, 2002). This program aims to utilise an RMF to both generate and to maintain a

prolate FRC. The program produced quasi steady state FRCs with densities of $n = 1 – 3$ x 10^{19} m^{-3} which were maintained as long as RMF power was supplied (Guo et al, 2002).

While FRCs can be generated and sustained using the RMF alone in the TCS chamber, these FRCs have sub 100 eV temperatures. Translation experiments have a hot FRC generated in the modified LSX equipment (LSX/mod) and transferred to a separate burn chamber (TCS), where the flux is maintained by an RMF (Hoffmann et al, 2002).

1.5 The Clemente Scheme

The plasma current generated by an RMF technique, or an FRC maintained by an RMF, will gradually decay over time. This is due to the rotation of the ion fluid, which will be driven by collisions between the electron and ion fluid. The plasma will eventually achieve a true steady state where both electron and ions rotate synchronously with the RMF, and the driven current is zero. In order to provide RMF driven plasmas with lifetimes greater than the ion collision time, requires a method of controlling the ion motion. It is possible that the steady state may be maintained by collisions of the ions with neutral species, wall interactions and diffusion effects (Hoffman, 2003).

The Clemente scheme for steady state operation longer than the ion relaxation time utilises two counter-rotating RMFs (Clemente, 1998). One RMF (the (-) RMF) entrains the electron fluid, which in the steady state rotates almost synchronously with the (-) RMF, and a second RMF (the (+) RMF) entrains the ion fluid.

It has been shown that steady state solutions for the Clemente scheme exist. (Hugrass, 2000). For the electron and ion fluids to be entrained in the steady state requires that the conditions

$$\left(\frac{\xi^-}{\zeta_e{}^-}\right) << 1 \quad \left(\frac{\xi^+}{\zeta_e{}^+}\right) << \frac{\delta}{R}, \tag{1.11}$$

be satisfied throughout the plasma, where

$$\zeta_e^{\pm} = \frac{e\,|B^{\pm}{}_r\,|}{\omega^{\pm} m_e} \qquad \xi^{\pm} = \frac{\nu_{ei}}{\omega^{\pm}}. \tag{1.12}$$

The Clemente scheme provides a true steady state, where the electron fluid rotates synchronously with the (-) RMF and the ion fluid rotates synchronously with the (+) RMF, providing a constant driven current.

For the Clemente scheme to be feasible, requires that the (+) RMF penetrates much farther than a classical skin depth, and that the steady states for the ion fluid are accessible from reasonable initial conditions. It is the purpose of this research to demonstrate the existence of global steady states where both RMFs penetrate much farther than the classical skin depth and entrain the electron and ion fluids. This work will also investigate the accessibility of the steady states for the Clemente scheme from reasonable initial conditions.

1.6 Outline of Thesis

The objective of this thesis is to investigate the accessibility of the Clemente steady states in a preformed FRC by performing a transient analysis using a simplified 1-D two fluid numerical model. The initial conditions from which the Clemente steady states are accessible are examined by means of numerical simulation.

Chapter 2 describes a simplified two-fluid model for the Clemente scheme and derives equations of motion for this physical model. Chapter 3 analyses the Clemente steady states for a single layer of the plasma, showing the conditions required for entrainment of the electron and ion fluids by the (-) and (+) RMF, respectively, and the conditions required so that the electrons remain entrained by the (-) RMF once the (+) RMF is applied. Chapter 4 analyses the accessibility of the Clemente scheme, demonstrating the requirements for full penetration of the RMFs, and the existence of a global steady state at every layer of the plasma. Chapter 5 presents results for a numerical model and simulation results for the Clemente scheme where the radial motion is suppressed. In Chapter 6 the physical model for a preformed FRC is examined where radial motion of

the plasma is allowed, and simulation results presented. Conclusions and further work are presented in Chapter 7.

CHAPTER 2 PHYSICAL MODEL AND EQUATIONS OF MOTION

The time-dependent equations of motion describing the penetration of two RMFs into an infinitely long plasma column are derived. A complete analysis should allow for radial motion of the plasma column. For the problem of penetration of the RMF into the plasma column, the radial motion may be neglected. The radial motion is thus suppressed in this initial model, but will be examined in Chapter 6 when the action of applied RMFs to a preformed FRCs is considered.

Section 2.1 presents the physical model and assumptions. In section 2.2 the transient equations of motion are developed for a single applied RMF where both electron and ion fluids are free to move in the z and θ directions. Section 2.3 presents the equations of motion for two applied RMFs. In Chapter 3 the derived equations of motion are used to analyse the steady states of the electron and ion fluids. Chapter 4 examines the accessibility of the steady states and the enhanced penetration of the applied RMFs for this model

2.1 Physical Model

An infinitely long cylindrical plasma is considered with radius R, and flux conserving rings positioned at a radius $b > R$ which are coaxial with the plasma column. Firstly we consider the transient influence of a single RMF applied to the plasma.

Initially, only a steady axial bias field B_a, is present. At $t = 0$, a transverse rotating magnetic field (RMF) having frequency ω, and magnitude B_ω is applied to the plasma column. The amplitude of the applied RMF rises in a time τ_r which is characteristic of the RF source used to generate the RMF.

$$B_t(t) = \left(1 - e^{-t/\tau_r}\right) B_\omega \tag{2.1}$$

The total magnetic field will then consist of an axial magnetic field $B_z(r)$ and a transverse rotating field. The externally applied magnetic field can then be expressed in cylindrical coordinates as

$$\mathbf{B} = \mathrm{Re}\left\{B_r \exp\left[j(\omega t - \theta)\right]\hat{\mathbf{r}} + B_\theta \exp\left[j(\omega t - \theta)\right]\hat{\boldsymbol{\theta}}\right\} + B_z \hat{\mathbf{z}}\,, \tag{2.2}$$

where B_r and B_θ are the complex phasors of the r and θ components of the magnetic field respectively.

For the externally applied field to an infinitely long plasma column, in the steady state any physical quantity can be represented by a Fourier series expansion in $(\omega t - \theta)$. It was demonstrated by Hugrass (1982) that all the relevant physical quantities can be classified into two groups. The first group consists of the transverse components of the electric field, the current density and fluid velocities, the number density, the pressure and the axial component of the magnetic fields. A quantity of the first group has a constant (dc) part which does not depend on θ, and only even harmonics of $(\omega t - \theta)$,

$$Q = \sum_{m=0}^{\infty} Q_{2m}(r) \exp i2m(\omega t - \theta). \tag{2.3}$$

The second group consists of the axial components of the electric field, the current density and fluid velocities and the transverse components of the magnetic field. A quantity of the second group has only odd harmonics of $(\omega t - \theta)$,

$$Q = \sum_{m=0}^{\infty} Q_{2m+1}(r)\exp i(2m+1)(\omega t - \theta). \tag{2.4}$$

The effects of the second and higher harmonics are very small and can be neglected (Milroy, 1999), and hence quantities of the first group are constant (dc) and quantities of the second group are ac and vary as exp[$i(\omega t - \theta)$].

The ac quantities are represented by their (constant) complex phasors. Thus a quantity x of the second group is given by

$$\begin{aligned} x(r,\vartheta,t) &= x_o(r)\cos(\omega \mathrm{t} - \theta - \varphi(\mathrm{r})) \\ &= \mathrm{Re}\{X(r)\exp i(\omega t - \theta)\} \end{aligned}, \tag{2.5}$$

and is represented by the complex phasor X

$$X(r) = x_o(r)\exp(-i\varphi_x(\mathrm{r})). \tag{2.6}$$

The phasor for $\partial x/\partial t$ is

$$X'(r) = i\omega X(r). \tag{2.7}$$

For quantities of the second group,

$$\frac{\partial}{\partial \theta} = -i \qquad \frac{\partial}{\partial z} = 0 \tag{2.8}$$

,

and for quantities of the first group,

$$\frac{\partial}{\partial \theta} = 0 \qquad \frac{\partial}{\partial z} = 0. \tag{2.9}$$

For the slowly varying transient states considered here, the dc quantities of the steady state as well as the complex phasors of the ac quantities vary slowly with time. In particular, a quantity x of the second group is given by

$$\begin{aligned} x(r,\theta,t) &= x_o(r,t)\cos(\omega t - \theta - \varphi_x(r,t)) \\ &= \mathrm{Re}\{X(r,t)\exp i(\omega t - \theta)\} \end{aligned}, \tag{2.10}$$

and is represented by the complex phasor X

$$X(r,t) = x_o(r,t)\exp(-i\varphi_x(r,t)) . \tag{2.11}$$

The phasor for $\partial x/\partial t$ is

$$X'(r,t) = i\omega X(r,t) + \frac{\partial X(r,t)}{\partial t} . \tag{2.12}$$

The meaning of the term slowly here is that $|(\partial/\partial t)| << |\omega|$. This condition must be satisfied in order that we can still represent the ac quantities by their complex phasors.

In the following analysis, the time dependant equation for the phasor X of a quantity x of the second group takes the form

$$\frac{\partial X(r,t)}{\partial t} = F(r,t) - i\omega X(r,t) \ , \tag{2.13}$$

where the complex function F is obtained from the equation of motion for x. For the slowly-varying steady states considered here

$$\left|\frac{\partial X(r,t)}{\partial t}\right| << \omega\left|X(r,t)\right| , \tag{2.14}$$

and hence

$$X'(r,t) \cong i\omega X(r,t) \cong F(r,t) . \tag{2.15}$$

In the steady state of course

$$\frac{\partial X(r,t)}{\partial t} = 0 \ , \tag{2.16}$$

and hence

$$X'(r,t) = i\omega X(r,t) = F(r,t) . \tag{2.17}$$

The approximation given in equation (2.15) could be made everywhere except in the time-dependent equation for x where one calculates the quantity $\partial X(r,t)/\partial t$.

The product of two quantities of the second group x and y has an average part

$$\langle xy \rangle = \frac{1}{2} x_o y_o \cos(\varphi_x - \varphi_y) = \frac{1}{2} \mathrm{Re}\{X \bar{Y}\}, \tag{2.18}$$

where $\bar{Y}$ is the complex conjugate of Y. In what follows we will not strictly follow the convention of using a lower case character for a quantity of the second group and the upper case character for its phasor. We prefer to conform to the convention of using upper case A and B for the vector potential and the magnetic field. For these quantities, the same upper case characters will be used to denote both the quantity and its complex phasor. The meaning of A and B will be always obvious from the context and we will not alert the reader on every occasion.

The r-component of the plasma velocity is a quantity of the first group and is thus independent of θ. It follows from the equation of continuity that v_r must vanish in the steady state unless there is a source or sink on the axis. A complete analysis of the transient behaviour of the plasma should allow for the motion of the plasma in the r direction and the consequent adjustment of the radial profile of the plasma pressure. These effects, however, are not essential for the study of the penetration of the RMF into the plasma and would introduce unnecessary complications. The effect of the motion of the plasma in the radial direction will be considered in Chapter 5.

2.2 Equations of Motion

The equations of motion for the electron and ion fluids are

$$m_e n\left(\frac{\partial \mathbf{v_e}}{\partial t} + \mathbf{v_e} \bullet \nabla \mathbf{v_e}\right) = -en(\mathbf{E} + \mathbf{v_e} \times \mathbf{B}) - \nabla P_e + m_e n \nu_{ei}(\mathbf{v_i} - \mathbf{v_e}), \tag{2.19}$$

$$m_i n\left(\frac{\partial \mathbf{v_i}}{\partial t} + \mathbf{v_i} \bullet \nabla \mathbf{v_i}\right) = en(\mathbf{E} + \mathbf{v_i} \times \mathbf{B}) - \nabla P_i + m_e n \nu_{ei}(\mathbf{v_e} - \mathbf{v_i}), \tag{2.20}$$

where m_e is the electron mass, m_i the ion mass, $\mathbf{v_e}$ the electron velocity, $\mathbf{v_i}$ the ion velocity, n is the number density, ν_{ei} is the electron ion collision frequency, P_e is the

electron pressure and P_i the ion pressure. In these equations, quasi-neutrality is assumed so that $n_e = n_i = n$.

Using Faraday's law

$$\nabla \times \mathbf{E} = -\frac{\partial \mathbf{B}}{\partial t}, \tag{2.21}$$

we obtain the following expression for the phasor of the z component of the electric field

$$E_z = -i\omega A_z - \frac{\partial A_z}{\partial t} = \omega r B_r - \frac{\partial A_z}{\partial t}. \tag{2.22}$$

The small term $\partial A_z/\partial t$ is retained in equation (2.22) because its contribution to the time-dependent equation for A_z becomes large for certain values of the electron and ion slips as will become clear from equation (2.38) below.

The derivation of the time-dependent equations is greatly simplified if we note that the phasor for the time derivative of v_{ez} (V'_{ez}) is approximately related to the phasor for v_{ez} (V_{ez}) by the equation

$$V'_{ez} \approx i\omega V_{ez} \quad , \tag{2.23}$$

and similarly for the ion fluid

$$V'_{iz} \approx i\omega V_{iz}. \tag{2.24}$$

Using equations (2.22) to (2.24), the z-components of the equations of motion can be written as

$$im_e n\left(\omega V_{ez} - \frac{v_{e\theta}}{r} V_{ez}\right) = -en\left(E_z - \frac{v_{e\theta}}{\omega r}\left(E_z + \frac{\partial A_z}{\partial t}\right)\right) + \frac{m_e \nu_{ei}}{e} J_z, \tag{2.25}$$

$$im_i n\left(\omega V_{iz} - \frac{v_{i\theta}}{r} V_{iz}\right) = -en\left(E_z - \frac{v_{i\theta}}{\omega r}\left(E_z + \frac{\partial A_z}{\partial t}\right)\right) + \frac{m_e \nu_{ei}}{e} J_z. \tag{2.26}$$

Defining the slips of the electron and ion fluids with respect to the RMF

$$S_e = 1 - \frac{v_{e\theta}}{\omega r} \qquad S_i = 1 - \frac{v_{i\theta}}{\omega r}, \tag{2.27}$$

equations (2.25) and (2.26) then reduce to

$$i\omega m_e n S_e \, V_{ez} = -en\left(S_e E_z + (S_e - 1)\frac{\partial A_z}{\partial t} \right) + \frac{m_e \nu_{ei}}{e} J_z, \tag{2.28}$$

$$i\omega m_i n S_i \, V_{iz} = en\left(S_i E_z + (S_i - 1)\frac{\partial A_z}{\partial t} \right) - \frac{m_e \nu_{ei}}{e} J_z. \tag{2.29}$$

Subtracting these two expressions provides an expression for the axial current density

$$J_z = -\frac{ie^2 n}{m_e \omega}\left[E_z + \left(1 - \frac{1}{S_e}\right)\frac{\partial A_z}{\partial t} - \frac{1}{S_e}\frac{m_e \nu_{ei}}{e^2 n} J_z \right. \\ \left. + \frac{m_e}{m_i}\left(E_z + \left(1 - \frac{1}{S_i}\right)\frac{\partial A_z}{\partial t} - \frac{1}{S_i}\frac{m_e \nu_{ei}}{e^2 n} J_z \right) \right]. \tag{2.30}$$

Equations (2.28) and (2.29) are used to derive a generalised Ohm's law for the z-component of the electric field

$$E_z = \eta^* J_z + \left[\frac{1}{S_e} - 1 + \frac{m_e}{m_i}\left(\frac{1}{S_i} - 1 \right) \right] \frac{\partial A_z}{\partial t}, \tag{2.31}$$

where the effective resistivity η^* is the given by

$$\eta^* = \eta\left(\frac{1}{S_e} + \frac{m_e}{m_i}\frac{1}{S_i} + i\frac{1}{\xi} \right), \tag{2.32}$$

the classical resistivity is given by

$$\eta = \frac{m_e m_i}{m_e + m_i}\frac{\nu_{ei}}{e^2 n} = \frac{m_e \, {}^{*}\nu_{ei}}{e^2 n}, \tag{2.33}$$

the reduced mass is given by

$$m_e^* = \frac{m_e m_i}{m_e + m_i}, \tag{2.34}$$

and

$$\xi = \frac{\nu_{ei}}{\omega} \tag{2.35}$$

is the normalised collision frequency.

The current density is also related to the magnetic field by Ampere's law

$$J_\theta = -\frac{1}{\mu_0}\frac{\partial B_z}{\partial r}, \tag{2.36}$$

$$J_z = -\frac{1}{\mu_0}\nabla^2 A_z. \tag{2.37}$$

Equations (2.31) and (2.37)are used to derive the time-dependant equation for A_z

$$\frac{\partial A_z}{\partial t} = \left[\frac{\eta^*}{\mu_0}\nabla^2 A_z - i\omega A_z\right] \Bigg/ \left[\frac{1}{S_e} + \frac{m_e}{m_i}\left(\frac{1}{S_i} - 1\right)\right], \tag{2.38}$$

where the Laplacian of A_z is given by

$$\nabla^2 A_z = \frac{1}{r}\frac{\partial}{\partial r}\left(r\frac{\partial A_z}{\partial r}\right) - \frac{A_z}{r^2}. \tag{2.39}$$

Note that the denominator in equation (2.39) becomes very small when

$$S_i = \frac{1}{1 - \frac{m_e}{m_i}\frac{1}{S_e}} \approx -\frac{m_e}{m_i}S_e, \tag{2.40}$$

at a certain layer. For the Clemente scheme, this occurs when S_i is small and negative. At this particular layer, $\frac{\eta^*}{\mu_0}\nabla^2 A_z$ becomes almost equal to $-i\omega A_z$. The value of $\frac{\partial A_z}{\partial t}$ does not become large at this layer.

The steady part of the force density on the electron fluid in the θ-direction is determined by

$$F_e = -en\langle v_{ez} B_r \rangle. \tag{2.41}$$

When the terms involving the time derivative of A_z are neglected this leads to

$$F_e = -\frac{1}{2} en \,\mathrm{Re}\left\langle \frac{ieE_z B_r}{m_e \omega S_e}\left(S_e - \frac{\eta}{\eta^*}\right)\right\rangle, \tag{2.42}$$

$$F_e = \frac{nm_e \omega^2 r \zeta_e{}^2}{2S_e \xi\left[\left(\frac{1}{S_e} + \frac{m_e}{m_i}\frac{1}{S_i}\right)^2 + \frac{1}{\xi^2}\right]}, \tag{2.43}$$

where

$$\zeta_e = \frac{e|B_r|}{\omega m_e}. \tag{2.44}$$

Similarly, the steady part the of force density on the ion fluid in the θ-direction is

$$F_i = en\langle v_{iz} B_r \rangle, \tag{2.45}$$

$$F_i = \frac{nm_i \omega^2 r \zeta_i{}^2}{2S_i \xi\left[\left(\frac{1}{S_e} + \frac{m_e}{m_i}\frac{1}{S_i}\right)^2 + \frac{1}{\xi^2}\right]}, \tag{2.46}$$

where

$$\zeta_i = \frac{e|B_r|}{\omega m_i} = \frac{m_e}{m_i}\zeta_e. \tag{2.47}$$

A time-dependant equation for B_z is obtained from the θ-component of the equation of motion of the electron fluid

$$E_\theta = -\langle v_{ez} B_r \rangle + \eta J_\theta , \tag{2.48}$$

and the θ-component of Faraday's law

$$\frac{\partial B_z}{\partial t} = -(\nabla \times \mathbf{E})_z = -\frac{1}{r}\frac{\partial}{\partial r}(rE_\theta). \tag{2.49}$$

Assuming that the electron-ion collision frequency is constant, this provides

$$\frac{\partial B_z}{\partial t} = \frac{\eta}{\mu_0}\nabla^2 B_z - \frac{1}{r}\frac{\partial}{\partial r}\left(r\langle v_{ez} B_r \rangle\right), \tag{2.50}$$

where the electron inertia terms are neglected. If we consider the steady state behaviour of equation (2.50), in the absence of an externally applied field, this becomes a diffusion equation and hence the field will be spread evenly through the plasma giving zero driven current. The presence of the externally applied field may provide a driven current in the steady state, given by

$$J_\theta = \frac{\langle v_{ez} B_r \rangle}{\eta}. \tag{2.51}$$

The θ-component of the plasma momentum density is given by

$$P_\theta = m_e n v_{e\theta} + m_i n v_{i\theta}. \tag{2.52}$$

A time dependant equation for the θ-component of the plasma momentum density may be found from the θ-components of the equation of motion.

$$m_e \frac{\partial v_{e\theta}}{\partial t} = -e\left(E_\theta + \langle v_{ez} B_r \rangle\right) + m_e \nu_{ei}\left(v_{i\theta} - v_{e\theta}\right), \tag{2.53}$$

$$m_i \frac{\partial v_{i\theta}}{\partial t} = -e\left(E_\theta + \langle v_{iz} B_r \rangle\right) + m_e \nu_{ei}\left(v_{e\theta} - v_{i\theta}\right). \tag{2.54}$$

Adding equations (2.53) and (2.54) gives

$$\frac{\partial P_\theta}{\partial t} = \langle J_z B_r \rangle. \tag{2.55}$$

Since the θ-component of the current density is given by

$$J_\theta = ne\left(v_{i\theta} - v_{e\theta}\right), \tag{2.56}$$

the θ-components of the fluid velocities are then given by

$$v_{i\theta} = \frac{1}{\left(m_e + m_i\right)n}\left(P_\theta + \frac{m_e J_\theta}{e}\right), \tag{2.57}$$

$$v_{e\theta} = \frac{1}{\left(m_e + m_i\right)n}\left(P_\theta - \frac{m_i J_\theta}{e}\right). \tag{2.58}$$

The values of the slips may then be calculated from the θ-components of the fluid velocities.

2.3 The Clemente Scheme

The Clemente scheme requires the introduction of a second RMF. The first RMF is given a frequency close to the electron rotational frequency and the second RMF has a frequency close to the ion rotational frequency. For the scheme envisaged here (and for the application of the Clemente scheme to a preformed FRC) the two RMFs will be counter-rotating since the electron and ion fluids are counter-rotating. The RMF which is applied to entrain the electron fluid is denoted the (-) RMF and the RMF which is applied to entrain the ion fluid is denoted the (+) RMF. Quantities relating to the (+) and (-) RMF are denoted by the + and – superscripts, respectively.

The externally applied total magnetic field then consist of an axial magnetic field B_z and two transverse rotating fields. The total magnetic field is then given by

$$\begin{aligned}\mathbf{B} = \quad & \mathrm{Re}\left\{\left(B_r^{-}\exp\left[j\left(\omega^{-}t-\theta\right)\right]+B_r^{+}\exp\left[j\left(\omega^{+}t-\theta\right)\right]\right)\hat{\mathbf{r}}\right\}+ \\ & \mathrm{Re}\left\{\left(B_\theta^{-}\exp\left[j\left(\omega^{-}t-\theta\right)\right]+B_\theta^{+}\exp\left[j\left(\omega^{+}t-\theta\right)\right]\right)\hat{\boldsymbol{\theta}}\right\}+ \\ & B_z\,\hat{\mathbf{z}}\end{aligned} \tag{2.59}$$

Under the influence of the two RMFs, the time-dependent equations are given by

$$\frac{\partial A_z^{\pm}}{\partial t} = \left(\frac{\eta^{*\pm}}{\mu_0} \nabla^2 A_z^{\pm} - i\omega^{\pm} A_z^{\pm} \right) \Bigg/ \left[\frac{1}{S_e^{\pm}} + \frac{m_e}{m_i} \left(\frac{1}{S_i^{\pm}} - 1 \right) \right] \tag{2.60}$$

$$\frac{\partial B_z}{\partial t} = \frac{\eta}{\mu_0} \nabla^2 B_z - \frac{1}{r} \frac{\partial}{\partial r} r \left(\left\langle v_{ez}^{-} B_r^{-} \right\rangle + \left\langle v_{ez}^{+} B_r^{+} \right\rangle \right) \tag{2.61}$$

$$\frac{\partial P_\theta}{\partial t} = \frac{1}{n} \left\langle J_z^{-} B_r^{-} + J_z^{+} B_r^{+} \right\rangle \tag{2.62}$$

$$v_{e\theta} = \frac{1}{(m_e + m_i) n} \left(P_\theta - \frac{m_i J_\theta}{e} \right) \tag{2.63}$$

$$v_{i\theta} = \frac{1}{(m_e + m_i) n} \left(P_\theta + \frac{m_e J_\theta}{e} \right) \tag{2.64}$$

$$J_\theta = -\frac{1}{\mu_0} \frac{\partial B_z}{\partial r} \tag{2.65}$$

$$J_z^{\pm} = -\frac{1}{\mu_0} \nabla^2 A_z^{\pm} \tag{2.66}$$

Where the + and − superscripts refer to the (+), and (–) RMFs respectively. The penetration of the RMF into the plasma is determined by the effective resistivity $\eta^{*\pm}$ with respect to each RMF, given by

$$\eta^{*\pm} = \eta \left(\frac{1}{S_e^{\pm}} + \frac{m_e}{m_i} \frac{1}{S_i^{\pm}} + i \frac{1}{\xi^{\pm}} \right), \tag{2.67}$$

where

$$\xi^{\pm} = \frac{\nu_{ei}}{\omega^{\pm}}, \tag{2.68}$$

is the normalised collision frequency with respect to each RMF.

In the Clemente scheme, either RMF may penetrate further than determined by the classical skin depth due to enhanced effective resistivity. The (-) RMF may penetrate the plasma with enhanced skin depth since $S_e^{-} << 1$ and the (+) RMF may penetrate the

plasma with enhanced skin depth since $S_i^+ << m_e/m_i$. This effect will be further examined in Chapter 4.

The steady part of the θ-component of the force density due to each RMF on the electron fluid is given by

$$F_e^{\pm} = -en\left\langle v_{ez}^{\pm} B_r^{\pm} \right\rangle, \tag{2.69}$$

$$F_e^{\pm} = \frac{nm_e\omega^{\pm 2} r\zeta_e^{\pm 2}}{2S_e^{\pm}\xi^{\pm}\left[\left(\frac{1}{S_e^{\pm}} + \frac{m_e}{m_i}\frac{1}{S_i^{\pm}}\right)^2 + \frac{1}{\xi^{\pm 2}}\right]}. \tag{2.70}$$

The sign of the force density on the electron fluid is always in a direction of attempting to entrain the electron fluid to the frequency of the RMF (the sign of the force density on the electron fluid is determined by the sign of the electron slip with respect to the RMF). If the rotational frequency of the electron fluid is less than that of the RMF, the RMF provides an accelerating torque. If the rotational frequency is greater than that of the RMF, the RMF provides a retarding torque on the electron fluid.

Similarly, the steady part of the θ-component of the force density due to each RMF on the ion fluid is given by

$$F_i^{\pm} = -en\left\langle v_{iz}^{\pm} B_r^{\pm} \right\rangle, \tag{2.71}$$

$$F_i^{\pm} = \frac{nm_i\omega^{\pm 2} r\zeta_i^{\pm 2}}{2S_i^{\pm}\xi^{\pm}\left[\left(\frac{1}{S_e^{\pm}} + \frac{m_e}{m_i}\frac{1}{S_i^{\pm}}\right)^2 + \frac{1}{\xi^{\pm 2}}\right]}. \tag{2.72}$$

The sign of the force density on the ion fluid is always in a direction of attempting to entrain the ion fluid to the frequency of the RMF (the sign of the force density on the ion fluid is determined by the sign of the ion slip with respect to the RMF). If the rotational frequency of the ion fluid is less than that of the RMF, the RMF provides an accelerating torque. If the rotational frequency is greater than that of the RMF, the RMF exerts a retarding torque on the ion fluid.

CHAPTER 3 THE CLEMENTE STEADY STATES

In this chapter the steady states relevant to the Clemente scheme are considered. The Clemente steady states correspond to almost synchronous rotation of the electron fluid with the (-) RMF and almost synchronous rotation of the ion fluid with the counter-rotating (+) RMF. Hence we will be interested in the steady states with small values of S_e^- and S_i^+. The steady states for a single layer of the plasma are examined for both the (-) and (+) RMF. The accessibility of these local steady states is examined in Chapter 4.

Section 3.1 describes the electron fluid steady states under the influence of a single applied RMF. The requirements for the existence of a steady state with small electron slip and the method of determining operating points is discussed. Section 3.2 extends these results for the case when two RMFs are applied and presents requirements for the existence the Clemente steady state for the electron fluid. Section 3.3 outlines the steady states for the ion fluid when two RMFs are applied and conditions required for the existence of the small slip operating point. Section 3.4 summarises the conditions required for the successful implementation of the Clemente scheme.

3.1 Electron Fluid Steady States

An external RMF can be used to generate or maintain a plasma current. For a current generation scheme the current is initially zero ($S_e = S_i = 1$) and the RMF transfers angular momentum to the electron fluid. In the steady state the electron fluid will rotate almost synchronously with the RMF ($S_e << 1$). The collision force between the electron and ion fluid has two main effects. It provides a drag force opposing the RMF current

drive, and hence requires that the RMF magnitude be large enough to overcome this opposition. The collision force also causes momentum transfer from the electron to the ion fluid providing a steady state where the ions will rotate synchronously with the electron fluid resulting in zero driven current. Loss of current due to ion rotation has not currently been observed, possibly because the particle confinement time is not long enough in current experiments (Hoffman, 2003). Conventional RMF current drive schemes may only be applicable for short confinement times without a method for controlling the loss of current due to ion rotation.

3.1.1 An analogy to the induction motor

The steady state solutions for a single applied RMF to a plasma column may be described using the analogy of a polyphase induction motor (Hugrass, 1985). For the induction motor, a torque is exerted on the rotor by an RMF, which is opposed by a torque exerted by the mechanical load, both of which depend on the slip of the rotor with respect to the RMF. The torque exerted by the RMF on the rotor is independent of the mechanical load, and the torque exerted by the mechanical load is independent of the RMF. The steady states of the system, or *operating points*, occur when the torque exerted by the RMF is exactly balanced by the torque applied by the mechanical load, so that the net torque is zero,

$$T_{RMF} + T_{load} = 0 \,. \tag{3.1}$$

The steady state value of the slip of the rotor-load system is hence determined by the intersection of the curve representing the torque imparted by the RMF (T_{RMF}) on the rotor and a *load line* representing the opposing torque exerted by the mechanical load (-T_{load}).

The induction motor and the current drive systems both involve the transfer of angular momentum by means of an RMF. In the current drive scheme, the electron fluid is analogous to the rotor, and the ion fluid is analogous to the mechanical load. For the case of an RMF applied to a plasma column, the plasma does not necessarily rotate as a rigid rotor, and hence we consider the force densities at a single layer of the plasma.

Since the electron and ion rotational velocities will be functions of radius, the slips of the electron and ion fluids will vary with radius.

For the RMF current drive system, the steady states, or *operating points*, are determined by the intersection of the force density imparted by the RMF on a layer of the electron fluid and a *load line*. For the current drive system, the load line represents the collisional force density exerted by the interaction of the electron fluid with the ion fluid. The steady states for the electron fluid under the application of a single RMF are hence solutions to

$$F_e + F_{coll} = 0 \tag{3.2}$$

where F_e is the force density on exerted by the RMF on the electron fluid at this layer and F_{coll} is the force density on the electron fluid due to collisions with the ion fluid at this layer.

Each layer of the plasma may have different operating points. Also for the plasma column, the RMF magnitude (and hence the force) will be a function of radius, since the local value of $|B_r|$ is determined by the penetration of the (+) RMF in the plasma.

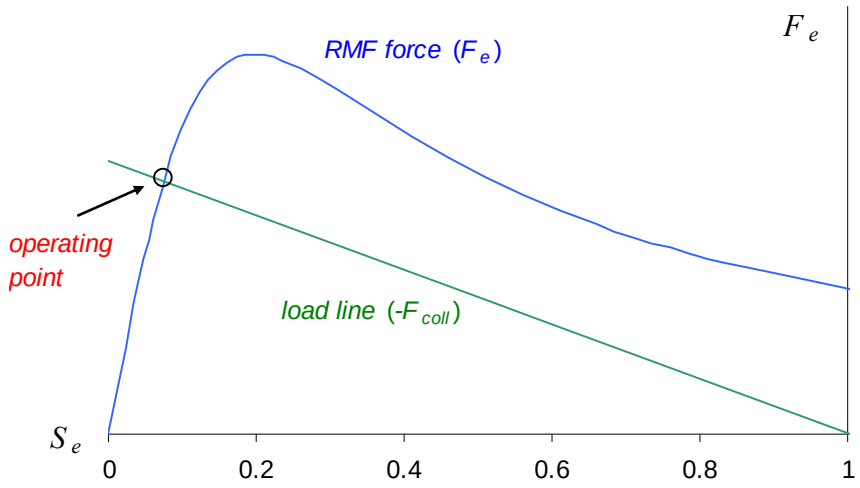

Figure 3.1. Method of determining operating points for RMF current drive ($\xi = 0.2$ and $\zeta_e = 1$).

Figure 3.1 shows an example of the method of determining operating points for the current drive scheme, showing the force density due to the RMF, the load line ($-F_{coll}$)

and the operating point as the intersection of these two curves. The operating point is determined for the case $\xi = 0.2$ and $\zeta_e = 1$. This diagram shows a single operating point for the electron fluid for a single layer of the plasma. The curves are plotted against the slip of the electron fluid with respect to the applied RMF at this layer.

The collision force density is determined by the relative velocities of the electron and ion fluids at this layer

$$F_{coll} = nm_e\nu_{ei}\left(\mathrm{v}_e - \mathrm{v}_i\right), \tag{3.3}$$

which can be represented in terms of the slip of the electron and ion fluid with respect to the RMF

$$F_{coll} = nm_e\nu_{ei}\omega r\left(S_e - S_i\right). \tag{3.4}$$

Figure 3.1 is shown with the ion fluid stationary, hence $S_i = 1$

For a single RMF the force density on the electron fluid is given by equation (2.44) and hence the operating points are solutions to

$$\frac{nm_e\omega^2 r\zeta_e^{\,2}}{2S_e\xi\left[\left(\frac{1}{S_e} + \frac{m_e}{m_i}\frac{1}{S_i}\right)^2 + \frac{1}{\xi^2}\right]} = -nm_e\nu_{ei}\omega r\left(S_e - S_i\right). \tag{3.5}$$

For a given value of the ion slip this equation is 3rd order in S_e. There are 3 solutions for S_e, one of which is always real and two solutions which are either real or complex. The operating points correspond to the real solutions of equation (3.5).

Firstly we will analyse the operating points for typical curves showing the possible cases and then derive an approximate expression for the steady state corresponding to almost synchronous rotation of the electron fluid with the RMF.

3.1.2 Analysis of operating points for the electron fluid

The force densities can be represented in dimensionless units by dividing by the factor

$$F_0 = nm_e\omega^2 r\,, \tag{3.6}$$

which provides a dimensionless representation for the force density on the electron fluid

$$\frac{F_e}{F_0} = \frac{\zeta_e^{\,2}}{2S_e\xi\left[\left(\frac{1}{S_e} + \frac{m_e}{m_i}\frac{1}{S_i}\right)^2 + \frac{1}{\xi^2}\right]}, \tag{3.7}$$

and the collision force

$$\frac{F_{coll}}{F_0} = \xi\left(S_e - S_i\right). \tag{3.8}$$

The relative magnitudes of the two forces at a given plasma layer are thus dependant upon the two dimensionless parameters ξ and ζ_e, and the rotational velocities of the two fluids.

There may be either 1 or 3 operating points for the electron fluid. The following figures show the three possible cases for the electron fluid operating points. The figures show the dimensionless force densities where the ions are assumed stationary, and hence the force due to collisions is zero at $S_e = 1$.

Figure 3.2 shows the case for the existence of 1 operating point with $S_e << 1$ where $\xi =$ 0.2 and $\zeta_e = 1$. The RMF magnitude is large enough so that the peak of the RMF force density on the electron fluid is greater than the force density due to collisions. This operating point is often termed the *synchronous rotation* operating point, however since the electron slip is not zero, the electron fluid rotates at a frequency slightly less than that of the RMF. The RMF exerts zero force on the electron fluid at $S_e = 0$, and since the force due to collisions is non-zero at $S_e = 0$. the electron fluid cannot rotate synchronously with the RMF.

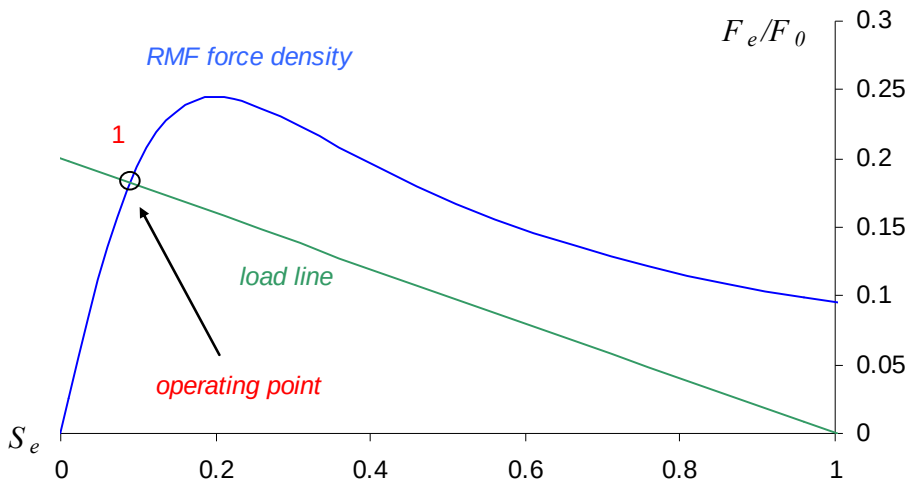

Figure 3.2. Electron fluid operating points ($\xi = 0.2$ and $\zeta_e = 1$).

Figure 3.3 shows the case for $\xi = 0.2$ and $\zeta_e = 0.5$. The RMF magnitude is not large enough, and the peak of the force on the electron fluid due to the RMF is less than that due to collisions. In this case there is no steady state corresponding to synchronous rotation. The operating point corresponds to a very small driven current.

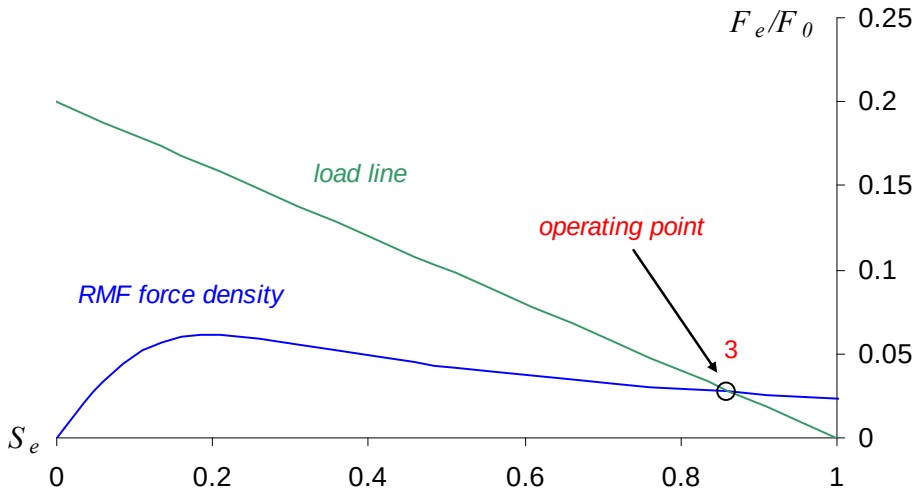

Figure 3.3. Electron fluid operating points ($\xi = 0.2$ and $\zeta_e = 0.5$).

Figure 3.4 shows the case for $\xi = 0.1$ and $\zeta_e = 0.65$. There are three possible operating points. All three operating points correspond to equilibria, where (1) and (3) are stable equilibria since small perturbations from the operating point provides a restoring force returning to the operating point. Operating point (2) is unstable since the total force in this region is always away from the operating point and hence a small perturbation from the operating point provides a force away from the operating point. The stable steady states for the electron fluid at this layer therefore correspond to operating points (1) and (3). Operating point (1) corresponds to almost synchronous rotation of the electron fluid with the RMF and solution (3) to a very small driven current. Which of the two stable steady states is accessed depends on the initial conditions.

The scenarios shown are determined by the peak value and width of the RMF force density on the electron fluid and the magnitude of the force density due to collisions with the ion fluid. For a current drive scheme where the initial condition is $S_e = 1$ requires a scenario outlined in Figure 3.2, since the steady state for almost synchronous rotation of the electron fluid is accessible from this initial condition. The scenario shown in Figure 3.4 cannot be accessed from the initial condition $S_e = 1$ and hence is only applicable for maintaining the plasma current and cannot be used for current generation.

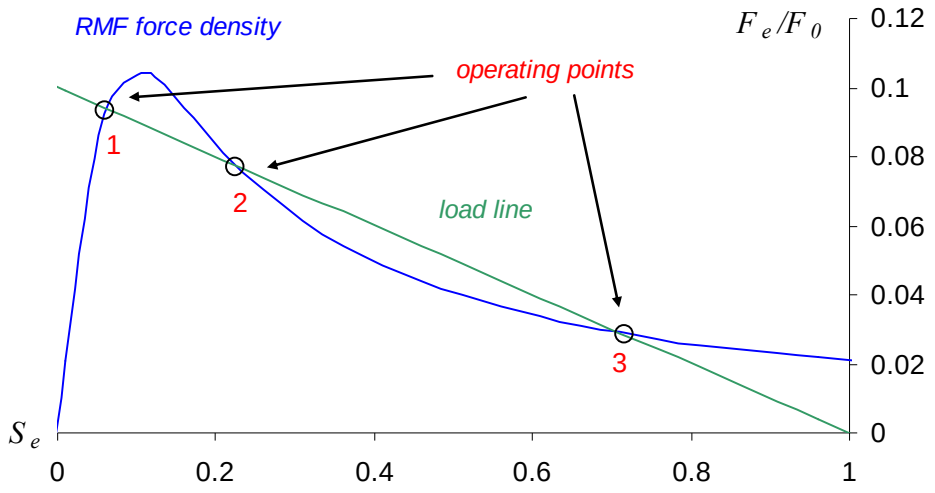

Figure 3.4. Electron fluid operating points ($\xi = 0.1$ and $\zeta_e = 0.65$).

3.1.3 The effect of ζ_e and ξ on operating points

The peak of the RMF force density on the electron fluid occurs at

$$S_e = \frac{\xi}{\sqrt{1+\left(\frac{m_e}{m_i}\frac{1}{S_i}\xi\right)^2}} \cong \xi \tag{3.9}$$

Hence the operating point where the electron fluid rotates almost synchronously with the (-) RMF is one with $S_e < \xi$.

If we assume

$$S_e >> \frac{m_e}{m_i}|S_i|, \tag{3.10}$$

the RMF force density has peak value

$$F_e(peak) \cong \frac{n m_e \omega^2 r \zeta_e^{\,2}}{4}. \tag{3.11}$$

The width of the RMF force density curve can be described by the width at half-maximum value

$$\Delta S_e = 2\sqrt{3}\xi. \tag{3.12}$$

The slip at which the RMF force density has peak value and the range of slip values over which the RMF has a significant effect is determined by the parameter ξ. The peak value of the RMF force density is determined by the parameter ζ_e. Hence these two dimensionless parameters

$$\zeta_e = \frac{e|B_r|}{m_e \omega} \qquad \xi = \frac{\nu_{ei}}{\omega}, \tag{3.13}$$

determine the number of operating points and their location, for a given value of S_i. The parameter ξ is a measure of the *collisionality* of the plasma. The parameter ζ_e is determined by the magnitude of the external RMF.

The effect of the value of ξ is shown by the set of RMF force density curves in Figure 3.5 where ζ_e is held constant and the ion fluid is stationary ($\zeta_e = 0.5$ and $S_i = 1$ for all curves). As ξ increases, the peak of the RMF force density occurs at larger values of S_e, and the force density is significant over a larger range of values of S_e (as demonstrated in equations (3.9) and (3.12) respectively).

The effect of the value of ζ_e is shown by the set of RMF force density curves in Figure 3.6 where ξ is held constant and the ion fluid is stationary ($\xi = 0.05$ and $S_i = 1$ for all curves). As ζ_e increases the RMF force increases. For low values of ζ_e there is no operating point with $S_e < \xi$ since collisions dominate in this region. As ζ_e is increased, there are 3 operating points and hence 2 stable steady states, one with $S_e < \xi$ and one with $S_e \cong 1$. The steady state obtained is determined by the initial conditions. For large values of ζ_e, there is only one operating point corresponding to $S_e < \xi$ irrespective of initial conditions.

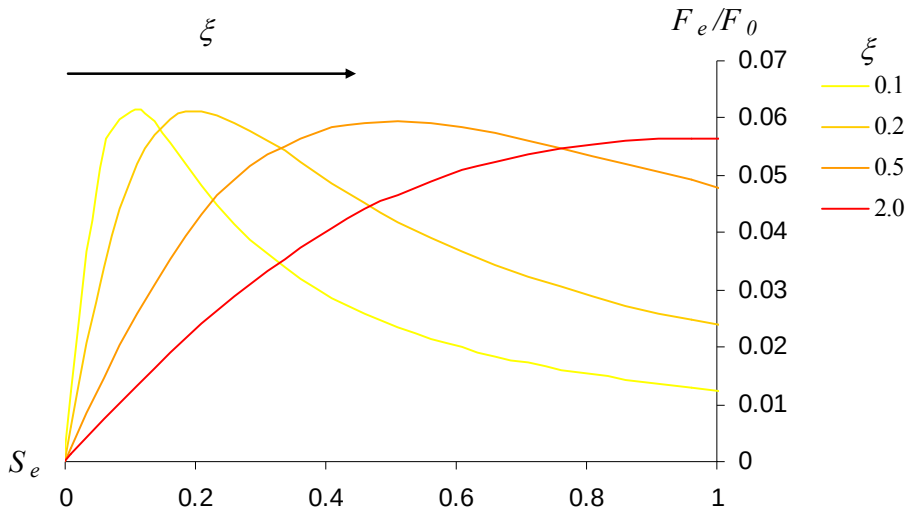

Figure 3.5. Effect of ξ on RMF force density ($\zeta_e = 0.5$ and $S_i = 1$ for all curves).

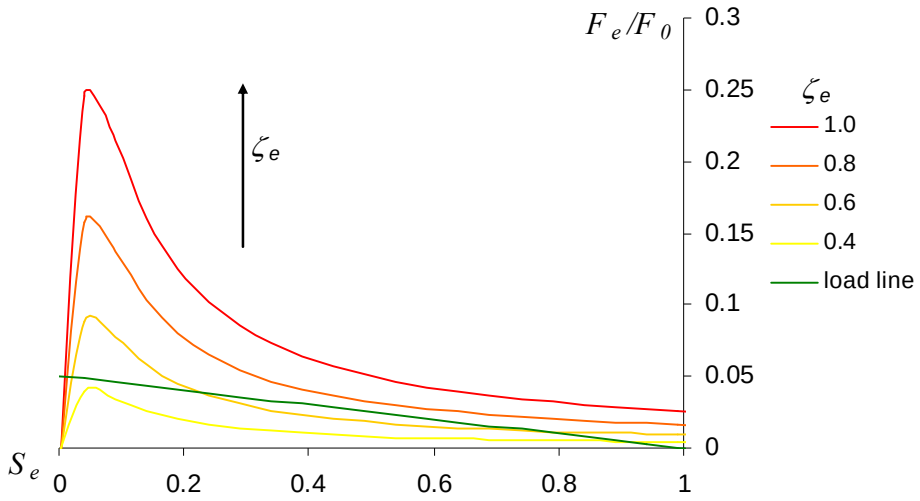

Figure 3.6. Effect of ζ_e on RMF force density (ξ = 0.05 and S_i = 1 for all curves).

The existence of an operating point with the electron fluid rotating almost synchronously with the RMF (i.e. $S_e < \xi$) is hence dependant on the relative magnitude of the applied RMF and the opposing force density due to collisions with the ion fluid.

A requirement for the existence of a $S_e < |\xi|$ operating point is that the peak force density exerted by the RMF exceeds the force density due to collisions. For a single RMF and stationary ion fluid (S_i = 1), the force due to collisions with the ion fluid has an upper bound

$$F_{coll} < nm_e\omega r\nu_{ei}, \tag{3.14}$$

and hence we require

$$\frac{nm_e\omega^2 r\zeta_e^{\,2}}{4} > nm_e\omega r\nu_{ei}, \tag{3.15}$$

providing a condition on the parameter ζ_e for the existence of this operating point.

$$\zeta_e^{\,2} > 4\xi. \tag{3.16}$$

This relates the electron cyclotron frequency to the collision frequency and RMF frequency

$$\omega_{ce}{}^2 > 4\nu_{ei}\omega\,. \tag{3.17}$$

Hence the magnitude of the RMF must exceed a minimum value to provide a steady state corresponding to almost synchronous rotation of the electron fluid with the applied RMF, as demonstrated in Figure 3.6.

In earlier RMF current drive literature (Blevin & Thoneman, 1962), it was assumed that the conditions required for the electron fluid to be entrained by the RMF,

$$\omega_{ce} >> \nu_{ei}\,, \tag{3.18}$$

and

$$\omega_{ce} >> \omega\,. \tag{3.19}$$

Equation (3.17) is a less stringent condition on these parameters for RMF current drive. The value of ω_{ce} in equation (3.17) is to be calculated from the local value of B_r, not the external value.

Figures 3.2-3.4 presented earlier show the requirement of this condition. The curves shown in Figure 3.2 ($\xi = 0.2$, $\zeta_e = 1.0$) and Figure 3.4 ($\xi = 0.1$, $\zeta_e = 0.65$) satisfy the condition in equation (3.16), and hence the $S_e < |\xi|$ operating point exists. The curve shown in Figure 3.3 ($\xi = 0.2$, $\zeta_e = 0.5$) does not satisfy the condition in equation (3.16), and hence there is no $S_e < \xi$ operating point.

3.1.4 Approximate solution for $S_e < \xi$ operating point

We now derive an approximate expression for the electron fluid operating point with $S_e < \xi$. The collision force is again approximated by equation (3.8) which provides a second order equation for S_e

$$S_e^{\,2} - \frac{\zeta_e^{\,2}}{2} S_e + \xi^2 = 0 . \tag{3.20}$$

The required small slip solution is then

$$S_e = \frac{\zeta_e^{\,2}}{4}\left(1 - \sqrt{1 - \left(\frac{4\xi}{\zeta_e^{\,2}}\right)^2}\right), \tag{3.21}$$

corresponding to the stable $S_e < \xi$ operating point. A comparison of the approximate operating points in the region of the peak of the RMF force, and the actual operating points is shown in Figure 3.7 (for the case $\xi = 0.1$ and $\zeta_e = 0.65$). The figure demonstrates that equation (3.21) is an upper bound for the steady state value of the slip, since the collision force is slightly overestimated in the region of the operating point. The existence of this small slip solution requires that equation (3.21) be real, again giving the condition in equation (3.16).

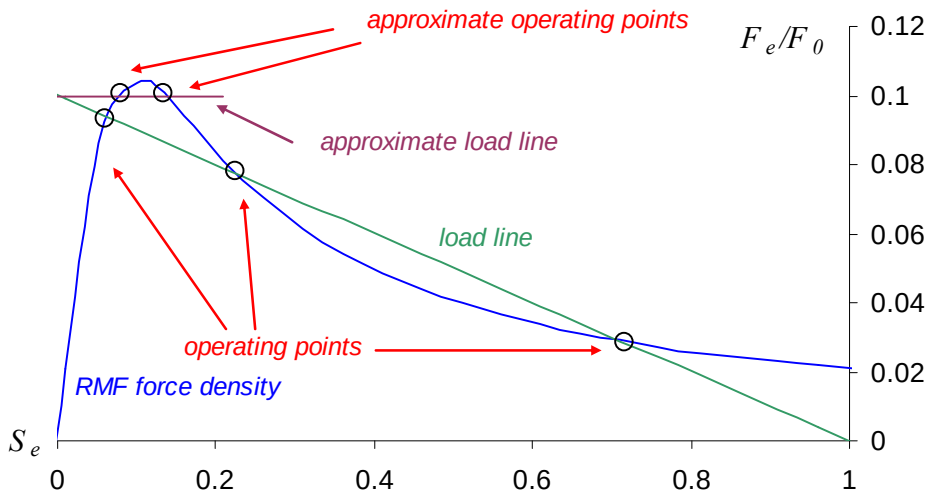

Figure 3.7. Approximate electron fluid small slip operating points ($\xi = 0.1$ and $\zeta_e = 0.65$).

The case where the RMF force is much larger than the collision force, $\zeta_e^2 >> 4\xi$, provides a binomial approximation for the $S_e < \xi$ operating point

$$S_e \cong 2\left(\frac{\xi}{\zeta_e}\right)^2 . \tag{3.22}$$

This expression shows that as the RMF magnitude is increased, the electron fluid rotates with smaller slip (is more tightly bound to the RMF), and as ξ increases the electron fluid rotates with larger slip (since the collision force density is larger). This trend holds even when the condition $\zeta_e^2 >> 4\xi$ is not satisfied as the following figures demonstrates. Figure 3.8 shows the operating points for two values of ξ when ζ_e is held constant ($\zeta_e = 0.5$) As ξ is increased, the operating point occurs at a larger value of S_e.

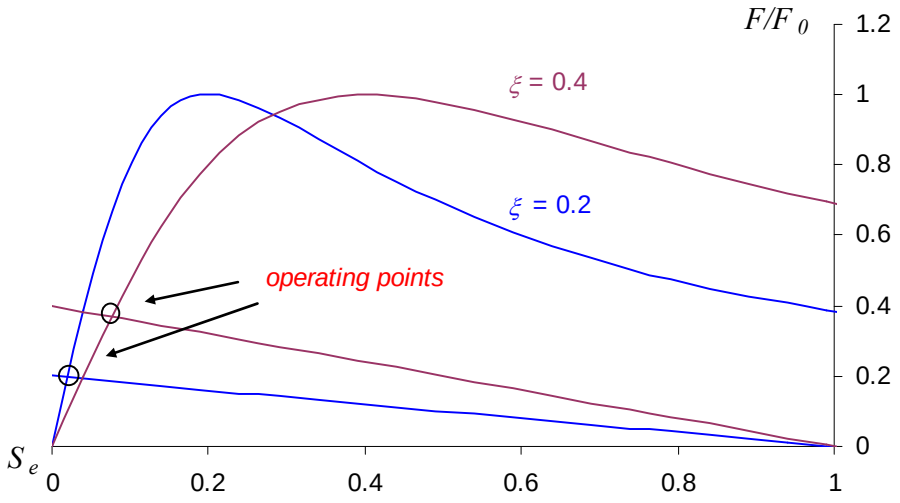

Figure 3.8. Electron fluid operating points for two values of ξ ($\zeta_e = 0.5$).

Figure 3.9 shows the operating points for two values of ζ_e when ξ is held constant ($\xi = 0.2$) As ζ_e is increased, the operating point occurs at a smaller value of S_e.

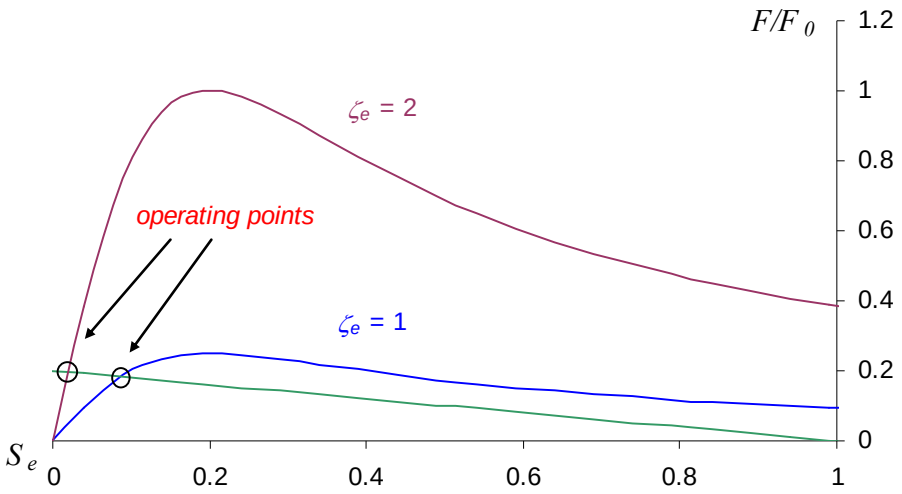

Figure 3.9. Electron fluid operating points for two values of ζ_e ($\xi = 0.2$).

Again the figures shown in this section apply only to a layer of the plasma, and hence we are considering the local operating points from the local values of $\xi(r)$ and $\zeta_e(r)$.

3.2 Electron Fluid Steady States for 2 RMFs

3.2.1 Method of determining operating points for 2 RMFs

We now consider the operating points for the electron fluid for the case required for the Clemente scheme, where there are two counter-rotating RMFs. The method of determining operating points described for a single applied RMF can be extended for two applied RMFs. The operating points are the intersection of the net force density $F_e^- + F_e^+$ and the collisional load line. Since for the Clemente scheme, the RMFs are counter-rotating, the two RMF forces densities are opposite in sign. We take $\omega^- > 0$ and $\omega^+ < 0$ and hence ξ^- will be positive and ξ^+will be negative.

The steady states under the application of two external RMFs are thus solutions to the equation

$$F_e^{+} + F_e^{-} = -F_{coll} = -nm_e\nu_{ei}\omega^{-}r\left(S_e^{-} - S_i^{-}\right). \tag{3.23}$$

For the Clemente scheme, the ions are not stationary but rather will be rotating with a frequency close to the (+) RMF ($S_i^{+} \cong 0$), and hence

$$S_i^{-} \cong \left(1 - \frac{\omega^{+}}{\omega^{-}}\right). \tag{3.24}$$

In determining the operating points in section 3.1.4, it was assumed that the ions were stationary. When we allow the ions to be counter-rotating, this increases the collision force on the electron fluid, and will increase the electron slip at the operating point.

If we consider the steady states for the electron fluid when the (-) RMF is applied, the second order equation for the electron slip in equation (3.20) is now given by

$$S_e^{2} - \frac{\zeta_e^{2}}{2}S_e + \left(1 - \frac{\omega^{+}}{\omega^{-}}\right)\xi^{2} = 0, \tag{3.25}$$

which has small slip solution

$$S_e^{-} \cong \frac{\zeta_e^{-}}{4\left(1 - \frac{\omega^{+}}{\omega^{-}}\right)}\left(1 - \sqrt{1 - \left(4\left(1 - \frac{\omega^{+}}{\omega^{-}}\right)\frac{\xi^{-}}{\zeta_e^{-}}\right)^{2}}\right). \tag{3.26}$$

For $\zeta_e^{2} >> 2\left(1 - \omega^{+}/\omega^{-}\right)\xi$, we have the expression

$$S_e^{-} \cong 2\left(1 - \frac{\omega^{+}}{\omega^{-}}\right)\left(\frac{\xi^{-}}{\zeta_e^{-}}\right)^{2}. \tag{3.27}$$

For the illustrative figures that follow we consider the case where the (+) RMF is equal in magnitude to the (-) RMF, and is counter-rotating with a frequency of equal magnitude. So we have $\omega^{+} = -\omega^{-}$, $|B_r^{+}| = |B_r^{-}|$, and it is assumed $S_i^{-} \cong 2$ in determining the load line.

Figure 3.10 shows the operating points for a layer of the electron fluid with the ion fluid counter-rotating when the (-) RMF is applied. For the case shown here ($\xi^- = 0.2$, $\zeta_e^- = 2.0$, $S_i^- = 2$), there is only one operating point corresponding to almost synchronous rotation with the (-) RMF.

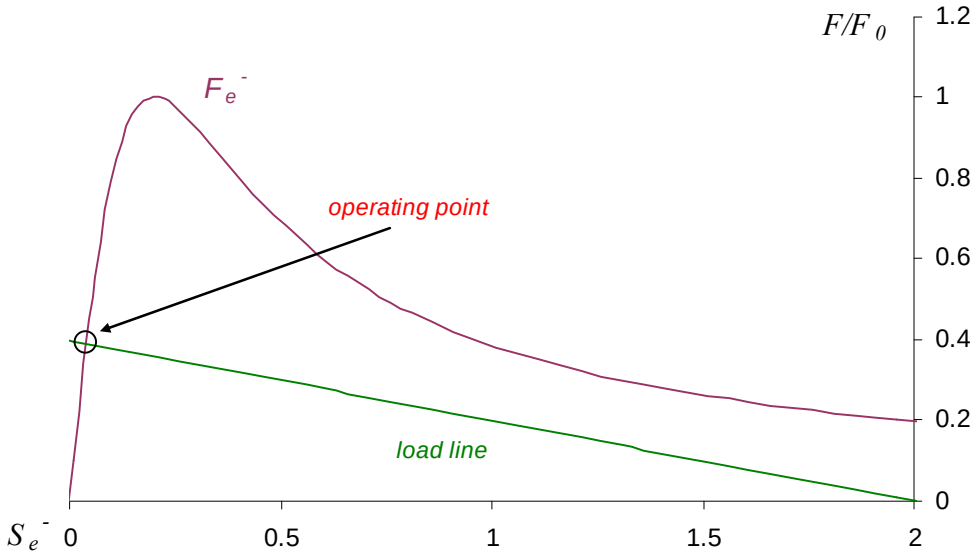

Figure 3.10. Operating points for the electron fluid for the (-) RMF ($\xi^- = 0.2$, $\zeta_e^- = 2.0$, $S_i^- = 2$).

Figure 3.11 shows the operating points for the electron fluid when two counter-rotating RMFs are applied (for the case $\xi^- = |\xi^+| = 0.2$, $\zeta_e^- = \zeta_e^+ = 2.0$, $S_i^- = 2$). There are now three operating points one of which (operating point 2) does not correspond to a stable steady state. The two stable steady states are almost synchronous rotation with either the (-) RMF (operating point 1) or the (+) RMF (operating point 3). The operating point obtained is dependant on the initial conditions. For the Clemente scheme the (-) RMF is applied first, so that the initial condition before the (+) RMF is applied is that the electron fluid is at the $S_e^- < \xi^-$. operating point (operating point 1). Hence the operating point obtained for the example curves shown will be almost synchronous rotation of the electron fluid with the (-) RMF. For the case shown, the operating point for the electron fluid is not significantly affected by the application of the (+) RMF.

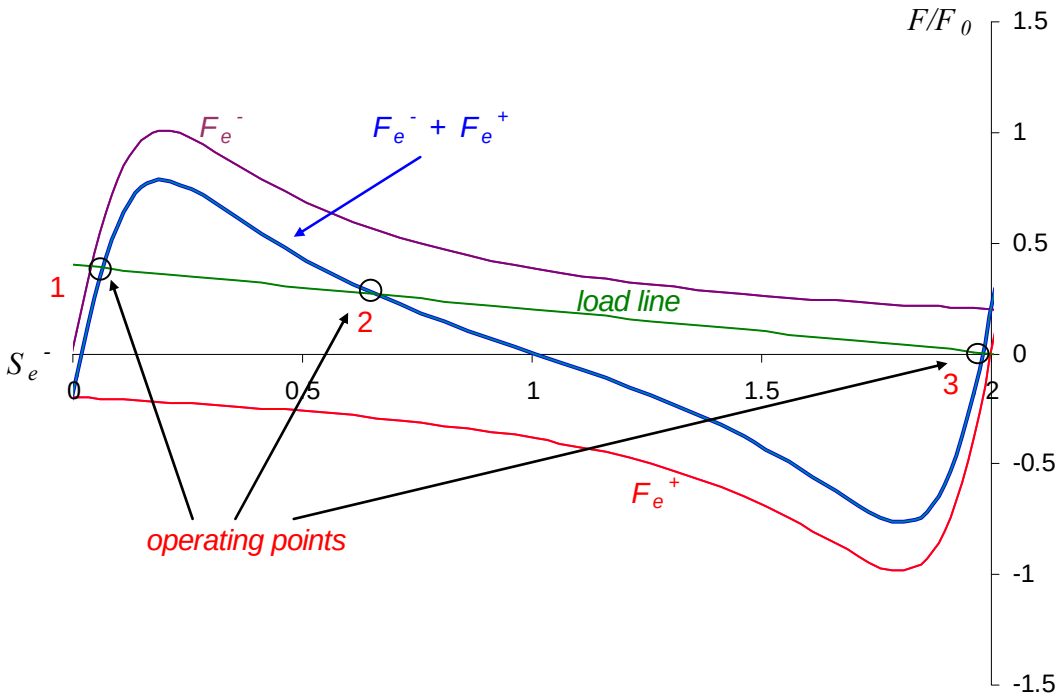

Figure 3.11. Operating points for the electron fluid, for two applied RMFs ($\xi^- = |\xi^+| = 0.2$, $\zeta_e^- = |\zeta_e^+| = 2.0$, $S_i^- = 2$).

3.2.2 A condition for the existence of $S_e^- < \xi^-$ operating point.

The existence of an operating point with $S_e^- < \xi^-$ requires that the peak value of the net force due to the RMFs exceeds the force due to collisions. The collision force is approximated by assuming the electron fluid rotates synchronously with the (-) RMF and the ion fluid rotates synchronously with the (+) RMF.

$$F_{coll} = nm_e\nu_{ei}r\left(\omega^- - \omega^+\right) \tag{3.28}$$

If we assume that the force density exerted by the (+) RMF in the region of the operating point for the electron fluid is negligible ($|F_e^-| >> |F_e^+|$ in this region) the condition is

$$\frac{nm_e\omega^{-2}r\left(\zeta_e^{-}\right)^2}{4} > nm_e r\nu_{ei}\left(\omega^{-}-\omega^{+}\right). \tag{3.29}$$

The condition for ζ_e^- required for the existence of a $S_e^- < \xi^-$ operating point is then given by

$$\left(\zeta_e^{-}\right)^2 > 4\left(1-\frac{\omega^{+}}{\omega^{-}}\right)\xi^{-}. \tag{3.30}$$

This again relates the electron cyclotron frequency with respect to the (-) RMF to the collision frequency and RMF frequency

$$\left(\omega_{ce}^{-}\right)^2 > 4\nu_{ei}\left(\omega^{-}-\omega^{+}\right). \tag{3.31}$$

If this expression is compared to equation (3.17), the effect of ion counter-rotation makes the restriction on the electron cyclotron frequency more restrictive, since the force density due to collisions will be greater.

For the case where the RMF frequencies are equal in magnitude $\omega^+ = -\omega^-$, the condition on ζ_e^- is

$$\left(\zeta_e^{-}\right)^2 > 8\xi^{-}, \tag{3.32}$$

and the condition on the electron cyclotron frequency for this case is

$$\left(\omega_{ce}^{-}\right)^2 > 8\nu_{ei}\omega^{-}. \tag{3.33}$$

This condition for the existence of an operating point requires a critical value of the field strength for the (-) RMF, which is dependant on the collision frequency. For more collisional plasmas, the minimum RMF magnitude required for the existence of the $S_e^- < \xi^-$ operating point must be greater.

3.2.3 Effect of (+) RMF on electron fluid operating points

For the Clemente scenario to be viable, it is imperative that the application of the (+) RMF does not stop the electron fluid from rotating synchronously with the (–) RMF. The net force on the electron fluid under the application of two counter-rotating fields is now examined. We consider firstly the case where the angular frequencies of (+) and (-) fields are equal in magnitude, but opposite in sign, $\omega^+ = -\omega^-$. For this situation, the plasma current is maintained, provided that the condition $|\xi^+| < 1$ is satisfied. In section 3.6 we show that when the (+) field has a smaller frequency than the (-) field ($|\omega^+| < \omega^-$) the condition for maintaining the plasma current is less restrictive.

Figure 3.10 demonstrated the operating point for the (-) RMF for the case $\xi^- = 0.2$. For the load line shown, there is only one possible operating point, which is almost synchronous rotation with the (-) RMF. This steady state will be accessible irrespective of the initial conditions for the electron fluid. In Figure 3.11, the operating points are shown when the (+) RMF is also applied. This figure shows the case where the RMFs are equal in magnitude ($|B_r^-| = |B_r^+|$) and have frequencies of equal magnitude ($\omega^+ = -\omega^-$). There are now 3 possible operating points (one of which (2) is unstable). The steady state is determined by the initial conditions. Since the electron fluid was initially rotating almost synchronously with the (-) RMF, the operating point accessed will be (1) which corresponds to the Clemente steady state for the electron fluid. The application of the (+) RMF increases the slip of the electron fluid operating point slightly, but does not stop the electron fluid from rotating almost synchronously with the (-) RMF with small slip, since F_e^+ is much smaller than F_e^- in this region. This is the situation in general for the case $|\xi^+| < 1$ when $\omega^+ = -\omega^-$, and $|B_r^-| = |B_r^+|$.

Figure 3.12 shows the operating point for the (-) RMF for the case $\xi^- = 2.0$ and $\zeta_e^- = 7.0$. For the load line shown, there is again only one possible operating point, which is almost synchronous rotation with the (-) RMF. In Figure 3.13, the operating points are shown when the (+) RMF is also applied (for the case $\xi^- = |\xi^+| = 2.0$, $\zeta_e^- = \zeta_e^+ = 7.0$, $S_i^- = 2$). This figure again demonstrates the case where the RMFs are equal in magnitude ($|B_r^-| = |B_r^+|$) and have frequencies of equal magnitude ($\omega^+ = -\omega^-$). There is now only one

possible operating point with large slip, which does not correspond to the Clemente steady state. The application of the (+) RMF stops the electron fluid from rotating almost synchronously with the (-) RMF with small slip since F_e^+ is larger than F_e^- in this region. This is the situation in general for the case $|\xi^+| > 1$.

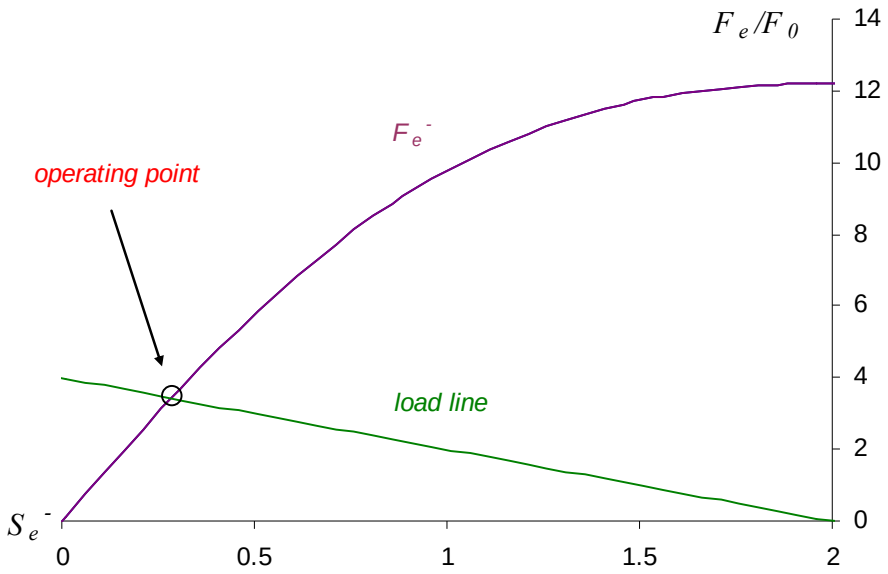

Figure 3.12. Operating points for the electron fluid under the (-) RMF with $\xi^- = 2.0$ ($\zeta_e^- = 7.0$, $S_i^- = 2$).

It is thus seen that the Clemente scheme cannot be implemented successfully (following the scenario described above) unless the criterion $|\xi^+| < 1$ is satisfied for the case $\omega^+ = -\omega^-$. This criterion does not apply to the case where the frequency of the (+) RMF significantly differs in magnitude from the (-) RMF.

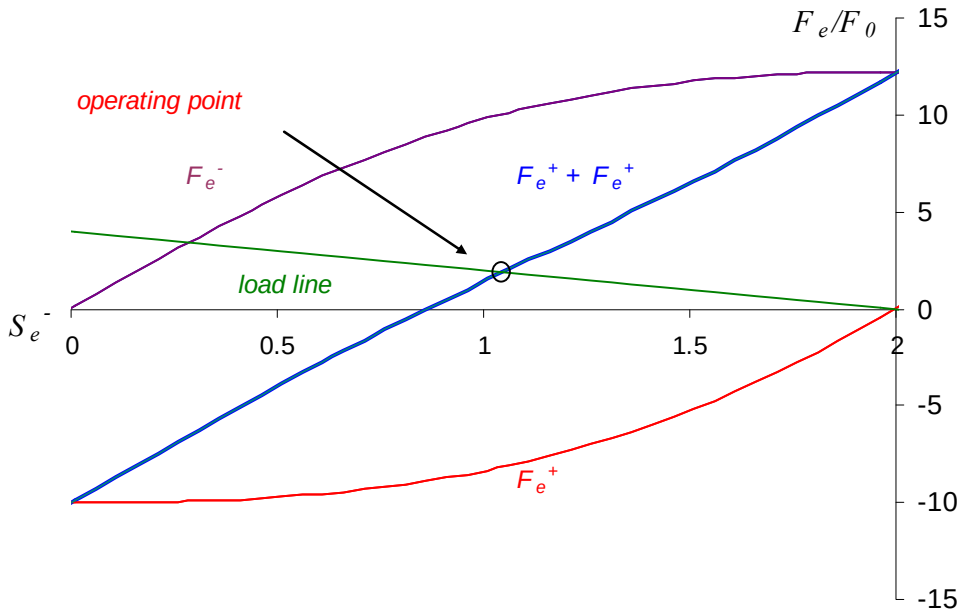

Figure 3.13. Operating points for the electron fluid under 2 RMF with $|\xi^+| = \xi^- = 2.0$ ($\zeta_e^- = |\zeta_e^+| = 2.0$, $S_i^- = 2$).

A condition required for the electron fluid to remain entrained by the (-) RMF when the (+) RMF is applied is that the peak value of F_e^- is greater in magnitude than F_e^+ at this point.

$$F_e^-(peak) > \left|F_e^+\right| \tag{3.34}$$

The peak value of the force on the electron fluid due to the (-) RMF is given by

$$F_e^-(peak) \cong \frac{nm_e\omega^{-2}r\left(\zeta_e^-\right)^2}{4}. \tag{3.35}$$

The force due to the (+) RMF in the region of the $S_e^- < \xi^-$ operating point is given by the approximate expression,

$$F_e^{+} \cong \frac{nm_e\left(\omega^{+}\right)^2 r\left(\zeta_e^{+}\right)^2 \xi^{+}}{2S_e^{+}}, \tag{3.36}$$

which is an upper bound on the for force in this region. If we assume an approximate expression for S_e^{+},

$$S_e^{+} \cong \left(1-\frac{\omega^{-}}{\omega^{+}}\right) \tag{3.37}$$

The requirement is given by;

$$\frac{nm_e\left(\omega^{-}\right)^2 r\left(\zeta_e^{-}\right)^2}{4} > \frac{nm_e\left(\omega^{+}\right)^2 r\left(\zeta_e^{+}\right)^2 \left|\xi^{+}\right|}{2\left(1-\frac{\omega^{-}}{\omega^{+}}\right)}, \tag{3.38}$$

providing a condition on ξ^{+}

$$\left|\xi^{+}\right| < \frac{1}{2}\left(\frac{B_r^{-}}{B_r^{+}}\right)^2\left(1-\frac{\omega^{-}}{\omega^{+}}\right). \tag{3.39}$$

This condition can be expressed as a requirement on the collision frequency

$$\nu_{ei} < \frac{1}{2}\left(\frac{B_r^{-}}{B_r^{+}}\right)^2\left(\omega^{-}-\omega^{+}\right). \tag{3.40}$$

If $\omega^{+} = -\omega^{-}$, and $|B_r^{-}| = |B_r^{+}|$ then the condition reduces to

$$\left|\xi^{+}\right| < 1, \tag{3.41}$$

or

$$\nu_{ei} < \omega^{-}. \tag{3.42}$$

The Clemente scheme is therefore applicable to *collisionless* plasmas, where the collision frequency is smaller that the difference between the frequencies of the applied RMFs. It should be emphasised that this condition is necessary but not sufficient for the

existence of a steady state corresponding to synchronous rotation of the electron fluid with the (-) RMF.

This requirement in equation (3.39) for the existence of a steady state with $S_e^- < \xi^-$ is more stringent when we require that the peak of the force curve due to the (-) RMF be greater in magnitude than the sum of the force due to collisions and the force exerted on the electron fluid by the (+) RMF. The requirement is given by

$$F_e^-(peak) > |F_{coll}| + |F_e^+|, \tag{3.43}$$

or

$$\frac{nm_e(\omega^-)^2 r(\zeta_e^-)^2}{4} > nm_e \nu_{ei} r(\omega^- - \omega^+) + \frac{nm_e(\omega^+)^2 r(\zeta_e^+)^2 |\xi^+|}{2\left(1 - \frac{\omega^-}{\omega^+}\right)}. \tag{3.44}$$

This places a condition on the electron cyclotron frequency with respect to the (-) RMF

$$\zeta_e^{-2} > \frac{4\xi^-\left(1 - \frac{\omega^+}{\omega^-}\right)}{1 - \frac{2|\xi^+|}{\left(1 - \frac{\omega^-}{\omega^+}\right)}\left(\frac{B_r^+}{B_r^-}\right)^2}. \tag{3.45}$$

The requirement that the right hand side of equation (3.45) be positive again shows the condition on the value of ξ^+ for the existence of the $S_e^- < \xi^-$ operating point.

$$|\xi^+| < \frac{1}{2}\left(\frac{B_r^-}{B_r^+}\right)^2\left(1 - \frac{\omega^-}{\omega^+}\right) \tag{3.46}$$

For the case $\omega^+ = -\omega^-$, and $|B_r^-| = |B_r^+|$

$$\left|\xi^{+}\right| < 1, \tag{3.47}$$

and we see that the critical field strength for the (-) RMF required for the existence of a synchronous rotation operating point is greater when the (+) field is applied. This places a condition on the electron cyclotron frequency with respect to the (-) RMF

$$\left(\omega_{ce}{}^{-}\right)^2 > \frac{4\nu_{ei}\left(\omega^{-} - \omega^{+}\right)}{1 - \dfrac{2\left|\xi^{+}\right|}{\left(1 - \dfrac{\omega^{-}}{\omega^{+}}\right)}\left(\dfrac{B_r{}^{+}}{B_r{}^{-}}\right)^2}, \tag{3.48}$$

for the case $\omega^{+} = -\omega^{-}$, and $\left|B_r{}^{-}\right| = \left|B_r{}^{+}\right|$

$$\left(\omega_{ce}{}^{-}\right)^2 > \frac{8\nu_{ei}\omega^{-}}{1 - \left|\xi^{+}\right|}, \tag{3.49}$$

or

$$\left(\zeta_e{}^{-}\right)^2 > \frac{8\xi^{-}}{1 - \left|\xi^{+}\right|}. \tag{3.50}$$

The condition required for the existence of the $S_e{}^{-} < \xi^{-}$ operating point for the electron fluid in equation (3.16), and the more general condition of equation (3.30) are made more stringent by the application of the (+) RMF.

3.2.4 Approximate solution for the $S_e{}^{-} < \xi^{-}$ operating point for 2 RMFs

The operating points are solutions to the equation

$$F_e{}^{-} + F_e{}^{+} = -F_{coll}. \tag{3.51}$$

The operating point of interest is one where the electron fluid rotates almost synchronously with the (-) RMF. Hence we may approximate the collision force by the expression

$$F_{coll} = nm_e \nu_{ei} \left(\omega^+ - \omega^-\right) r \,. \tag{3.52}$$

Equation (3.51) is then given by

$$\frac{nm_e \left(\omega^-\right)^2 r \left(\zeta_e{}^-\right)^2}{2} \frac{S_e{}^- \xi^-}{\left(S_e{}^-\right)^2 + \left(\xi^-\right)^2} + \frac{nm_e \left(\omega^+\right)^2 r \left(\zeta_e{}^+\right)^2 \xi^+}{2\left(1 - \dfrac{\omega^-}{\omega^+}\right)} = nm_e \nu_{ei} \left(\omega^- - \omega^+\right) r \,, \tag{3.53}$$

or in terms of dimensionless parameters only

$$\frac{\left(\zeta_e{}^-\right)^2}{2} \left[\frac{S_e{}^-}{\left(S_e{}^-\right)^2 + \left(\xi^-\right)^2} - \left(\frac{\omega^-}{\omega^- - \omega^+} \right) \left| \frac{B_r{}^+}{B_r{}^-} \right|^2 \right] = \left(1 - \frac{\omega^+}{\omega^-}\right). \tag{3.54}$$

This provides a second order equation for $S_e{}^-$

$$\left(S_e{}^-\right)^2 - \frac{S_e{}^-}{\dfrac{2}{\left(\zeta_e{}^-\right)^2}\left(1 - \dfrac{\omega^+}{\omega^-}\right) + \left(\dfrac{\omega^-}{\omega^- - \omega^+} \right) \left| \dfrac{B_r{}^+}{B_r{}^-} \right|^2} + \left(\xi^-\right)^2 = 0 \,, \tag{3.55}$$

which has small slip solution

$$S_e{}^- = \frac{1 - \sqrt{1 - \left[2\xi^- \left(\dfrac{2}{\left(\zeta_e{}^-\right)^2}\left(1 - \dfrac{\omega^+}{\omega^-}\right) + \dfrac{\omega^-}{\omega^- - \omega^+} \left| \dfrac{B_r{}^+}{B_r{}^-} \right|^2 \right) \right]^2}}{\dfrac{4}{\left(\zeta_e{}^-\right)^2}\left(1 - \dfrac{\omega^+}{\omega^-}\right) + \dfrac{2\omega^-}{\omega^- - \omega^+} \left| \dfrac{B_r{}^+}{B_r{}^-} \right|^2} \,. \tag{3.56}$$

The existence of this solution (equation (3.56) is real) requires the condition that the peak of the force density due to the (-) RMF be larger than the sum of the force density due to collisions and the force density applied by the (+) RMF on the electron fluid in this region. This condition is described in terms of the dimensionless parameters

$$\zeta_e^{-2} > \frac{4\xi^-\left(1-\frac{\omega^+}{\omega^-}\right)}{1-2\xi^+\frac{\omega^+}{\omega^- - \omega^+}\left|\frac{B_r^+}{B_r^-}\right|^2}, \tag{3.57}$$

again showing that the critical value of ζ_e^- required for the existence of the small slip operating point (in equation (3.30) for a single RMF) is increased by the application of the (+) RMF.

The case where the (-) RMF force density is much larger than the effect of the collision force and the effect of (+) RMF in this region

$$\zeta_e^{-2} >> \frac{4\xi^-\left(1-\frac{\omega^+}{\omega^-}\right)}{1-2\xi^+\frac{\omega^+}{\omega^- - \omega^+}\left|\frac{B_r^+}{B_r^-}\right|^2}, \tag{3.58}$$

provides a binomial approximation for the $S_e^- < \xi^-$ operating point

$$S_e^- \cong 2\left(1-\frac{\omega^+}{\omega^-}\right)\left(\frac{\xi^-}{\zeta_e^-}\right)^2 + \left(\xi^-\right)^2\frac{\omega^-}{\omega^- - \omega^+}\left|\frac{B_r^+}{B_r^-}\right|^2. \tag{3.59}$$

The slip of the $S_e^- < \xi^-$ operating point for the electron fluid is increased by the application of the (+) RMF. As was demonstrated in Figure 3.7, the approximations used show that this is an upper bound for the steady state value of the slip.

Equation (3.59) can be compared to the relation derived by Hugrass (2000),

$$S_e^- \cong 2\left(1-\frac{\omega^+}{\omega^-}\right)\left(\frac{\xi^-}{\zeta_e^-}\right)^2, \tag{3.60}$$

where it was assumed that

$$\left|\frac{F_e^-}{F_e^+}\right| >> 1 \qquad \text{and} \qquad S_e^- << 1.$$

The first of these conditions is not true in general for the Clemente scheme where the frequencies of the (-) and (+) RMFs are equal in magnitude. The (+) RMF may exert a significant force on the electron fluid over a wide range of slips. The range of slips over which the (+) RMF exerts a significant force is determined by the value of ξ^+. For small values of ξ^+, the force due to the (+) RMF on the electron fluid is highly peaked, the magnitude being much smaller than the peak value in the region of the $S_e^- < \xi^-$ operating point. Hence the (+) RMF has negligible effect on the operating point if either the (+) RMF has a much smaller magnitude ($\left|B_r^-\right| >> \left|B_r^+\right|$), or if the force density curve due to the (+) RMF with slip is highly peaked ($\left|\xi^+\right| << 1$), and hence the magnitude of the force due to the (+) RMF in the region of the $S_e^- < \xi^-$ operating point is significantly less than the peak value.

3.2.5 Electron fluid operating points for the case $\omega^- > |\omega^+|$.

In previous sections, it has been assumed that the RMFs are equal in magnitude ($\left|B_r^-\right| = \left|B_r^+\right|$) and have frequencies of equal magnitude ($\omega^+ = -\omega^-$). We now consider the case where the frequencies of the applied RMFs may have different magnitudes $\omega^- > |\omega^+|$. In this case the curves are not symmetrical and hence may allow a small slip operating point for the electron fluid when $|\xi^+| > 1$. The full condition on ξ^+

$$\left|\xi^+\right| < \frac{1}{2}\left|\frac{B_r^-}{B_r^+}\right|^2\left(1-\frac{\omega^-}{\omega^+}\right), \tag{3.61}$$

shows that the requirement on ξ^+ is less stringent when the magnitude of frequency of the (+) RMF is less than that of the (-) RMF. The condition is also less stringent if $\left|B_r^-\right| > \left|B_r^+\right|$ since in this case the net force is dominated by F_e^-.

Figure 3.14 and Figure 3.15 demonstrate the same parameters presented in Figure 3.11 ($\xi^- = 0.2$, $\zeta_e^- = 2.0$), and in Figure 3.13 ($\xi^- = 2.0$, $\zeta_e^- = 7.0$), respectively , but with $\omega^+ = -0.1\omega^-$. The operating point for the electron fluid is not changed significantly by the application of the (+) RMF for either case. Both situations allow a steady state where the electron fluid rotates synchronously with the (-) RMF after application of the (+) RMF. Hence allowing the majority of the current to be carried by the electrons may allow access to the Clemente steady states for plasmas where $\nu_{ei} > |\omega^+|$.

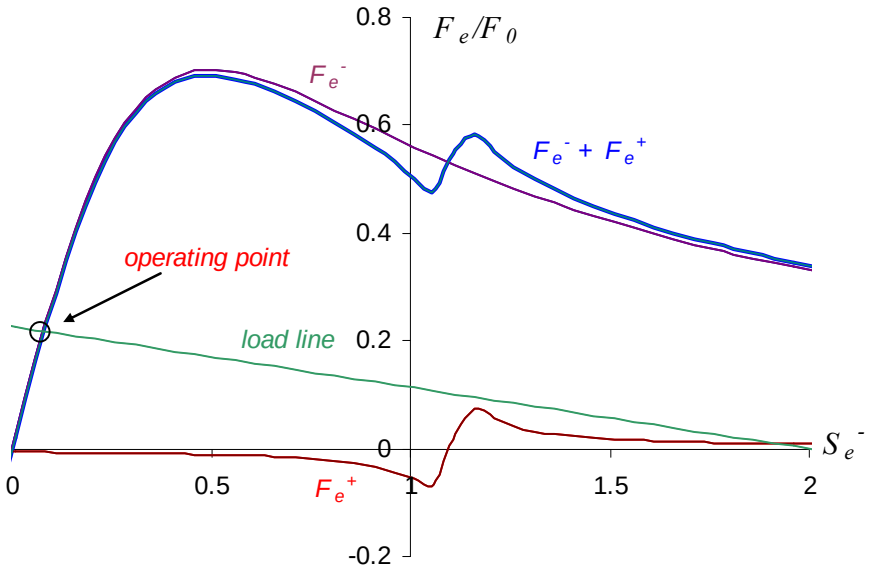

Figure 3.14. Operating points for the electron fluid under 2 RMFs where $\xi^- = 0.2$ and $\omega^+ = -0.1\omega^-$ ($|\xi^+| = 2$, $\zeta_e^- = 2.0$, $S_i^- = 2$).

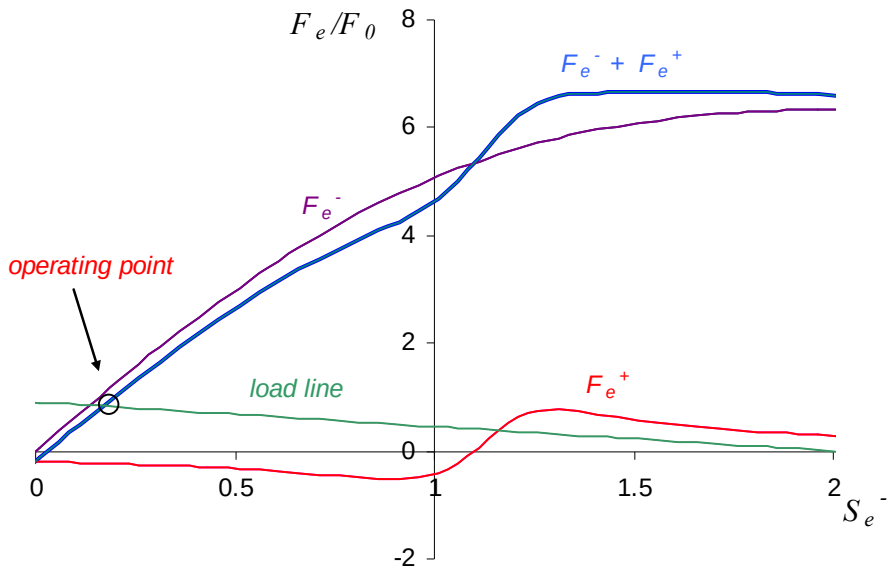

Figure 3.15. Operating points for the electron fluid under 2 RMF for $\xi^- = 2.0$, where $\omega^+ = -0.1\omega^-$ ($|\xi^+| = 20$, $\zeta_e^- = 7.0$, $S_i^- = 2$).

3.2.6 Condition for the existence of multiple operating points

In general, the steady states for the electron fluid are solutions to the cubic equation in S_e^-

$$\left(S_e^-\right)^3 - S_i^-\left(S_e^-\right)^2 + \left(\frac{\left(\zeta_e^-\right)^2}{2} + \left(\xi^-\right)^2\right) S_e^- - \left(\xi^-\right)^2 S_i^- = 0\,. \tag{3.62}$$

The determinant of the cubic equation with coefficients α_0, α_1, α_2, α_3 is given by

$$\Delta_3 = 4\alpha_1{}^3 - \alpha_1{}^2\alpha_2{}^2 4\alpha_0\alpha_2{}^3 - 18\alpha_0\alpha_1\alpha_2\alpha_3 + 27\alpha_0{}^2\alpha_3{}^2\,. \tag{3.63}$$

There are 3 real roots for the case $\Delta_3 < 0$. For conventional current drive the initial condition for the ion fluid is $S_i^- = 1$. Using the condition for the existence of a small slip operating point

$$\left(\zeta_e^{-}\right)^2 > 2\xi^{-} S_i^{-}, \tag{3.64}$$

leads to the requirement for three real roots

$$\xi^{-} < 0.135 \qquad (S_i^{-} = 1) \tag{3.65}$$

For the Clemente scheme with $\omega^{+} = -\omega^{-}$ case we have $S_i^{-} = 2$, the condition for the existence of a small slip operating point

$$\left(\zeta_e^{-}\right)^2 > 4\xi^{-} S_i^{-}, \tag{3.66}$$

leads to the requirement for three real roots

$$\xi^{-} < 0.394 \qquad (S_i^{-} = 2). \tag{3.67}$$

In general, the critical value of ξ^{-} increases with S_i^{-}, as shown in Figure 3.16.

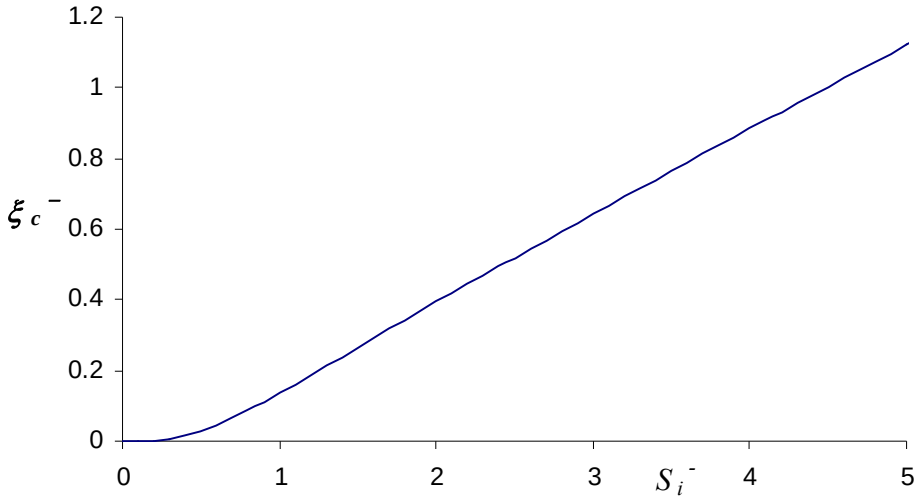

Figure 3.16. Variation of ξ_c^{-} with ion slip.

Hence the case of three operating points need only be considered for small values of ξ^{-}. If $\xi^{-} < \xi_c^{-}$, the steady state value of S_e^{-} will depend on the initial conditions. The number of operating points that exist will then be determined by the value of ζ_e^{-}. If ξ^{-} is sufficiently large ($\xi^{-} > \xi_c^{-}$), there is only one operating point, and hence the steady

state value of S_e^- will be independent of the initial conditions for the electron fluid. The number of operating points that exist will then be determined by the value of ζ_e^-.

3.3 Ion Fluid Steady States

3.3.1 Method of determining operating points for the ion fluid

The induction motor analogy and method of determining operating points for the electron fluid under a single RMF, is here applied to the case of the ion fluid under the action of two RMFs. The ion fluid is now analogous to the rotor, and the electron fluid is now analogous to the mechanical load. The operating points are determined by the intersection of the net force density imparted by the RMFs and a *load line* which is determined by the collisional force exerted by the interaction of the ion fluid with the electron fluid.

An operating point for the ion fluid may thus be found by the intersection of the curve representing the steady part of the net force density on the ion fluid due to the two applied RMFs, and a *load line* representing the collisional drag from interaction with the electron fluid. The operating points are thus the solutions to the equation

$$F_i^+ + F_i^- = -F_{coll} = nm_i\nu_{ie}\omega^+ r\left(S_i^+ - S_e^+\right) \tag{3.68}$$

Again the operating points are only applicable for a layer of the plasma fluid, and hence we consider the force densities at a layer of the plasma. Chapter 4 will extend these results to the entire plasma.

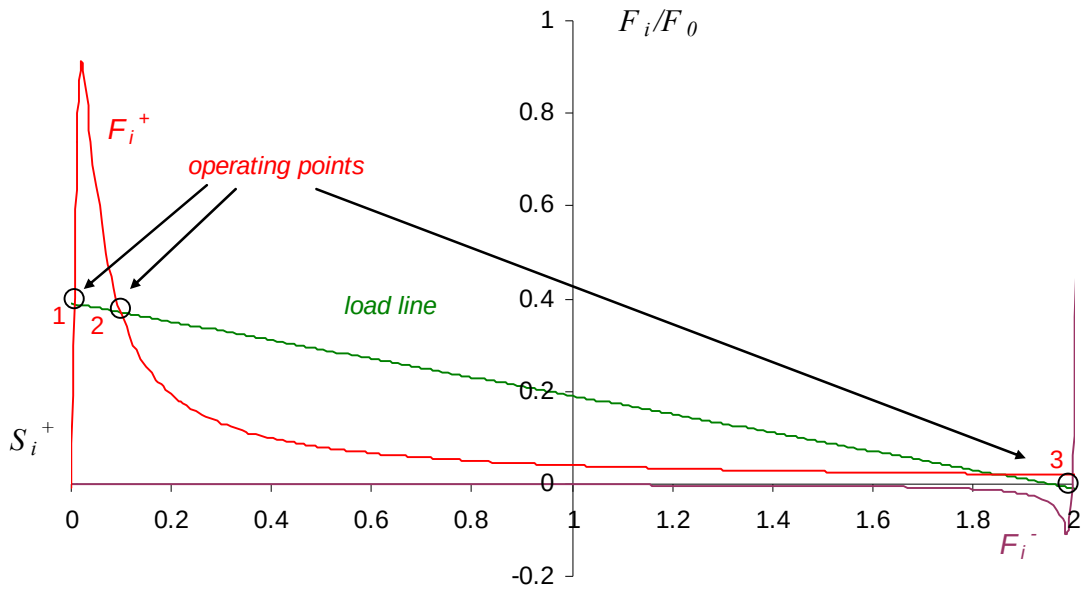

Figure 3.17. Ion fluid operating points ($\xi^- = |\xi^-| = 0.2$, $\zeta_e^+ = |\zeta_e^-| = 2.0$, $S_i^- = 0.05$, $m_e/m_i = 0.1$).

Figure 3.17 shows the method of determining operating points for a layer of the ion fluid. For the curves shown, the electron fluid at this layer is assumed to be rotating almost synchronously with the (-) RMF and we again assume $\omega^+ = -\omega^-$, and $\left|B_r^-\right| = \left|B_r^+\right|$ for the purpose of this demonstration. The force densities only have significant magnitudes in the region of small slip, and hence the net force density may be approximated by the (+) RMF force density when S_i^+ is small. For the purpose of demonstration, the force density curves are plotted for the case $m_e/m_i = 0.1$, for physical values of m_e/m_i the curve is much more sharply peaked, approaching a delta function.

The steady part of the θ-component of the force density due to each RMF on the ion fluid was given as equation (2.72)

$$F_i^{\pm} = \frac{n m_i \omega^{\pm 2} r \zeta_i^{\pm 2}}{2 S_i^{\pm} \xi^{\pm}} \Bigg/ \left[\left(\frac{1}{S_e^{\pm}} + \frac{m_e}{m_i} \frac{1}{S_i^{\pm}} \right)^2 + \frac{1}{\xi^{\pm 2}} \right], \tag{3.69}$$

where $\zeta_i = e|B_r|/\omega m_i$.

The force density on the ion fluid due to either RMF has peak value at

$$S_i^{\pm} = \frac{\frac{m_e}{m_i}\left|\xi^{\pm}\right|}{\sqrt{1+\left(\frac{\xi^{\pm}}{S_e{}^{\pm}}\right)^2}} \cong \frac{m_e}{m_i}\left|\xi^{\pm}\right|, \tag{3.70}$$

with a half peak width of

$$\Delta S_i^{\pm} \cong 2\sqrt{3}\left(\frac{m_e}{m_i}\right)\left|\xi^{\pm}\right|. \tag{3.71}$$

The force density on the ion fluid is only appreciable for ion slips in an extremely small range about $S_i^+ = (m_e/m_i)|\xi^+|$. Outside this very small range of ion slips, the motion of the ion fluid in the θ-direction is dominated by collisions with the electron fluid, the (+) RMF effectively transferring no angular momentum to the ion fluid.

3.3.2 Effect of (-) RMF on ion fluid operating points

We require that the (-) RMF exert negligible force on the ion fluid in the region of the peak of the (+) RMF force for the Clemente steady states to exist. The force on the ion fluid due to either RMF is more strongly peaked than on the electron fluid, and hence the condition required is less stringent than that for the electron fluid.

A condition required for the Clemente steady state for the ion fluid is that the peak value of F_i^+ is greater in magnitude than F_i^- at this point.

$$\left|F_i^+(peak)\right| > F_i^- \tag{3.72}$$

The peak value of the force on the ion fluid due to the (+) RMF is given by

$$\left|F_i^+(peak)\right| \cong \frac{nm_e\omega^{+2}r\zeta_e{}^{+2}}{4}. \tag{3.73}$$

The force due to the (-) RMF in the region of the operating point is approximated by

$$F_i^- = \frac{nm_e{}^2\omega^{-2}r\zeta_e{}^{-2}\xi^-}{2m_iS_i^-}, \tag{3.74}$$

which is an upper bound on the force in this region. If we assume an approximate expression for S_i^-

$$S_i^- \cong \left(1-\frac{\omega^+}{\omega^-}\right), \tag{3.75}$$

the requirement is given by

$$\frac{nm_e\omega^{+2}r\zeta_e{}^{+2}}{4} > \frac{nm_e{}^2\omega^{-2}r\zeta_e{}^{-2}\xi^-}{2m_i\left(1-\frac{\omega^+}{\omega^-}\right)}. \tag{3.76}$$

This relation can be expressed in terms of the normalized collision frequency

$$\xi^- < \frac{1}{2}\frac{m_i}{m_e}\left(\frac{B_r{}^+}{B_r{}^-}\right)^2\left(1-\frac{\omega^+}{\omega^-}\right), \tag{3.77}$$

or in terms of the collision frequency

$$\nu_{ei} < \frac{1}{2}\frac{m_i}{m_e}\left(\frac{B_r{}^+}{B_r{}^-}\right)^2\left(\omega^- - \omega^+\right). \tag{3.78}$$

If $\omega^+ = -\omega^-$ and $\left|B_r{}^-\right| = \left|B_r{}^+\right|$ then the condition reduces to

$$\xi^- < \frac{m_i}{m_e}, \tag{3.79}$$

or

$$\nu_{ei} < \frac{m_i}{m_e}\omega^-. \tag{3.80}$$

This condition is much less stringent for the (-) RMF than for the (+) RMF, since the force on the ion fluid is more strongly peaked than the force on the electron fluid by a factor of m_i/m_e. It should be emphasised that this condition is necessary but not

sufficient for the existence of a steady state corresponding to synchronous rotation of the ion fluid with the (+) RMF.

3.3.3 Analysis of operating points for the ion fluid

Since the force density due to the (-) RMF on the ion fluid is negligible in the region of the Clemente steady state for the ion fluid, we may consider only the (+) RMF in determining the operating points. There are in general three cases for the ion fluid operating points, however only 2 cases are likely unless the collision frequency is extremely large. There are either 1 or 3 operating points which correspond to the real solutions of the equation

$$F_i^+ + F_i^- = -F_{coll} \tag{3.81}$$

Figure 3.18 demonstrates the case where the peak force density due to the (+) RMF is larger than the force density due to collisions. In this case there are 3 real operating points, one of which (2) is unstable and does not correspond to a steady state for the ion fluid. The steady states correspond to almost synchronous rotation with either the (+) RMF or the (-) RMF. Since the peak of the (+) RMF force curve is at $S_i^+ = (m_e/m_i)|\xi^+|$, the operating point of interest is at $S_i^+ < (m_e/m_i)|\xi^+|$.

Figure 3.19 demonstrates the case where the peak value of the force density due to the (+) RMF is smaller than the force density due to collisions. In this case there is only one operating point, where the ions rotate synchronously with the electron fluid.

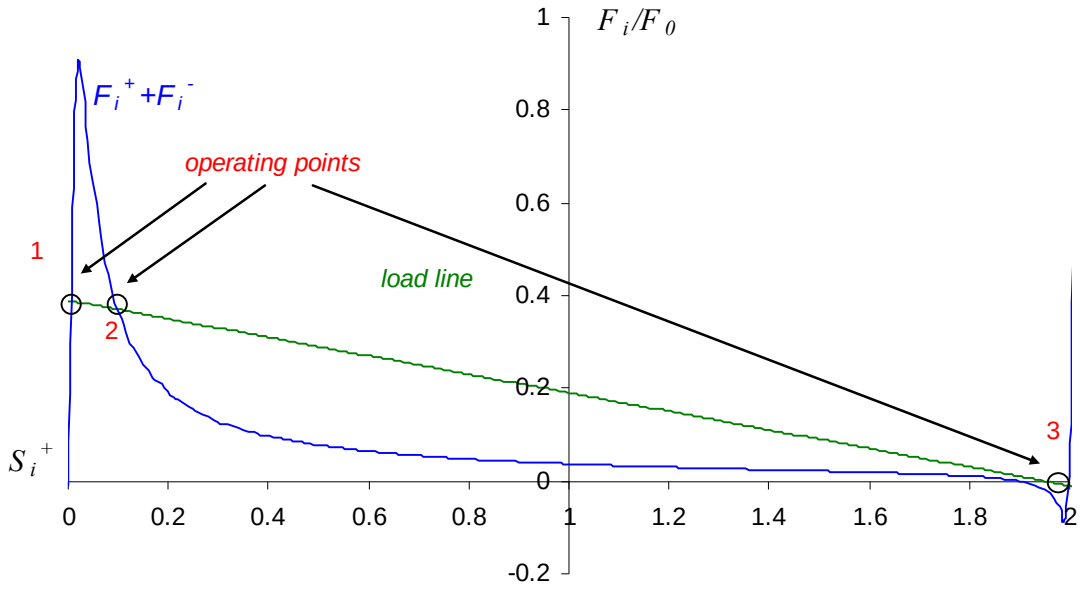

Figure 3.18. Ion fluid operating points for $\xi^- = |\xi^-| = 0.2$, $\zeta_e^+ = |\zeta_e^-| = 2.0$, $S_i^- = 0.05$, $m_e/m_i = 0.1$.

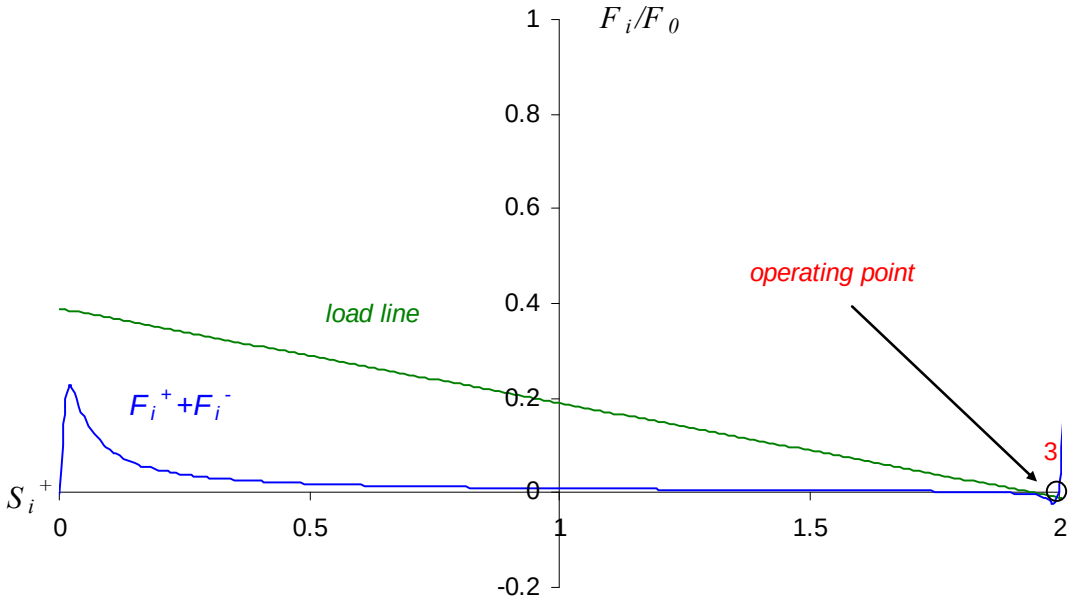

Figure 3.19. Ion fluid operating point for $\xi^- = |\xi^-| = 0.2$, $\zeta_e^+ = |\zeta_e^-| = 1.0$, $S_i^- = 0.05$, $m_e/m_i = 0.1$.

The requirement for the existence of the $S_i^+ < (m_e/m_i)|\xi^+|$ operating point is that the force density exerted by the RMF on the ion fluid exceeds the force density due to collisions.

If we assume that $|F_i^+| >> |F_i^-|$, and approximate the collision force density by assuming synchronous rotation of the electron fluid with the (-) RMF and the ion fluid with the (+) RMF, the requirement is

$$\frac{nm_e\left(\omega^+\right)^2 r\left(\zeta_e{}^+\right)^2}{4} > nm_e\nu_{ei}\left(\omega^- - \omega^+\right)r, \tag{3.82}$$

which gives the condition

$$\left(\zeta_e{}^+\right)^2 > 4\left(\left(\frac{\omega^-}{\omega^+}\right)^2 \xi^- - \xi^+\right) = 4\left(1 - \frac{\omega^-}{\omega^+}\right)\left|\xi^+\right|. \tag{3.83}$$

This again relates the electron cyclotron frequency to the collision and RMF frequencies

$$\left(\omega_{ce}{}^+\right)^2 > 4\left(\omega^- - \omega^+\right)\nu_{ei}. \tag{3.84}$$

For the case $\omega^+ = -\omega^-$

$$\zeta_e{}^{+2} > 8\left|\xi^+\right|, \tag{3.85}$$

or

$$\left(\omega_{ce}{}^+\right)^2 > 8\left|\omega^+\right|\nu_{ei}. \tag{3.86}$$

For the Clemente scheme, there is a similar requirement on $\zeta_e{}^+$, for a small slip operating point to exist for the ion fluid, as was derived in section 3.1.4 for $\zeta_e{}^-$, for a small slip operating point to exist for the electron fluid. The magnitude of the (+) RMF must exceed a critical value (determined by ξ^+) to provide the existence of a steady state corresponding to synchronous rotation of the ion fluid with the (+) RMF.

3.3.4 Approximate relation for the $S_i^+ < (m_e/m_i)|\xi^+|$ operating point

The operating points for the ion fluid are solutions to the equation

$$F_i^+ + F_i^- = -F_{coll}\,. \tag{3.87}$$

The operating point of interest is one where the ion fluid rotates almost synchronously with the (+) RMF. Hence we may approximate the collision force by the expression

$$F_{coll} = nm_e\nu_{ei}\left(\omega^- - \omega^+\right)r\,. \tag{3.88}$$

As demonstrated in section 3.3.2, the effect of the (-) RMF on the operating points is negligible if $\nu_{ei} < \dfrac{m_i}{m_e}\left|\omega^+\right|$, hence we may assume that $\left|F_i^+\right| > \left|F_i^-\right|$ in the region of the steady state corresponding to synchronous rotation.

Equation (3.87) is then given by

$$\frac{nm_i\omega^{+2}r\zeta_e^{+2}}{2}\frac{S_i^+\xi^+}{\left(m_iS_i^+/m_e\right)^2+\xi^{+2}} = nm_e\nu_{ei}\left(\omega^+ - \omega^-\right)r\,. \tag{3.89}$$

This provides a second order equation for S_i

$$S_i^{+2} - \frac{1}{2}\frac{m_e}{m_i}\frac{\zeta_e^{+2}}{\left(1-\dfrac{\omega^-}{\omega^+}\right)}S_i^+ + \left(\frac{m_e}{m_i}\xi^+\right)^2 = 0\,, \tag{3.90}$$

which has small slip solution

$$S_i^+ = \frac{1}{4}\frac{m_e}{m_i}\frac{\left(\zeta_e^+\right)^2}{\left(1-\dfrac{\omega^-}{\omega^+}\right)}\left(1-\sqrt{1-\left[\frac{4\xi^+}{\left(\zeta_e^+\right)^2}\left(1-\frac{\omega^-}{\omega^+}\right)\right]^2}\right). \tag{3.91}$$

The existence of this solution (equation (3.91) is real) requires the condition that the peak of the force due to the applied RMF be larger than the force due to collisions.

$$\left(\zeta_e^{+}\right)^2 > 4\left|\xi^{+}\right|\left(1-\frac{\omega^{-}}{\omega^{+}}\right) \tag{3.92}$$

The case where the RMF force is much larger than the collision force

$$\left(\zeta_e^{+}\right)^2 >> 4\left|\xi^{+}\right|\left(1-\frac{\omega^{-}}{\omega^{+}}\right), \tag{3.93}$$

provides a binomial approximation

$$S_i^{+} \cong 2\left(\frac{m_e}{m_i}\right)\left(1-\frac{\omega^{-}}{\omega^{+}}\right)\left(\frac{\xi^{+}}{\zeta_e^{+}}\right)^2. \tag{3.94}$$

The approximations used show that this is an upper bound for the steady state value of the ion slip.

This relation is in agreement with Hugrass (2000) where it was assumed that

$$\left|\frac{F_i^{+}}{F_i^{-}}\right| >> 1 \qquad \text{and} \qquad S_i^{+} << \frac{m_e}{m_i} \tag{3.95}$$

It has been demonstrated that the first condition is true in general since the (-) RMF exerts a significant force on the ion fluid only over a very small range of slips. The second condition has not been assumed, but it is a result of the approximation in equation (3.93). The slip of the ion fluid at the operating point corresponding to almost synchronous rotation with the (+) RMF is smaller than the slip at which the peak of the force curve occurs. Hence the synchronous rotation operating point is one with $S_i^{+} < (m_e/m_i)|\xi^{+}|$. As the (+) RMF magnitude is increased, the ion slip will become closer to zero for this operating point as the condition in (3.93) is satisfied.

3.4 Summary of conditions required for the existence of the Clemente steady states

This chapter has outlined the conditions for the Clemente steady states to exist at a single layer of the plasma for both the electron and ion fluid. The successful application of the Clemente scheme requires the following.

(1) The existence of a small slip operating point for the electron fluid requires that the force density due to the (-) RMF must exceed the sum of the force density due to the (+) RMF and the force density due to collisions with the ion fluid in the region of the operating point. This is an extension of the condition derived for the (-) RMF in the absence of the (+) RMF.

(2) The existence of a small slip operating point for the ion fluid requires that the force density due to the (+) RMF must exceed the force density due to collisions with the electron fluid in the region of the operating point. The force density due to the (-) RMF is negligible in this region.

(3) The existence of a small slip operating point for the electron fluid requires an upper bound on the normalised collision frequency with respect to the (+) RMF.

(4) The existence of a small slip operating point for the ion fluid requires an upper bound on the normalised collision frequency with respect to the (-) RMF. However this is less restrictive by a factor m_e/m_i than condition (3)

These conditions can be expressed in terms of the dimensionless parameters.

(1)
$$\zeta_e^{-2} > \frac{4\xi^-\left(1-\frac{\omega^+}{\omega^-}\right)}{1-2\xi^+\frac{\omega^+}{\omega^- - \omega^+}\left|\frac{B_r^+}{B_r^-}\right|^2} \tag{3.96}$$

(2)
$$\zeta_e^{+2} > 4\left|\xi^+\right|\left(1-\frac{\omega^+}{\omega^-}\right) \tag{3.97}$$

(3)
$$\left|\xi^{+}\right| < \frac{1}{2}\left|\frac{B_r^{-}}{B_r^{+}}\right|^2\left(1-\frac{\omega^{-}}{\omega^{+}}\right) \tag{3.98}$$

(4)
$$\xi^{-} < \frac{1}{2}\frac{m_i}{m_e}\left(\frac{B_r^{+}}{B_r^{-}}\right)^2\left(1-\frac{\omega^{+}}{\omega^{-}}\right) \tag{3.99}$$

These relations refer to only a layer of the plasma fluid. The existence of operating points for the Clemente scheme is determined by the local values of $\zeta_e^{\pm}$ and $\xi^{\pm}$, and these conditions must be satisfied at every layer. In order to determine whether an operating point exists for the entire fluid requires an analysis of the penetration of the RMFs. We have also yet to consider the initial conditions from which these local steady states may be accessible. The penetration of the RMFs into the plasma and the accessibility of the steady states will be examined in Chapter 4.

CHAPTER 4 ACCESSIBILITY OF THE CLEMENTE STEADY STATES

Chapter 3 examined the existence of the Clemente steady states for a single layer of the plasma, and the local values of plasma and RMF parameters (ξ and ζ_e) required for their existence. Since the local value of ζ_e is not determined solely by the external RMF magnitude, but also by the penetration of the RMF into the plasma, the external RMF magnitudes required for the successful application of the Clemente scheme cannot be deduced immediately from the results presented in section 3.4. In this chapter, the accessibility of the Clemente steady states is examined. The parameters required for complete penetration of the RMFs is described, and the initial conditions from which the steady states may be accessed are examined.

Section 4.1 describes the enhanced penetration of the RMFs into the plasma in terms of effective resistivity and skin depth. Section 4.2 examines the enhanced steady state penetration of the (-) RMF, and Section 4.3 the enhanced steady state penetration of the (+) RMF. In both cases it is shown that the slips in the steady state provide the conditions required for enhanced penetration of the RMF. The accessibility of the steady states for the electron fluid is considered in Section 4.4 and the accessibility of the steady states for the ion fluid is considered in Section 4.5. A scenario for the application of the Clemente scheme with electrons and ions initially counter-rotating is outlined in Section 4.6 and the initial conditions required for the ion fluid. We show that it is difficult for the (+) RMF to penetrate into the plasma and entrain the ion fluid if the ions initially rotate as a rigid body. The penetration of the (+) RMF into the plasma is possible for a narrow class of initial conditions, namely that the initial rotational velocity

of the ion fluid varies with radius in a suitable manner, which may be induced during the transient phase of the (-) RMF. A frequency modulation technique can allow access to the Clemente steady states without the need for an initial radial profile.

4.1 Effective Resistivity and Effective Skin Depth

4.1.1 Effective resistivity and skin depth for a single applied RMF

We examine first the steady state behaviour when a single RMF is applied. The vector potential under the application of a single RMF is described by the time-dependant equation

$$\frac{\partial A_z}{\partial t} = \left[\frac{\eta^*}{\mu_0}\nabla^2 A_z - i\omega A_z\right] \Big/ \left[\frac{1}{S_e} + \frac{m_e}{m_i}\left(\frac{1}{S_i} - 1\right)\right]. \tag{4.1}$$

The steady state solutions for A_z satisfy the diffusion equation

$$\frac{\eta^*}{\mu_0}\nabla^2 A_z - i\omega A_z = 0. \tag{4.2}$$

Equation (4.2) can be written as

$$r^2\frac{d^2 A_z}{dr^2} + r\frac{dA_z}{dr} - \left(\frac{i\mu_0\omega r^2}{\eta^*} + 1\right)A_z = 0. \tag{4.3}$$

For the special case where η^* is a constant, equation (4.3) has the general solution

$$A_z = aI_1(cr) + bK_1(cr), \tag{4.4}$$

where a and b are arbitrary constants, I_1 is the modified Bessel function of order 1 of the first kind, K_1 is the modified Bessel functions of order 1 of the second kind, and

$$c^2 = \frac{i\omega\mu_0}{\eta^*}. \tag{4.5}$$

The modified Bessel function K_1 is not well behaved at $r = 0$. The solution which is well behaved at $r = 0$ and satisfies the boundary condition at $r = R$ (see equation (5.14)) is

$$A_z(r) = \frac{2}{cR}\frac{I_1(cr)}{I_0(cR)}A_{ext}(R), \tag{4.6}$$

where $A_{ext}(R)$ is the externally applied vector potential at $r = R$ in the absence of the plasma, and I_0 is the modified Bessel function of order zero of the first kind.

The effective skin depth δ^*, is defined by

$$\frac{1}{\delta^*} = \mathrm{Re}\left[\sqrt{\frac{i\omega\mu_0}{\eta^*}}\right]. \tag{4.7}$$

For the special case $cR >> 1$ (which is equivalent to $\delta^* << R$) one can use the asymptotic expansion of the modified Bessel functions (Abramawitz, 1964) to obtain the approximate expression

$$A_z(r) = \frac{1}{c\sqrt{rR}}e^{-c(R-r)}A_{ext}(R), \tag{4.8}$$

which is valid for the outer layers of the plasma ($r \cong R$). It is seen from equation (4.8) that the vector potential at the plasma surface is

$$A_z(R) = \frac{A_{ext}(R)}{cR}, \tag{4.9}$$

and hence

$$|A_z(R)| << |A_{ext}(R)|. \tag{4.10}$$

Also the vector potential decays inside the plasma as $\exp\left(-(R-r)/\delta^*\right)$. Hence the RMF will not penetrate into the plasma for $R >> \delta^*$. If R is not much greater than δ^*, the

expansion used to derive equation (4.8) is not valid, however the magnitude of the RMF inside the plasma will be much smaller than the externally applied field when $R > \delta^*$.

For the special case $cR << 1$ (which is equivalent to $\delta^* >> R$) one can use the limiting form of the modified Bessel functions for small arguments (Abramawitz, 1964) to obtain the approximate expression

$$A_z(r) = \frac{r}{R} A_{ext}(R) = A_{ext}(r). \tag{4.11}$$

Since the magnitude of the RMF (from equation (2.21)) is given by

$$B_r(r) = \frac{iA_z(r)}{r}, \tag{4.12}$$

the RMF fully penetrates the plasma for $\delta^* >> R$. If R is not much smaller than δ^*, the expansion used to derive equation (4.11) is not valid, however the magnitude of the RMF inside the plasma will not be much smaller the externally applied field when $R < \delta^*$.

We are interested in the case where η^* varies with r. For this case the above analytical solutions are not valid, however one can assert that the RMF penetrates into the plasma if the local value of δ^*, defined by equation (4.7), is everywhere larger than R.

In the absence of plasma rotation ($S_e = S_i = 1$), and electron inertia ($\nu_{ei} >> \omega$) the effective skin depth is given by

$$\delta^* = \sqrt{\frac{2\eta}{\omega\mu_0}} = \delta, \tag{4.13}$$

where δ is the classical skin depth with respect to the RMF. When the electron fluid is rotating (and assuming $S_e << (m_i/m_e)S_i$) the effective skin depth is equal to the skin depth calculated at the Doppler-shifted frequency of the RMF, as observed in the frame of reference rotating with the electron fluid (Hugrass, 1998),

$$\delta^* = \sqrt{\frac{2\eta}{\mu_0 S_e}} = \sqrt{\frac{\omega}{\left(\omega - \frac{v_{e\theta}}{r}\right)}}\,\delta\,. \tag{4.14}$$

Hence the penetration of the RMF may be much greater than the classical skin depth δ, because

$$\eta^* > \eta \qquad \text{when} \quad S_e^{-} < 1, \tag{4.15}$$

throughout the plasma.

An important plasma parameter in determining RMF penetration is

$$\lambda = \frac{R}{\delta}\,. \tag{4.16}$$

For $\lambda >> 1$, we require $\delta^* >> \delta$ for the RMF to completely penetrate the plasma.

4.1.2 Effective resistivity and skin depth for a two applied RMFs

When two RMFs are applied, the steady state solutions for both RMFs satisfy a diffusion equation

$$\frac{\eta^{*\pm}}{\mu_0}\nabla^2 A_z^{\pm} - i\omega^{\pm} A_z^{\pm} = 0\,, \tag{4.17}$$

and thus, in the steady state for constant $\eta^{*\pm}$, each RMF may penetrate the plasma with the vector potential given by,

$$A_z^{\pm}(r) = \frac{2}{c^{\pm} R}\frac{I_1\left(c^{\pm} r\right)}{I_0\left(c^{\pm} R\right)} A_{ext}^{\pm}(R), \tag{4.18}$$

where

$$\left(c^{\pm}\right)^2 = \frac{i\omega^{\pm}\mu_0}{\eta^{*\pm}}. \tag{4.19}$$

The effective skin depth with respect to each RMF is given by,

$$\frac{1}{\delta^{*\pm}} = \mathrm{Re}\left[\sqrt{\frac{i\omega^{\pm}\mu_0}{\eta^{*\pm}}}\right]. \tag{4.20}$$

Again we have the two limiting cases for constant effective resistivity throughout the plasma

$$A_z{}^{\pm}(r) = \frac{1}{c^{\pm}\sqrt{rR}} e^{-c^{\pm}(R-r)} A_{ext}{}^{\pm}(R) \qquad \text{for} \qquad \delta^{*\pm} << R, \tag{4.21}$$

and

$$A_z{}^{\pm}(r) = \frac{r}{R} A_{ext}{}^{\pm}(R) \qquad \text{for} \qquad \delta^{*\pm} >> R. \tag{4.22}$$

Both the (-) and (+) RMF can only penetrate the plasma if $\delta^{*\pm} / R$ is sufficiently large. In the Clemente scheme, both RMFs may penetrate the plasma with enhanced skin depth. The enhanced penetration can be described as an increase in the local effective resistivity, or as an increase in the local effective skin depth.

For the case where both the electron and ion fluids are stationary ($S_e{}^{\pm} = S_i{}^{\pm} = 1$), the effective resistivities are given by

$$\eta^{*\pm} = \eta\left(1 + \frac{m_e}{m_i} + \frac{i}{\xi^{\pm}}\right). \tag{4.23}$$

If this is compared with the effective resistivities with respect to each of the applied RMFs,

$$\eta^{*\pm} = \eta\left(\frac{1}{S_e{}^{\pm}} + \frac{m_e}{m_i}\frac{1}{S_i{}^{\pm}} + \frac{i}{\xi^{\pm}}\right), \tag{4.24}$$

or

$$\eta^{*\pm} = \frac{\eta}{\left(1 - \frac{v_{e\theta}}{\omega^{\pm} r}\right)} + \frac{m_e}{m_i}\frac{\eta}{\left(1 - \frac{v_{i\theta}}{\omega^{\pm} r}\right)} + i\frac{\eta}{\xi^{\pm}}, \tag{4.25}$$

it is clear that the effective resistivity may be enhanced due to an increase in the first term on the right hand side of equation (4.25) for the case of small electron slip, and an increase in the second term due to small ion slip. Either effect leads to an increased effective skin depth and enhanced penetration of the RMF. The final term is the electron inertia which makes the effective resistivities in general complex.

In the Clemente scheme the penetration of the (-) RMF into the plasma may be enhanced because $\eta^{*^-} > \eta$ for $S_e{}^- < 1,$ and the penetration of (+) RMF into the plasma may be enhanced because $\eta^{*^+} > \eta$ for $S_i{}^+ < \frac{m_e}{m_i}$.

In the absence of plasma rotation ($S_e{}^{\pm} = S_i{}^{\pm} = 1$), and electron inertia ($\nu_{ei} >> \omega^{\pm}$) the effective skin depth is given by

$$\delta^{*\pm} = \sqrt{\frac{2\eta}{\omega^{\pm}\mu_0}} = \delta^{\pm}, \tag{4.26}$$

where $\delta^{\pm}$ the classical skin depth with respect to each applied RMF. For the case where $S_e{}^- << 1$, the effective skin depth with respect to the (-) RMF is given by

$$\delta^{*^-} = \sqrt{\frac{2\eta}{\omega^{-}\mu_0 S_e{}^-}}. \tag{4.27}$$

For the case where $S_i{}^+ << (m_e/m_i)\, S_e{}^+$, the effective skin depth with respect to the (+) RMF is given by

$$\delta^{*+} = \sqrt{\frac{2m_e\eta}{m_i\omega^+\mu_0 S_i{}^+}}\,. \tag{4.28}$$

In the Clemente scheme the penetration of the (-) RMF into the plasma may be enhanced because $\delta^{*-} > R$ for $S_e{}^- < 1$, and the penetration of (+) RMF into the plasma may be enhanced because $\delta^{*+} > R$ for $S_i{}^+ < \frac{m_e}{m_i}$.

The value of λ may be different for each applied RMF, since the RMFs may have frequencies of different magnitudes

$$\lambda^{\pm} = \frac{R}{\delta^{\pm}}\,. \tag{4.29}$$

For $\lambda^{\pm} >> 1$, we require $\delta^{*\pm} >> \delta^{\pm}$ for the RMF to completely penetrate the plasma.

The steady state values of the effective resistivity (and effective skin depth) are functions of the electron and ion slips. For the RMFs to have enhanced penetration in the steady state, requires that the steady state values of $\eta^{*\pm}$ (and hence $\delta^{*\pm}$) must be much larger than η (and $\delta^{\pm}$).

The ability for the (-) RMF to penetrate the plasma when $R > \delta^-$ is a nonlinear phenomena since complete penetration requires almost synchronous rotation of the electron fluid with the RMF. A global steady state for the electron fluid can be maintained when the steady state slip for synchronous rotation of the electron fluid with the RMF satisfies the condition for enhanced penetration of the RMF.

It was demonstrated in section 3.1.3 that the existence of the steady state for the electron fluid is determined by the parameters $\zeta_e{}^-$ and ξ^-. The magnitude of the (-) RMF will be attenuated in the plasma determined by δ^{*-}, which will determine the local value of $\zeta_e{}^-(r)$. Hence the existence of operating point at any point in the plasma is determined by the penetration of the (-) RMF into the plasma column. As has been observed by simulation (Hugrass and Grimm, 1981) and experiment (Hugrass et al, 1981), the ability

of the (-) RMF to maintain the steady state (once it has penetrated) is that the external magnitude of the (-) RMF exceed a critical value. It will be shown in the next section the physical basis of this phenomenon.

The ability of the (+) RMF to penetrate the plasma when $R > \delta^{+}$ requires synchronous rotation of the ion fluid. This can be achieved and maintained when the steady state for synchronous rotation satisfies the condition for enhanced penetration. For the ion fluid, the condition for enhanced penetration is more stringent (by a factor m_e/m_i), however the ion fluid is more closely bound to the (+) RMF than the electron fluid is to the (-) RMF in the steady state. The steady states value of S_i^{+} is in general much smaller than the steady state value of S_e^{-} (by a factor m_e/m_i). It will be shown in the following section that the condition for enhanced penetration of the (+) RMF is satisfied by the steady state ion slip value for almost synchronous rotation. For plasmas with $\lambda^{\pm} >> 1$ we require that the steady states correspond to enhanced penetration of the applied RMFs.

It was demonstrated in section 3.3.3 that the existence of the steady state for the ion fluid is determined by the parameters ζ_e^{+} and ξ^{+}. The magnitude of the (+) RMF will be attenuated in the plasma determined by δ^{*+}, which will determine the local value of $\zeta_e^{+}(r)$. Hence the existence of operating point at any point in the plasma is determined by the penetration of the (+) RMF into the plasma column. It will now be shown that the ability of the (+) RMF to maintain the steady state (once it has penetrated) is that the external magnitude of the (+) RMF exceed a critical value, in the same manner as for the (-) RMF.

4.2 Enhanced steady state penetration of the (-) RMF

The steady states for a layer of the electron fluid are now extended to a steady state for the entire fluid. If we firstly consider the collision frequency to be constant throughout the fluid, then the steady states conditions derived in section 3.2 will be determined by the global parameter ξ^{-}, and the local parameter $\zeta_e^{-}(r)$. The value of $\zeta_e^{-}(r)$ is determined by the external magnitude of the (-) RMF and the effective skin depth at each layer.

It has been demonstrated that the penetration of the (-) RMF is not solely governed by the classical skin effect, and may be enhanced when the electron slip is small with respect to the (-) RMF. This effect can be described in terms of an enhanced resistivity, or enhanced skin depth with respect to the (-) RMF. Both these parameters are local parameters and hence are functions of radius. A requirement for the existence of the Clemente steady states, for the case where $\lambda^- >> 1$, is that the effective resistivity with respect to the (-) RMF be large throughout the plasma. In the steady state the effective resistivity (and effective skin depth) can be determined by the value of S_e^- at the operating point. It will be shown that when the electron fluid is rotating synchronously with the (-) RMF, the steady state values of S_e^- correspond to the conditions required for enhanced penetration of the (-) RMF. Hence in the steady state, the effective skin depth and effective resistivity are greatly enhanced, allowing for the existence of a steady state for the entire electron fluid. Firstly we consider the enhanced penetration in the steady states for the application of the (-) RMF alone, and then consider the effect of the application of the (+) RMF in section 4.3.

Numerical (Milroy 1999, Hugrass & Grimm 1981) and experimental (Jones, 1999) studies have demonstrated that enhanced penetration of a single applied RMF can be maintained when the dimensionless parameter

$$\gamma = \frac{\zeta_e}{\xi}, \tag{4.30}$$

is greater than some critical value, dependant on λ. We now examine the physical basis for this behaviour, and extend the concept to the Clemente scheme. Hence we will consider the parameters

$$\gamma^{\pm} = \frac{\zeta_e^{\pm}}{\xi^{\pm}} \qquad \lambda^{\pm} = \frac{R}{\delta^{\pm}}. \tag{4.31}$$

These studies demonstrated that there is also a critical value of γ required for the RMF to access the steady states (which may be larger than the critical value required to maintain the steady state). The accessibility of the global steady states will be examined in sections 4.4 (for the electron fluid) and 4.5 (for the ion fluid).

4.2.1 Steady state values of $\eta^{*-}(r)$ and $\delta^{*-}(r)$ when the (-) RMF is applied

The $S_e^- < \xi^-$ steady state values for the electron fluid under one RMF (where they exist) are given by

$$S_e^- \cong \frac{\zeta_e^-}{4\left(1-\frac{\omega^+}{\omega^-}\right)}\left(1-\sqrt{1-\left(4\left(1-\frac{\omega^+}{\omega^-}\right)\frac{\xi^-}{\zeta_e^-}\right)^2}\right). \tag{4.32}$$

The figures in this section show the case where the two RMFs have frequencies of equal magnitude ($\omega^+ = -\omega^-$).

Figure 4.1 shows the value of S_e^- at the $S_e^- < \xi^-$ operating point (where it exists) for 3 different values of ξ^- against γ^-. The slip at the operating point is shown to decrease as γ^- increases. The plots are log-log and hence the linear region demonstrates that the power law approximation of equation (3.60) is valid for $\gamma^- >> 1$. The steady state value of S_e^- decreases as γ^- increases.

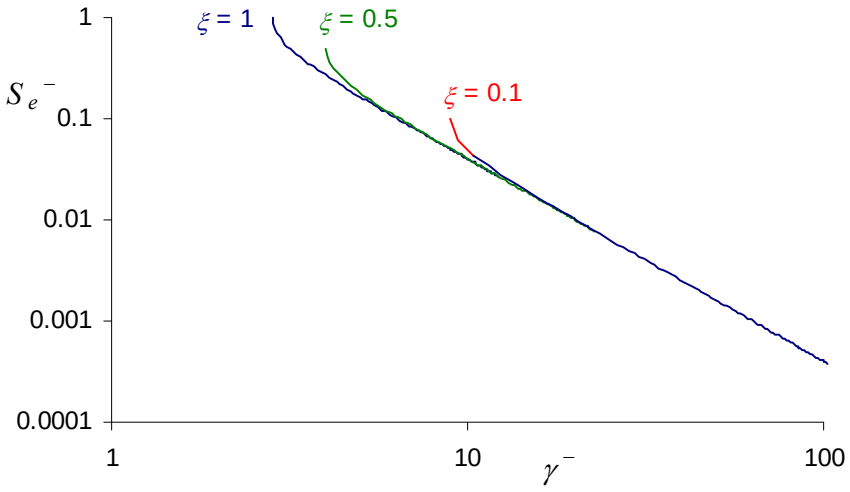

Figure 4.1. Steady state values of S_e^-.

Figure 4.2 presents the real part of the normalised effective resistivity with respect to the (-) RMF at the operating point, given by

$$\mathrm{Re}\left\{\frac{\eta^{*-}}{\eta}\right\} = \frac{1}{S_e^{-}} + \frac{m_e}{m_i}\frac{1}{S_i^{-}}, \tag{4.33}$$

against $\bar{\gamma}$ at the $S_e^{-} < \bar{\xi}$ operating point for the electron fluid (where it exists). The value of S_e^{-} is given by equation (4.32). The effective resistivity increases with $\bar{\gamma}$. For large values of $\bar{\gamma}$, the effective resistivity may be orders of magnitude larger than the plasma resistivity in the steady state.

The power law behaviour for $\bar{\gamma} >> 1$ in Figure 4.2, is consistent with the approximate expression

$$\eta^{*-} \cong \frac{\eta}{S_e^{-}} \cong \frac{\eta}{2\left(1-\dfrac{\omega^{+}}{\omega^{-}}\right)}\left(\frac{\varsigma_e^{-}}{\xi^{-}}\right)^2 = \frac{\eta\gamma^{-2}}{2\left(1-\dfrac{\omega^{+}}{\omega^{-}}\right)}. \tag{4.34}$$

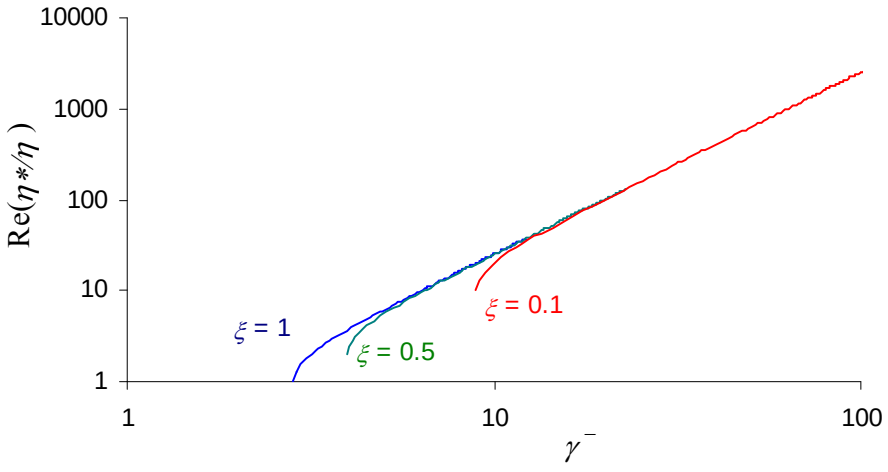

Figure 4.2. Steady state values of normalised effective resistivity.

The (local) effective skin depth may be determined from the effective resistivity by

$$\frac{1}{\delta^{*-}} = \mathrm{Re}\sqrt{\frac{i\omega^{-}\mu_0}{\eta^{*-}}}, \tag{4.35}$$

where η^{*-} is given by equation (4.24). The approximate expression of equation (4.34) does not show the weak dependence of ξ^{-} on η^{*-}. Figure 4.3 shows the resultant values of the effective skin depth against γ^{-} at the $S_e^{-} < \xi^{-}$ operating point for the electron fluid (where it exists), normalised by the classical skin depth. The effective skin depth increases linearly as the magnitude of the applied field is increased. For large values of γ^{-} (and small values of ξ^{-}) the effective skin depth may be significantly larger than the classical skin depth in the steady state.

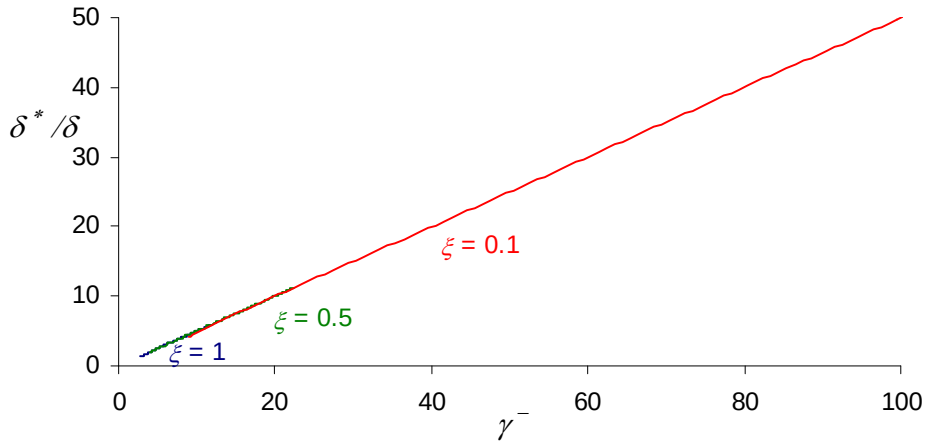

Figure 4.3. Steady state values of normalised effective skin depth.

An approximate expression for the effective skin depth in the steady state can be obtained from the expression for the effective resistivity in equation (4.34)

$$\frac{1}{\delta^{*-}} = \mathrm{Re}\sqrt{\frac{i\omega^{-}\mu_0}{\eta^{*-}}} \cong \left[2\left(1-\frac{\omega^{+}}{\omega^{-}}\right)\right]^{\frac{1}{2}} \frac{\xi^{-}}{\zeta_e^{-}} \mathrm{Re}\sqrt{\frac{i\omega^{-}\mu_0}{\eta}}. \tag{4.36}$$

The linear relationship of the effective skin depth with γ^{-} in Figure 4.3 is then consistent with the approximate expression

$$\frac{\delta^{*-}}{\delta^{-}} \cong \left[2\left(1-\frac{\omega^{+}}{\omega^{-}}\right)\right]^{-\frac{1}{2}} \frac{\zeta_e^{-}}{\xi^{-}} = \left[2\left(1-\frac{\omega^{+}}{\omega^{-}}\right)\right]^{-\frac{1}{2}} \gamma^{-}. \tag{4.37}$$

Figures 4.2 and 4.3, and the approximate expressions, demonstrate that if the $S_e^- < \xi^-$ steady state exists, there will be an enhanced penetration of the (-) RMF in the steady state. The enhanced penetration may be characterised by an increase effective skin depth and effective resistivity. In the steady state required for the Clemente scheme, the (-) RMF will penetrate much further than the classical skin depth. There exists a "global" steady state where the (-) RMF fully penetrates the plasma and captures the entire electron fluid, even though the plasma radius may be much larger than the classical skin depth. The effective resistivity scales with $(\gamma^-)^2$ and the effective skin depth increases linearly with γ^-.

Milroy (1999) in a numerical study showed that for a single RMF, with electrons and ions initially stationary and a uniform density profile, demonstrated that the steady states are accessible when the external RMF magnitude is increased past a critical value which becomes more restrictive for large λ.

$$\gamma^{-} = \frac{\zeta_e^{-}(ext)}{\xi^{-}} > 1.12\lambda^{-} \qquad \lambda^{-} \le 6.5 \tag{4.38}$$

$$\gamma^{-} = \frac{\zeta_e^{-}(ext)}{\xi^{-}} > 1.12\lambda^{-}\left(1.0 + 0.12\left(\lambda^{-} - 6.5\right)^{0.4}\right) \qquad \lambda^{-} > 6.5 \tag{4.39}$$

However, the RMF magnitude required to maintain the steady state is always given by equation (4.38). This was found by decreasing the RMF magnitude after full penetration had been achieved. This is due to the existence of multiple operating points for $\lambda^- > 6.5$ (Hugrass, 1984) for a given value of γ^-. The critical value of γ^- required to access the steady state is greater than that required to maintain it.

The value of the constant of proportionality in equation (4.38) would be dependant on the ion and electron fluid initial conditions, and hence for the Clemente scheme, dependant on the frequency ratio of the RMFs. If the ions are initially counter-rotating, the force due to collisions is larger than for the case where the ions are stationary.

Hence, it would be expected that the critical value γ_c^- would be larger for the case of counter-rotating ions.

Complete penetration will require a critical value of δ^{*-}. If we assume that full penetration is achieved when $\delta^{*-} > R$ then we require,

$$\frac{\delta^{*-}}{\delta^-} > \frac{\delta_c{}^{*-}}{\delta^-} \approx \lambda^- \quad . \tag{4.40}$$

If we apply the approximate expression in equation (4.37), this provides a critical value of γ^-,

$$\gamma^- > \gamma_c{}^- \approx \sqrt{2\left(1-\frac{\omega^+}{\omega^-}\right)}\lambda^- \quad , \tag{4.41}$$

which for the case considered by Milroy (ions stationary) provides.

$$\gamma_c{}^- \approx \sqrt{2}\lambda^- \tag{4.42}$$

Which is in close agreement with the numerical result in equation (4.38). Although the condition $\delta^{*-} > R$ for complete penetration is arbitrary, it is clear that the requirement of a critical value of the effective skin depth will lead to a linear relationship for the critical value of γ^- with λ^- for the steady state to be maintained.

4.2.2 Effect of the (+) RMF on steady state values of $\eta^{*-}(r)$ and $\delta^{*-}(r)$.

A requirement for the successful application of the Clemente scheme is that the steady state for the (-) RMF, once obtained, continues to exist under the application of the (+) RMF. We now examine the effective resistivity and effective skin depth when the (+) RMF is applied. The $S_e^- < \xi^-$ steady state values for the electron fluid for two applied RMFs (where they exist) are given by equation (3.56). The figures in this section show

the case where the two RMFs are equal in magnitude ($\left|B_r^-\right| = \left|B_r^+\right|$) and have frequencies of equal magnitude ($\omega^+ = -\omega^-$).

Figure 4.4 shows the value of S_e^- at the $S_e^- < \xi^-$ operating point (where it exists) for 3 different values of ξ^- when a (+) RMF of equal magnitude is applied. The slip at the operating point is shown to decrease as γ^- increases. The steady state value of S_e^- decreases as the magnitude of the (-) RMF is increased. A comparison with Figure 4.1 shows that the steady state value of S_e^- is less affected by the (+) RMF for small values of ξ^-. There is significant departure from the power law approximation given in equation (3.60) since the (+) RMF has a significant effect on the steady state.

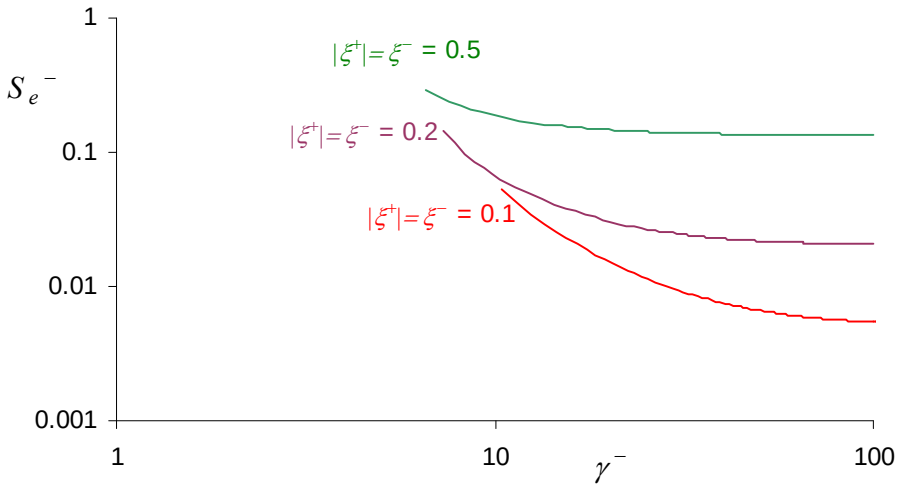

Figure 4.4. Steady state values of S_e^- for 2 RMFs.

Figure 4.5 presents the resultant values of the real part of the normalised effective resistivity with respect to the (-) RMF at the operating point, against γ^- at the $S_e^- < \xi^-$ operating point for the electron fluid (where it exists), when the (+) RMF of equal magnitude is applied. The effective resistivity again increases as the magnitude of the applied field is increased, and the increase is most significant for smaller values of ξ^- (since the force due to the (+) RMF is negligible in the region of the $S_e^- < \xi^-$ operating point for $|\xi^+| << 1$). For large values of γ^-, the effective resistivity may again be orders

of magnitude larger than the plasma resistivity in the steady state, however there is a significant departure from the power relation due to the application of the (+) RMF.

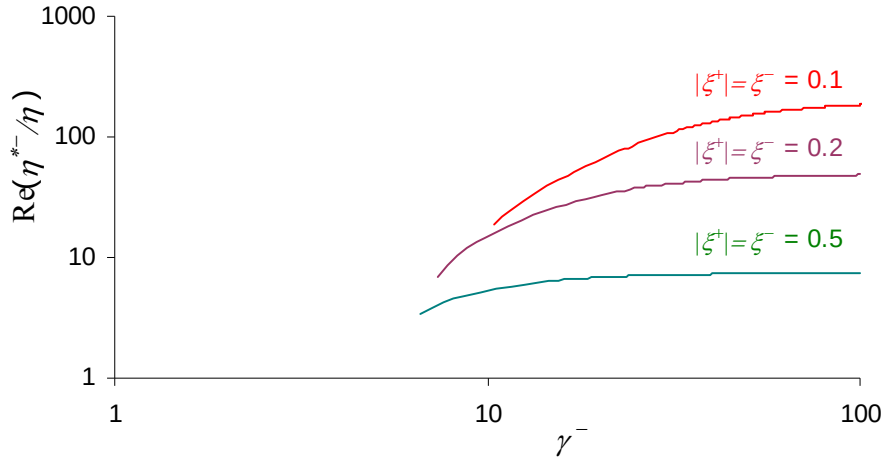

Figure 4.5. Steady state values of normalised effective resistivity for 2 RMFs.

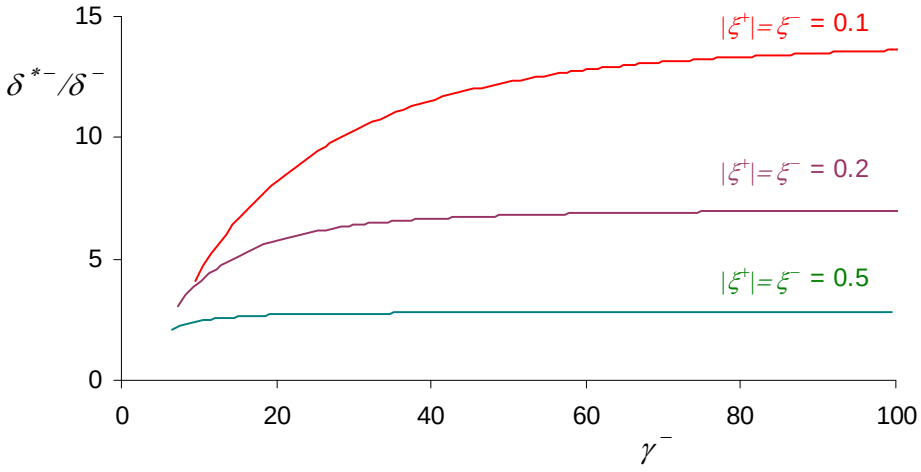

Figure 4.6. Steady state values of normalised effective skin depth for 2 RMFs.

Figure 4.6 shows the resultant values of the effective skin depth against γ^- at the $S_e^- < \xi^-$ operating point for the electron fluid (where it exists), normalised to the classical skin depth when the (+) RMF is applied. The effective skin depth again increases as the magnitude of the applied field is increased and the increase is most significant for

smaller values of ξ^-. For large values of γ^- (and small values of ξ^-) the effective skin depth may be significantly larger than the classical skin depth in the steady state.

For the Clemente scheme, there exists a steady state corresponding to almost synchronous rotation of the electron fluid with the (-) RMF, which also corresponds to enhanced penetration of the (-) RMF. When the (+) RMF is applied, the enhanced penetration of the (-) RMF is effected, but the penetration may still be orders of magnitude larger than described by the classical skin depth for sufficiently large values of γ^-. The enhanced penetration of the (-) RMF may be characterised by the effective resistivity or the effective skin depth. The enhanced penetration scales with the parameter γ^- and is dependant on ξ^+ when the (+) RMF is applied.

4.2.3 Effect of $\omega^- > \omega^+$ on steady state values of $\eta^{*-}(r)$ and $\delta^{*-}(r)$.

The steady state value of the electron slip is also determined by the relative frequencies of the applied RMFs. It was demonstrated in section 3.2.5 that if the (+) RMF has frequency much less than that of the (-) RMF, then the steady states are less affected by the application of the (+) RMF. It is now shown that this results in an increased value of the effective resistivity (and effective skin depth) in the steady state. Figures in this section show the case where the two RMFs are equal in magnitude ($\left|B_r{}^-\right| = \left|B_r{}^+\right|$), but may have different frequencies.

Figure 4.7 shows the value of S_e^- at the $S_e^- < \xi^-$ operating point (where it exists) for 3 different values of ω^+/ω^- for $\xi^- = 0.1$. The slip at the operating point is shown to decrease as $|\omega^+/\omega^-|$ decreases. The variation of S_e^- with γ^- more closely approaches the power law approximation (the (+) RMF has negligible effect) as the relative frequency of the (+) RMF is decreased.

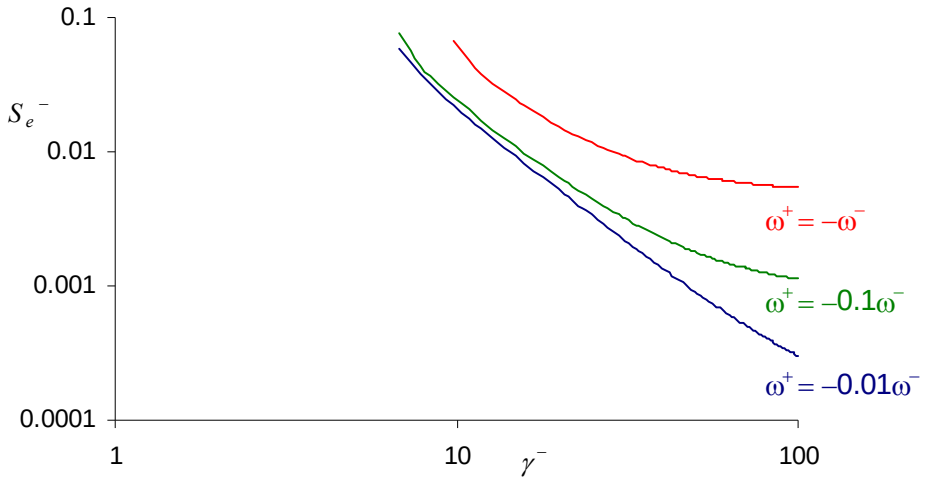

Figure 4.7. Steady state values of S_e^- for 2 RMFs.

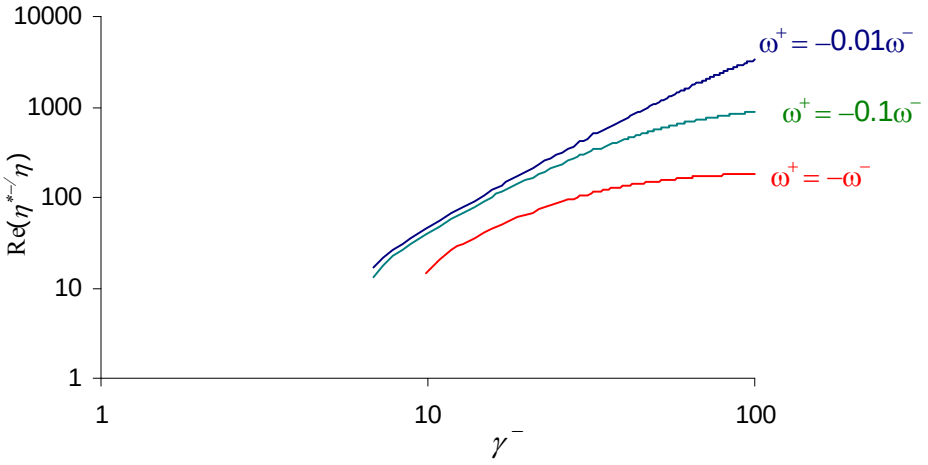

Figure 4.8. Steady state values of normalised effective resistivity for 2 RMFs.

Figure 4.8 presents the real part of the normalised effective resistivity at the $S_e^- < \xi^-$ operating point (where it exists) for 3 different values of ω^+/ω^- for $\xi^- = 0.1$. The ions are assumed to be rotating synchronously with the (+) RMF and hence we take

$$S_i^- = \left(1 - \frac{\omega^+}{\omega^-}\right). \tag{4.43}$$

The effective resistivity at the operating point is shown to increase as $|\omega^+/\omega^-|$ decreases. The variation of the effective resistivity with γ^- more closely approaches the power law approximation (the (+) RMF has insignificant effect) as the relative frequency of the (+) RMF is decreased.

Figure 4.9 shows the normalised effective skin depth at the $S_e^- < \xi^-$ operating point (where it exists) for 3 different values of ω^+/ω^- for $\xi^- = 0.1$. The effective skin depth at the operating point is shown to significantly increase as $|\omega^+/\omega^-|$ decreases. The variation of the effective resistivity with γ^- more closely approaches the linear approximation (the (+) RMF has insignificant effect) as the relative frequency of the (+) RMF is decreased.

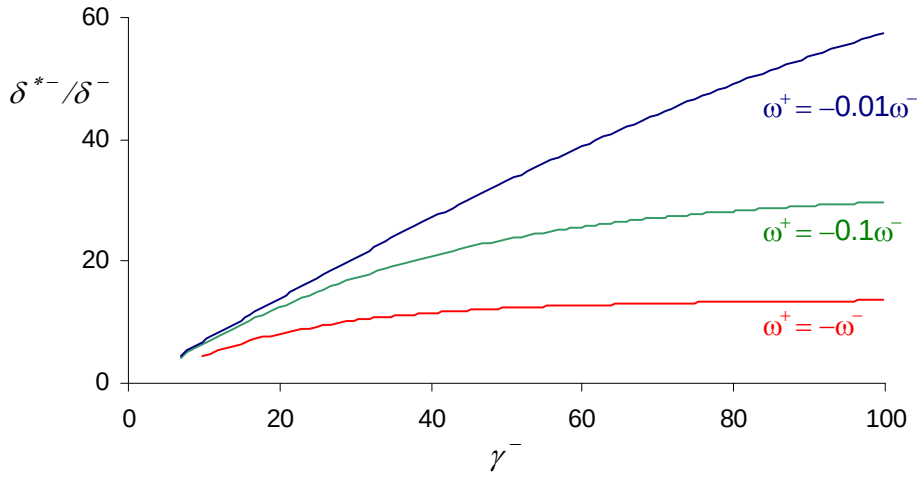

Figure 4.9. Steady state values of normalised effective skin depth for 2 RMFs.

It is seen that the penetration of the (-) RMF in the steady state may be enhanced by having the frequency of the (+) RMF smaller relative to the (-) RMF. As the ratio $|\omega^+/\omega^-|$ decreases, the penetration increases, as shown by an increase in the effective resistivity and effective skin depth.

The Clemente steady state for the electron fluid requires that when the (+) RMF is applied, the small slip steady state for the electron fluid continues to exist, and corresponds to enhanced penetration of the (-) RMF. This is shown to be true, although the enhanced penetration is limited by the application of the (+) RMF. The effect of the (+) RMF on the Clemente steady state for the electron fluid can be reduced by making the frequency of the (+) RMF much smaller in magnitude than the (-) RMF.

4.3 Enhanced steady state penetration of the (+) RMF

The penetration of the (+) RMF is not solely governed by the classical skin effect, and may be enhanced when the ion slip is very small. This can be described in terms of an enhanced resistivity, or enhanced skin depth with respect to the (+) RMF. Both these parameters are local parameters and hence are functions of radius. A requirement for the existence of the Clemente steady states for the case where $\lambda^+ >> 1$, is that the effective resistivity with respect to the (+) RMF be large throughout the plasma. In the steady state the effective resistivity (and effective skin depth) can be determined by the value of S_i^+ at the operating point. It will be shown that when the ion fluid is rotating almost synchronously with the (+) RMF, the steady state values of S_i^+ correspond to the conditions required for enhanced penetration of the (+) RMF. Hence, in the steady state, the effective skin depth and effective resistivity are greatly enhanced allowing the existence of a steady state for the entire ion fluid.

4.3.1 Steady state values of $\eta^{*+}(r)$ and $\delta^{*+}(r)$

The $S_i^+ < (m_e/m_i)|\xi^+|$ steady state values for the ion fluid (where they exist) are given by

$$S_i^+ = \frac{1}{4}\frac{m_e}{m_i}\frac{{\zeta_e^+}^2}{\left(1-\frac{\omega^-}{\omega^+}\right)}\left(1-\sqrt{1-\left[\frac{4\xi^+}{{\zeta_e^+}^2}\left(1-\frac{\omega^-}{\omega^+}\right)\right]^2}\right). \tag{4.44}$$

Figure 4.10 presents the value of S_i^+ at the $S_i^+ < \xi^+$ operating point for 3 different values of ξ^+. The two RMFs are equal in magnitude ($\left|B_r^-\right| = \left|B_r^+\right|$) and have frequencies of equal magnitude ($\omega^+ = -\omega^-$). The slip at the operating point is shown to decrease as γ^+ increases. Note that the power law approximation of equation (3.94) is valid as γ^+ becomes large. The steady state values of the ion slips are in general smaller than that for the electron slips by a factor m_e/m_i.

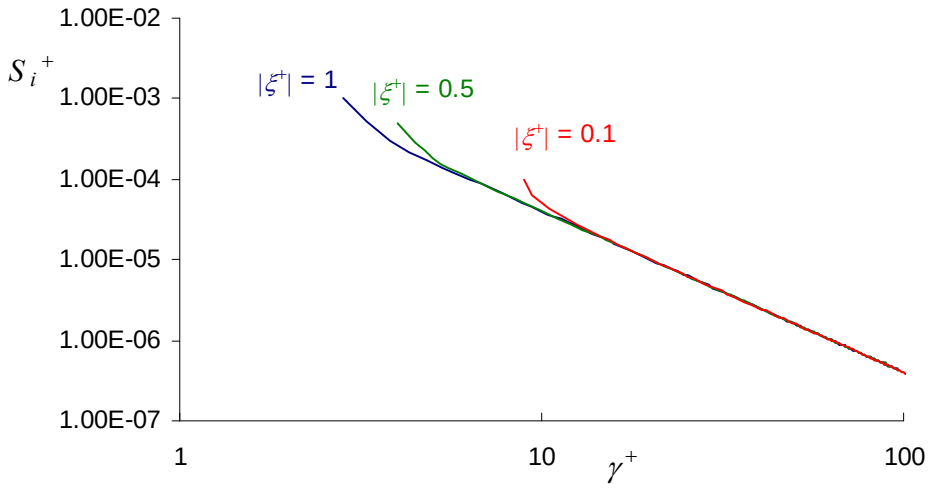

Figure 4.10. Steady state values of S_i^+.

Figure 4.11 shows the real part of the normalised effective resistivity with respect to the (+) RMF at the operating point, given by

$$\mathrm{Re}\left\{\frac{\eta^{*+}}{\eta}\right\} = \frac{1}{S_e^+} + \frac{m_e}{m_i}\frac{1}{S_i^+}, \tag{4.45}$$

against γ^- at the $S_i^+ < (m_e/m_i)|\xi^+|$ operating point for the ion fluid (where it exists). The electrons are assumed to be rotating synchronously with the (-) RMF and hence $S_e^+ = 2$ as $\omega^+ = -\omega^-$. The effective resistivity increases as the magnitude of the applied field is increased. The increase is most significant for smaller values of ξ^+. For large values of γ^+, the effective resistivity may be orders of magnitude larger than the plasma resistivity in the steady state.

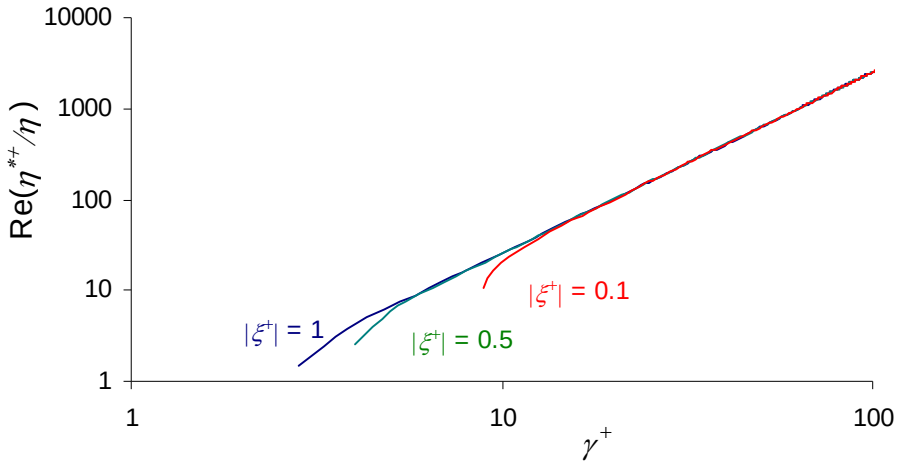

Figure 4.11. Steady state values of normalised effective resistivity for the (+) RMF.

The power law behaviour is consistent with the approximate expression (using equation (3.94))

$$\eta^{*+} \cong \frac{m_e}{m_i}\frac{\eta}{S_i^+} \cong \frac{\eta}{2\left(1-\frac{\omega^-}{\omega^+}\right)}\gamma^{+2}. \tag{4.46}$$

The (local) effective skin depth may be determined from the effective resistivity by

$$\frac{1}{\delta^{*+}} = \mathrm{Re}\sqrt{\frac{i\omega^+\mu_0}{\eta^{*+}}}. \tag{4.47}$$

where η^{*-} is given by equation (4.24).

Figure 4.12 presents the resultant values of the effective skin depth (with respect to the (+) RMF) against γ^+ at the $S_i^+ < (m_e/m_i)|\xi^+|$ operating point for the ion fluid (where it exists), normalised to the classical skin depth. The effective skin depth increases as the magnitude of the applied field is increased. For large values of γ^+ (and small values of ξ^+) the effective skin depth may be significantly larger than the classical skin depth in the steady state.

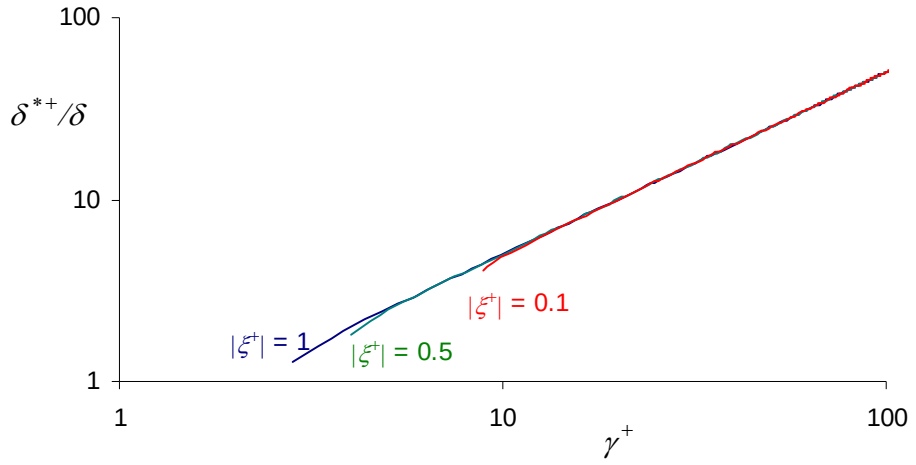

Figure 4.12. Steady state values of normalised effective skin depth for the (+) RMF.

An approximate expression for the effective skin depth can be obtained from the expression for the effective resistivity.

$$\frac{1}{\delta^{*+}} = \mathrm{Re}\sqrt{\frac{i\omega^+\mu_0}{\eta^{*+}}} \cong \sqrt{2\left(1-\frac{\omega^-}{\omega^+}\right)}\left(\frac{\xi^+}{\zeta_e{}^+}\right)\mathrm{Re}\sqrt{\frac{i\omega^+\mu_0}{\eta}}\,. \tag{4.48}$$

The linear relationship with γ^- is then consistent with the approximate expression

$$\delta^{*+} \cong \frac{\zeta_e{}^+}{\sqrt{2\left(1-\frac{\omega^-}{\omega^+}\right)}\xi^+}\delta^+ = \frac{1}{\sqrt{2\left(1-\frac{\omega^-}{\omega^+}\right)}}\gamma^+\delta^+ \tag{4.49}$$

If the $S_i^+ < (m_e/m_i)|\xi^+|$ steady state exists, there will be an enhanced penetration of the (+) RMF in the steady state. The enhanced penetration is characterised by an increase effective skin depth and effective resistivity.

Section 4.3 demonstrated the existence of the Clemente steady state for the electron fluid, where the (-) RMF penetrates much farther than the classical skin depth in the steady state. The Clemente steady states also exist for the ion fluid, and correspond to enhanced penetration of the (+) RMF in the steady state. The conditions required for the global steady states to exist are determined by

$$\frac{\delta^{*\pm}}{\delta^{\pm}} \cong \frac{\gamma^{\pm}}{\sqrt{2\left(1-\frac{\omega^{-}}{\omega^{+}}\right)}}. \tag{4.50}$$

The existence of a global steady state for $\lambda^{\pm} >> 1$ requires that the local effective skin depth with respect to each RMF must be significantly larger than the classical skin depth.

Complete penetration will require a critical value of δ^{*+}. If we assume that full penetration is achieved when $\delta^{*+} > R$ then we require,

$$\frac{\delta^{*+}}{\delta} > \lambda^{+} \tag{4.51}$$

If we apply the approximate expression in equation (4.49), this provides a critical value of γ^{+} for the case where $S_e^{+} = 2$

$$\gamma^{+} > \gamma_c{}^{+} = \sqrt{2\left(1-\frac{\omega^{-}}{\omega^{+}}\right)}\lambda^{+}. \tag{4.52}$$

For the case where $\omega^{+} = -\omega^{-}$ provides

$$\gamma^{+} > 2\lambda^{+}. \tag{4.53}$$

As for the electron fluid, the steady states for the ion fluid can be maintained if the external magnitude of the (+) RMF is sufficiently large. The magnitude required for the (+) RMF to maintain the steady state is the same as for the (-) RMF when $\omega^{+} = |\omega^{-}|$. Although the condition $\delta^{*+} > R$ for complete penetration is arbitrary, it is clear that the requirement of a critical value of the effective skin depth will lead to a linear relationship for the critical value of γ^{+} with λ^{+} for the steady state to be maintained.

4.3.2 Steady state values of $\eta^{*+}(r)$ and $\delta^{*+}(r)$ for the ion fluid with $\omega^- > |\omega^+|$

It has been demonstrated in section 3.3.2 that the (-) RMF exerts an insignificant force on the ion fluid steady state. The steady state values will vary for the ion fluid since the value of S_e^+ is determined by the relative magnitudes of the RMF frequencies.

Figure 4.13 shows the value of S_i^+ at the $S_i^+ < (m_e/m_i)|\xi^+|$ operating point (where it exists) for 3 different values of ω^+/ω^- for $\xi^+ = 0.1$. The electrons are assumed to be rotating synchronously with the (-) RMF and hence we take

$$S_e^+ \cong \left(1 - \frac{\omega^-}{\omega^+}\right). \tag{4.54}$$

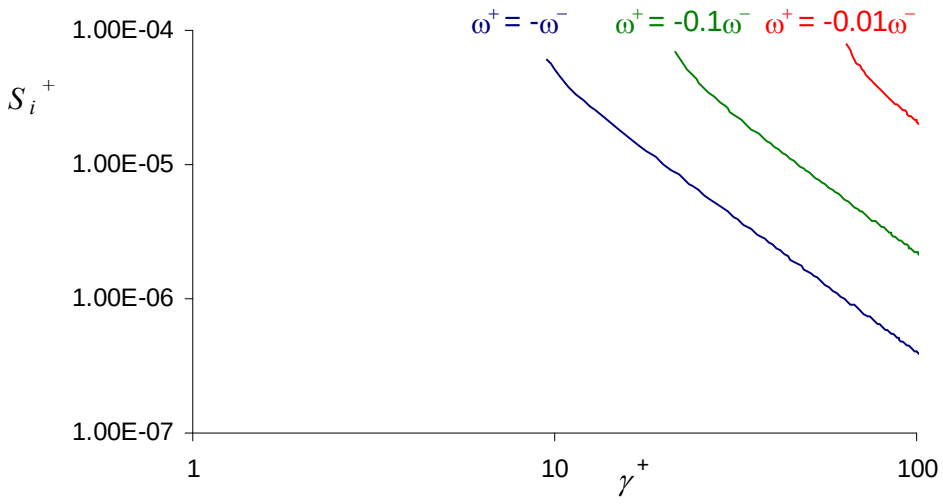

Figure 4.13. Steady state values of S_i^+.

The slip at the operating point is shown to decrease as $|\omega^+/\omega^-|$ increases. Figure 4.14 shows the value of real part of the effective resistivity at the $S_i^+ < (m_e/m_i)|\xi^+|$ operating point for 3 different values of ω^+/ω^- for $|\xi^+| = 0.1$. The effective resistivity at the operating point is shown to decrease as $|\omega^+/\omega^-|$ decreases.

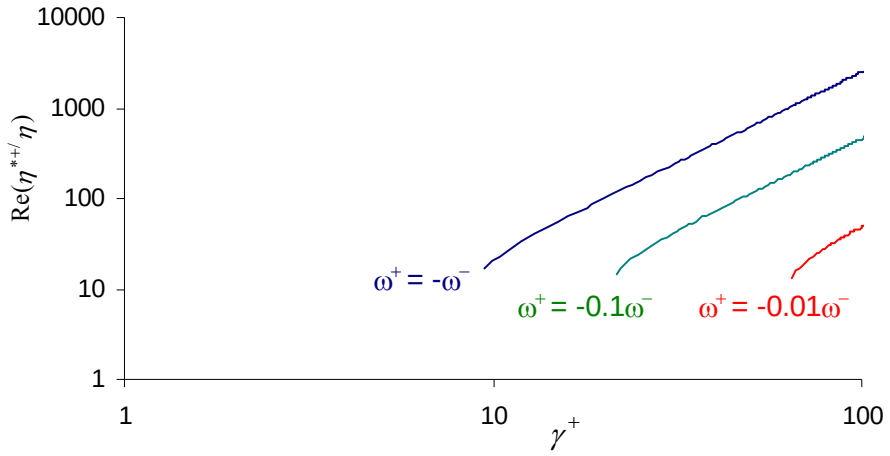

Figure 4.14. Steady state values of normalised effective resistivity for the (+) RMF.

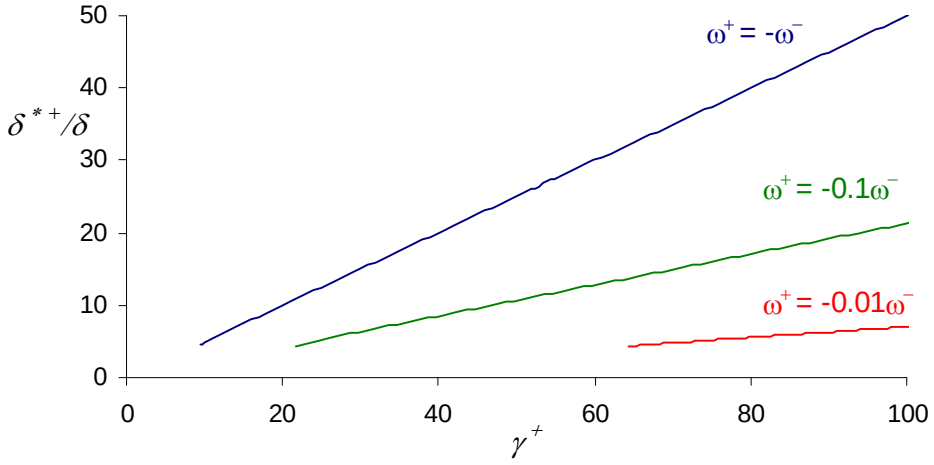

Figure 4.15. Steady state values of normalised effective skin depth for the (+) RMF.

Figure 4.15 presents the normalised effective skin depth at the $S_i^+ < (m_e/m_i)|\xi^+|$ operating point for 3 different values of ω^+/ω^- for $|\xi^+| = 0.1$. The effective skin depth at the operating point is shown to decrease as $|\omega^+/\omega^-|$ decreases.

These results would appear to demonstrate that the penetration of the (+) RMF is less effective for the case $\omega^- > \omega^+$. However, when the value of ω^+ is decreased, then the value of λ^+ is also decreased (by a factor $(\omega^+)^{½}$) which compensates for the decrease in

the effective skin depth (by a factor $(\omega^+)^{1/2}$). There is hence no net effect on the (+) RMF penetration in the steady state by decreasing the frequency of the (+) RMF. As demonstrated in section 4.2.3, the important effect of $\omega^- > |\omega^+|$ is that the steady states for the electron fluid are less affected by the application of the (+) RMF (the effect of the (-) RMF on the ion fluid steady states is negligible). Hence having $\omega^- > |\omega^+|$ may be a useful technique for employing the Clemente scheme.

4.4 Accessibility of the Electron Fluid Steady states

Sections 4.2 and 4.3 have demonstrated that the Clemente steady states correspond to enhanced penetration of both the (-) and the (+) RMFs. This allows for the existence of the Clemente steady states with $\lambda^{\pm} >> 1$. It is required that these steady states be accessible from the initial conditions. This section investigates the initial conditions allowing accessibility of the Clemente steady states for the electron fluid, and section 4.5 investigates the accessibility of the steady states for the ion fluid.

4.4.1 Initial conditions for the accessibility of the electron fluid steady states.

Figures 3.2 - 3.4 in section 3.2.1 demonstrated the 3 cases for the operating points for a layer of the electron fluid. We now consider the range of initial conditions leading to each operating point. Since the Clemente scheme involves entrainment of the (-) RMF before the (+) RMF is applied, we need only consider the (-) RMF to determine the accessibility of the steady state for the electron fluid. If the steady state for the electron fluid still exists after the (+) RMF is applied, the accessibility of the two-RMF operating point for the electron fluid will be trivial.

The accessibility of the three cases for steady states of the electron fluid considered in section 3.2.1 can be demonstrated in terms of the potential function for the electron fluid. The potential function for the electron fluid U_e is defined by

$$\frac{1}{F_0}\left(F_e^{-} + F_{coll}\right) = -\frac{dU_e}{dS_e^{-}} \tag{4.55}$$

where the normalised net force is determined by the derivative of the potential function. The time-evolution of the system will always be from high to low potential. The operating points for the electron fluid are hence the local minima and maxima of the potential. The local minima correspond to stable operating points and local maxima correspond to the unstable operating point.

The electron potential has approximate solution

$$U_e \cong \frac{1}{2}\zeta_e^{-}\xi^{-}\ln\left(S_e^{-} + \xi^{-2}\right) + \frac{1}{2}\xi^{-}S_e^{-}\left(\frac{S_e^{-}}{2} - S_i^{-}\right) \tag{4.56}$$

The 3 cases for the potential function with $S_i^{-} = 2$ and $\xi^{-} = 0.1$ are presented in Figures 4.15 – 4.17.

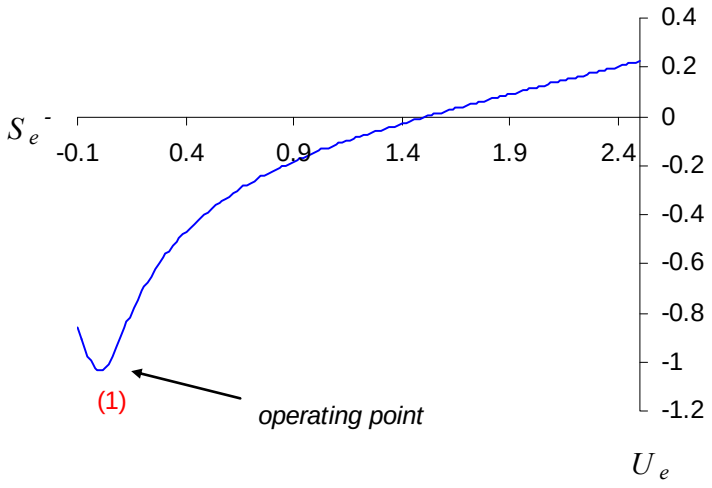

Figure 4.16. Potential function for the electron fluid with $\xi^{-} = 0.1$, $\zeta_e^{-} = 3$.

Figure 4.16 presents the case for $\xi^{-} = 0.1$, $\zeta_e^{-} = 3$ where there is only one operating point, corresponding to almost synchronous rotation of the electron fluid with the (-) RMF. If the slip is initially greater than the operating point, the net force density will be positive (the RMF force is greater than the force load line), and hence the (-) RMF will

drive the electron fluid toward the operating point. If the slip is initially less than the operating point, the net force density will be negative (the RMF force density is less than the collisional load line), and hence collisions with the ion fluid will relax the electron fluid toward the operating point. For this case then, the initial conditions are irrelevant, and this situation may be used for either maintaining a driven current, or producing current drive.

Figure 4.17 shows the case for $\xi^{-} = 0.1$, $\zeta_e^{-} = 1.2$ where there are three operating points. In this situation the steady state achieved is determined by the initial conditions. If the initial slip is less than operating point (1) collisions dominate, which drives the electron fluid toward (1). If the initial slip is greater than (1) but less than (2), the (-) RMF force density dominates which drives the electron fluid toward (1). If the initial slip is less than (2) but greater than (3), collisions dominate, driving the electron fluid toward (3). If the initial slip is greater than (3), the RMF dominates, driving the electron fluid toward (3), The meaning of initial condition in this context is the slip at the time when the local value of ζ_e^{-} becomes large enough for the existence of operating point (1).

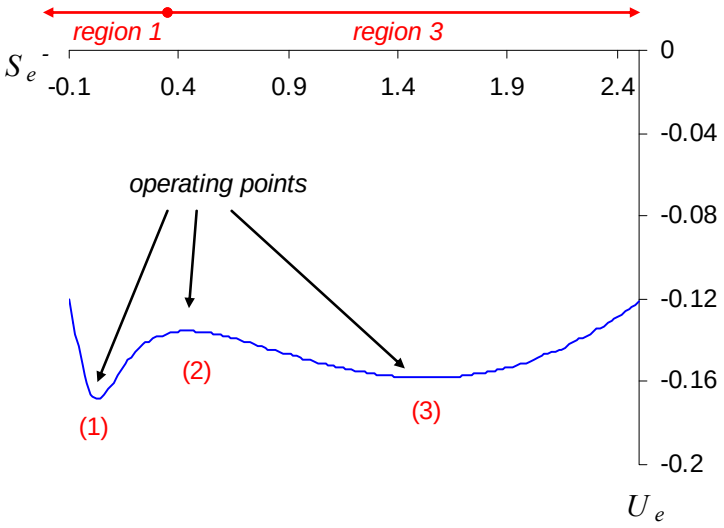

Figure 4.17. Potential function for the electron fluid with $\xi^{-} = 0.1$, $\zeta_e^{-} = 1.2$.

For this case there are three classes of initial conditions, or basins of attraction for the three operating points. If the initial slip is less than that of the (unstable) operating point (2) (region 1, the basin of attraction of operating point (1)) then the steady state achieved is operating point (1). If the initial slip is greater than that of operating point (2) (region 3, the basin of attraction of operating point (3)) then the steady state achieved is operating point (3). The basin of attraction of the operating point (2) consists only of the operating point itself. This situation can only be used for maintaining a driven current, since the operating point (1) cannot be accessed from the initial condition $S_e^- = 1$. The meaning of initial condition in this context is the slip at the time when the local value of ζ_e^- becomes large enough for the existence of operating point (1). The value of $\xi^- = 0.1$ was specifically chosen for the figures presented in this section. As was shown in section 3.2.6 , for $\xi^- > 0.394$ there is always only one operating point and hence the situation shown in Figure 4.17 cannot occur.

Figure 4.18 shows the case for $\xi^- = 0.1$, $\zeta_e^- = 0.5$, where there is now no small slip operating point. The net force density is always toward the zero current operating point (3), regardless of initial condition.

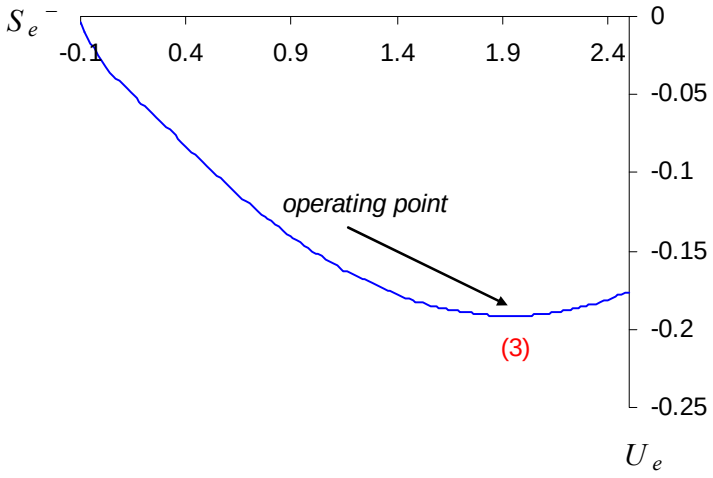

Figure 4.18. Potential function for the electron fluid with $\xi^- = 0.1$, $\zeta_e^- = 0.5$.

For the Clemente scheme, the (+) RMF is applied after the (-) RMF has already penetrated and entrained the electron fluid. If the application of the (+) RMF does not

remove the existence of the operating point (1), then the electron fluid will remain entrained by the (-) RMF when the (+) RMF is applied (with slightly increased slip).

The situations shown in Figures 4.16-4.18 apply locally. For the case $\lambda^- >> 1$ the initial penetration of the (-) RMF is significantly affected by the classical skin effect. If the classical skin effect were to dominate in the steady state, we would expect that only outer layers of the plasma would be captured, since the condition required for the existence of the $S_e^- < \xi^-$ operating point,

$$\zeta_e^-(r)^2 > 4\left(1-\frac{\omega^+}{\omega^-}\right)\xi^-(r), \tag{4.57}$$

and hence entrainment of the electron fluid, would be satisfied only in the outer layers.

There are two cases to consider for $\xi^- > 0.394$. Firstly, the external magnitude of the (-) RMF may be too low, so that the boundary value of ζ_e^- does not satisfy equation (4.57). This situation corresponds to Figure 4.18 at every layer and hence the electron fluid will not be captured, the only possible steady state being (3). Since the (-) RMF will be initially attenuated, the initial value of $\zeta_e^-(R)$ will be less than $\zeta_e^-(\text{ext})$.

Secondly, the external magnitude of the (-) RMF may be sufficiently large so that the boundary value of ζ_e^- satisfies equation (4.57). The initial penetration is determined by the classical skin effect, and hence ζ_e^- will be large in outer layers, but small at inner layers. Outer layers will correspond to the situation shown in Figure 4.16 where the local value of ζ_e^- is large enough to allow the existence of operating point (1). Since there is only one operating point at these layers, a steady state will be achieved with small slip. The inner layers will correspond to the situation shown in Figure 4.18 where the local value of ζ_e^- is small and hence only operating point (3) exists. The initial capture of outer layers gives a small slip. As seen in section 4.1.1 this leads to a large increase in the (local) effective resistivity and the (local) effective skin depth in this layer. This will allow the (-) RMF to penetrate further in the plasma, increasing ζ_e^- at successive layers where the situation in Figure 4.16 is achieved, where the only possible operating point is (1). In this manner, the criterion required for complete penetration of the (-) RMF and

entrainment of the electron fluid can be achieved successively as it penetrates the plasma.

Hence if ξ^- sufficiently large, we require no special initial conditions for the electron fluid. The only requirement is that the external magnitude of the (-) RMF exceed some critical value. This critical value may be larger than that required to maintain the steady state, due to initial attenuation of the RMF. Since the attenuation increases with λ^- (as the plasma radius becomes much larger than the skin depth), the critical value of γ^- required to access the steady state can be much larger than the critical value required to maintain the steady state when λ^- is large. Even if ξ^- is below the critical value for three operating points, the external RMF magnitude can be made large enough so that only one operating point exists. It would be expected that a (larger) critical value of γ^- would allow access to the $S_e^- < \xi^-$ steady state for this case from any initial condition.

4.5 Accessibility of the Ion Fluid Steady states

Sections 4.2 and 4.3 have demonstrated that the Clemente steady states correspond to enhanced penetration of both the (-) and the (+) RMFs. This allows for the existence of the Clemente steady states with $\lambda^{\pm} >> 1$. It is required that these steady states be accessible from the initial conditions. This section investigates the initial conditions allowing accessibility of the Clemente steady states for the ion fluid.

The accessibility of the two cases for steady states of the ion fluid considered in section 3.3.1 can also be demonstrated in terms of the potential function for the ion fluid. The potential function for the ion fluid U_i is defined by

$$\frac{1}{F_0}\left(F_i^{+} + F_{coll}\right) = -\frac{dU_i}{dS_i^{+}} \tag{4.58}$$

where the normalised net force is determined by the derivative of the potential function. The time-evolution of the system will always be from high to low potential. The operating points for the ion fluid are hence the local minima and maxima of the

potential. The local minima correspond to stable operating points and local maxima correspond to the unstable operating point.

The ion potential has approximate solution

$$U_i \cong \frac{1}{4}\frac{m_e}{m_i}\zeta_e^{+}\xi^{+}\ln\left(S_i^{+}+\left(\frac{m_e}{m_i}\xi^{+}\right)^2\right)+\frac{1}{2}\xi^{+}S_i^{+}\left(\frac{S_e^{+}}{2}-S_i^{+}\right) \tag{4.59}$$

The two cases for the potential function with $S_e^+ = 2$ and $\xi^+ = 0.1$ are shown in Figures 4.18 & 4.19 with $m_e/m_i = 0.00055$.

Figure 4.19 shows the case for $\xi^+ = 0.5$, $\zeta_e^+ = 20$, where there are three operating points. In this situation the steady state achieved is determined by the initial conditions. If the initial ion slip is less than operating point (1) collisions dominate, which drives the ion fluid (slowly) toward (1). If the initial ion slip is greater than (1) but less than (2), the (+) RMF force density dominates which drives the ion fluid toward (1) (this is a very small region for the ion fluid). If the initial slip is less than (2) but greater than (3), collisions dominate, driving the ion fluid toward (3). The meaning of initial condition in this context is the slip at the time when the local value of ζ_e^+ becomes large enough for the existence of operating point (1).

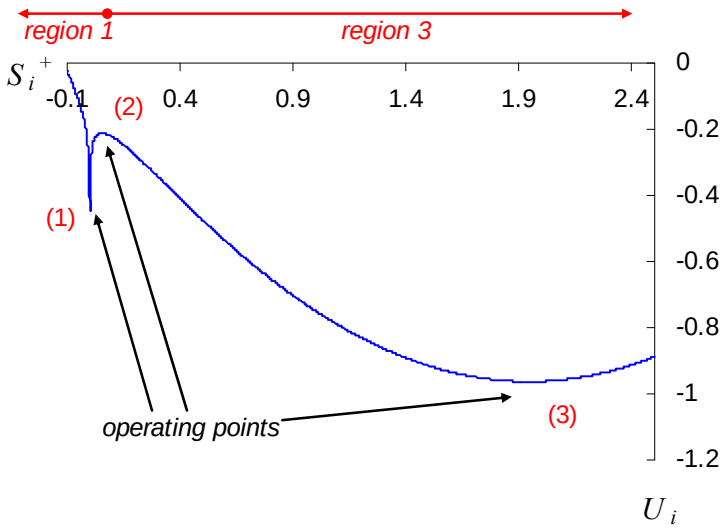

Figure 4.19. Potential function for the ion fluid for $\xi^+ = 0.5$, $\zeta_e^+ = 20$ showing net force density.

Figure 4.20 shows the case for $\xi^+ = 0.5$, $\zeta_e^+ = 1$, where there is now no small slip operating point. The net force density is always toward the zero current operating point (3), regardless of initial condition.

For the ion fluid, if the small slip operating point exists, there will be 3 operating points, and hence the operating point (1) can only be accessed from initial conditions in region 1. The only suitable initial condition for the ion fluid is that all layers of the ion fluid are in region 1, hence $S_i^+ < 0$.

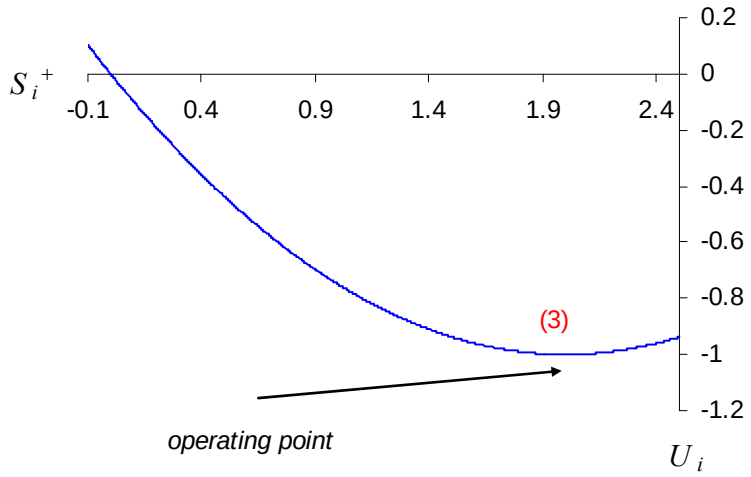

Figure 4.20. Potential function for the ion fluid for $\xi^+ = 0.5$, $\zeta_e^+ = 1$ showing net force density.

The situations shown in Figures 4.19 and 4.20 apply locally. For the case $\lambda^+ >> 1$ the initial penetration of the (+) RMF is significantly affected by the classical skin effect. If the classical skin effect were to dominate in the steady state, we would expect that only outer layers of the plasma would be captured, since the condition required for the existence of operating point (1)

$$\zeta_e^+(r)^2 > 4\left|\xi^+(r)\right|\left(1-\frac{\omega^-}{\omega^+}\right), \tag{4.60}$$

and hence entrainment, would only be satisfied only in the outer layers.

For the ion fluid there are two cases to consider. Firstly, the external magnitude of the (+) RMF may be too low, so that the boundary value of ζ_e^+ does not satisfy equation (4.60). This situation corresponds to Figure 4.20 at every layer and hence the ion fluid will not be captured, the only possible steady state being (3). Since the (+) RMF will be initially attenuated, the initial value of $\zeta_e^+(R)$ will be less than ζ_e^+(ext).

Secondly, the external magnitude of the (+) RMF may be sufficiently large so that the boundary value of ζ_e^+ satisfies equation (4.60). The initial penetration is determined by the classical skin effect, and hence ζ_e^+ will be large in outer layers, but small at inner layers. Outer layers will correspond to the situation shown in Figure 4.19 where the local value of ζ_e^+ is large enough to allow the existence of operating point (1). Since there is only one operating point at these layers, a steady state will be achieved with small slip. The inner layers will correspond to the situation shown in Figure 4.20 where the local value of ζ_e^+ is small and hence only operating point (3) exists. The initial capture of outer layers a leads to a large increase in the effective resistivity (with respect to the (+) RMF) and the effective skin depth in this layer. This will allow the (+) RMF to penetrate further in the plasma, increasing ζ_e^+ at successive layers where the situation in Figure 4.19 is achieved, where the operating point (1) exists. If the local value of S_i^+ at this layer is in region (1), then operating point (1) can be accessed allowing for further penetration of the (+) RMF. In this manner, the criterion required for complete penetration of the (+) RMF and entrainment of the ion fluid can be achieved successively as it penetrates the plasma. However, since the operating point (1) for the ion fluid is not unique (unless the magnitude of the (+) RMF is extremely large), the initial conditions for the ion fluid are essential for enhanced penetration of the (+) RMF. While an initial condition of $S_i^+ < 0$ (region 1) is suitable for capture of the outer layers of the ion fluid, it does not guarantee accessibility of the steady state for the inner layers, since they may have relaxed to region 3 before the local value of ζ_e^+ is large enough to allow the existence of operating point (1).

4.6 Initial Conditions for the Clemente Scheme

RMF current drive has been applied as both current generation and confinement schemes. The (-) RMF can be used to drive an electron current when the initial current is zero for sufficiently large values of γ^-. However it is not possible for the (+) RMF to drive an ion current when the initial ion current is zero, since the force density on the ion fluid is only significant for a very small region about $S_i^+ \cong \xi^+(m_e/m_i)$, (the (+) RMF applies negligible force when $S_i^+ = 1$). The Clemente scheme is therefore only applicable to confinement (although variation of either frequency may allow control of driven current).

The most likely scenario for the practical application of the Clemente scheme would involve the following sequence:

- A hot Field Reversed Configuration (FRC) is generated.
- The FRC is translated to a separate chamber.
- The (–) RMF is applied to the plasma to maintain the plasma current (and hence maintain the flux).
- The (+) RMF is applied to the plasma to entrain the ion fluid and prevent it from being dragged by the electron fluid through momentum transfer collisions.

When the Clemente Scheme is applied to a preformed FRC, since the electron and ion fluids are pre-rotating, the only requirement is to maintain the rotation of the two fluids. The RMFs may be applied so that the conditions required for enhanced penetration are satisfied by the initial conditions. The applied RMFs should be slightly smaller in frequency than the initial rotational frequency of the electron and ion fluids. This is a much less restrictive requirement than to begin with a non-rotating plasma.

It is not necessary that the ion fluid carry a significant amount of the current and the (+) and (-) RMFs need not be equal in magnitude. Having the electron fluid carry the majority of the current may be a useful initial condition for the Clemente scheme, since it minimises the effect of the (+) RMF on the electron fluid steady states. Since the

accessibility of the Clemente steady states will be strongly determined by the accessibility of the steady states for the ion fluid, we now consider possible initial conditions for the ion fluid in detail.

4.6.1 Rigid Rotor Initial Condition

The condition $S_i^+ \cong \xi^+ (m_e/m_i)$ is required for the effective resistivity with respect to the (+) RMF to become large. This condition must be satisfied for each layer of the ion fluid to allow capture by the (+) RMF. It is therefore necessary to start from suitable initial conditions where the ions rotate slightly faster than the (+) RMF, ie. the initial value for S_i^+ is small and negative. One possible initial condition is for the ion fluid to be initially rotating as a rigid rotor slightly faster than the (+) RMF, so that S_i^+ is initially small, negative and constant with r.

The initial penetration of the (+) RMF will be limited by the classical skin depth, hence the outer layers of the plasma will correspond to Figure 4.19 and the inner layers to Figure 4.20. Since the initial condition is in region 1, the outer layers of the ion fluid will relax collisionally to operating point (1), and be entrained by the (+) RMF. However by this time, the inner layers may have relaxed collisionally past the narrow slip range required for capture in this time to a slip greater than operating point (2). Due to the small value of S_i^+, which produces an increase in the effective resistivity and hence an increase in the effective skin depth in the outer layers, the (+) RMF will now penetrate further to the inner layers, but since the inner layers of the ion fluid have already relaxed to region 3, these layers will eventually relax to operating point (3), rotating synchronously with the electron fluid and the (-) RMF. In order to entrain the entire ion fluid, every layer of the fluid must be in region 1 when the local value of ζ_e^+ becomes large enough to provide for the existence of the operating point (1).

The (+) RMF penetration is not complete and is limited by the classical skin depth for the case where $\lambda^+ >> 1$ for a rigid rotor initial condition for the ion fluid when the (-) RMF has already penetrated (although not necessarily for the case where there is a rigid

rotor initial condition for both electron and ion fluid before the (-) RMF is applied, as will be discussed below). In the steady state, all but the outer layers of the ion fluid will rotate synchronously with the (–) RMF and hence the driven current will decay and the plasma equilibrium is lost.

4.6.2 Radial Profile Initial Condition

Another possible initial condition is to allow the initial ion slip to have a radial profile, where the slip increases with *r*. This allows each layer of the ion fluid to correspond to region (1) in Figure 4.19, when the local value of ζ_e^+ becomes large enough, and thus each layer successively passes the penetration criterion and attains the steady state operating point (1).

The condition $S_i^+ \cong \xi^+(m_e/m_i)$ must be satisfied for each successive layer of the ion fluid. Since the relaxation of the ions slip (through collisions with the electrons) may change the value of S_i^+ in the inner layers before the (+) RMF penetrates, it is required to choose a suitable radial profile for the initial value of S_i^+ to allow complete penetration and capture of all layers. Successive layers of the ion fluid become entrained by the (+) RMF as they relax (by momentum-transfer collisions with the electrons) to the favourable value of the slip $S_i^+ \cong (m_e/m_i)\xi^+$.

It should be noted here that the particular form of the initial ion slip profile is not critical. The ion fluid is entrained by the (+) RMF for any radial profile which allows each layer to successively relax through the very narrow range of slip where the force density on the ion fluid is appreciable, after the (+) RMF has already diffused up to this layer. If the (+) RMF diffuses to a layer after the ions have relaxed through this narrow slip range, the ions in this layer will not be captured, inhibiting further field penetration.

It is important to distinguish a difference between an initial condition for the ion fluid before the (-) RMF has penetrated, and an initial condition for the ion fluid after the (-) RMF has penetrated. While the steady states cannot be accessed if the ion fluid is rotating as a rigid rotor once the (-) RMF has penetrated (for $\lambda^+ >> 1$), a radial profile is

induced in the ion fluid by the act of penetration of the (-) RMF. If both the electron and ion fluid are initially rotating as a rigid rotor and the (-) RMF is applied first, then the outer layers of the electron fluid will be entrained first, with the inner layers relaxing significantly to the ion fluid. Since the ion fluid relaxation rate is proportional to ($v_{i\theta}$ - $v_{e\theta}$) the ion fluid relaxation rate will increase with r. This will have the effect of inducing a small radial profile on the ion fluid (with the inner layers rotating faster), which may allow complete entrainment of the ion fluid by the (+) RMF from the rigid rotor initial condition. When the plasma density is constant with r, once the (-) RMF has fully penetrated, the relaxation rate will now be constant with radius, and all layers of the ion fluid will be relaxing at the same rate. The layers will thus pass the favourable region for entrainment by the (+) RMF in sequence, thus allowing each layer to reach this region at a point when the local value of the magnitude of the (+) RMF is large enough to overcome the force due to collisions.

Since the penetration time of the (-) RMF increases with λ^{-}, this effect will be most pronounced when the plasma radius is much greater than the classical skin depth. This effect may be most important where the density is not constant with r. In this case, since the relaxation rate is proportional to $n(r)(v_{i\theta} - v_{e\theta})$, the variation of the velocity term is required to overcome the variation of the density term. The case of non-uniform density will be considered in Chapter 6.

4.6.3 Frequency Modulation

In practice, it may be extremely difficult to form an FRC with the profile of the ion rotational velocity tailored to suit the Clemente scheme. A more feasible alternative may involve decreasing the frequency of the (+) RMF gradually as it diffuses in and thus allowing the ion slip to remain small in each successive layer (Visentin, 2003). By decreasing the frequency of the (+) RMF, the value of S_i^{+} is decreased, and the favourable condition $S_i^{+} \cong \xi^{+}\left(m_e/m_i\right)$ may thus be reobtained.

For the case where ω is allowed to vary with time, quantities of the first group can be represented as a superposition of odd harmonics of $\left(\int \omega(t)dt - \theta\right)$

$$Q = \sum_{m=0}^{\infty} Q_{2m+1}(r)\exp i(2m+1)\left(\int \omega(t)dt - \theta\right) \tag{4.61}$$

Quantities of the second group can be represented as a superposition of a steady part (m = 0) and even harmonics of $\left(\int \omega(t)dt - \theta\right)$,

$$Q = \sum_{m=0}^{\infty} Q_{2m}(r)\exp i2m\left(\int \omega(t)dt - \theta\right) \tag{4.62}$$

where the effect of second and higher harmonics is small and may be neglected. Hence quantities of the first group are assumed to be functions of r only and quantities of the second group vary as

$$f(r)\exp i\left(\int \omega(t)dt - \theta\right) \tag{4.63}$$

For quantities of the second group,

$$\frac{\partial}{\partial t} = i\omega \qquad \frac{\partial}{\partial \theta} = -i \qquad \frac{\partial}{\partial z} = 0 \tag{4.64}$$

These relations are the same as for the case where ω is constant, and hence equations derived in sections 2.2 and 2.3 apply for the case where the frequency of either RMF is allowed to vary.

Consider the initial condition for the ion fluid to be initially rotating as a rigid rotor slightly faster than the (+) RMF, so that S_i^+ is initially small, negative and constant with r, but now allow the frequency of the (+) RMF to decrease. The initial penetration of the (+) RMF will again be limited by the classical skin depth, so that the outer layer corresponds to region (1) in Figure 4.19, and inner layers to Figure 4.20. The outer layers will be entrained (operating point 1), and the (+) RMF penetrates further, increasing the local value of ζ_e^+ so that the next layer corresponds to Figure 4.19. During the time required for the (+) RMF to penetrate, the next layer will have relaxed to point (3). By

decreasing the frequency of the (+) RMF, the slip is returned to region 1, and the layer can attain the operating point 1. Continuing to decrease the frequency of the (+) RMF allows each successive layer to be returned to region 1 and attain the operating point (1). This allows the entire ion fluid to be entrained by the (+) RMF, at which point the frequency is held constant to maintain the plasma current. The frequency of the (+) RMF should decrease at a rate greater than the ion relaxation time to allow complete penetration.

Frequency modulation once the Clemente steady states have been established may also allow the plasma current to be controlled. Increasing the frequency of either RMF increases the plasma current so long as both fluids remained entrained.

4.7 Summary of conditions required for the accessibility of the Clemente steady states

This chapter has outlined the conditions for the complete penetration of both the (-) and (+) RMF . The accessibility of the Clemente steady states requires the following.

(1) The penetration of the RMFs requires that the effective skin depth becomes sufficiently large for each RMF. It is demonstrated that the entrained steady states correspond to a greatly increased effective skin depth, and hence enhanced penetration of both the (-) and (+) RMF in the steady state. The enhanced penetration is decreased for the (-) RMF when the (+) RMF is applied, although having $\omega^- > \omega^+$ minimises this effect.

(2) For the steady states to be maintained requires critical values of $\gamma^{\pm}$ (the external magnitude of the RMFs must exceed a critical value). This critical value scales linearly with $\lambda^{\pm}$ for both RMFs.

(3) No special initial conditions are required for the electron fluid, since the steady state may be accessed from any initial condition if the external magnitude of the (-) RMF is sufficiently large. The critical value of γ^-

required to access the steady state for the electron fluid may be larger than that required to maintain it. The initial conditions for the ion fluid is that $S_i^+ < 0$ and that there is a radial profile on the ion slip (S_i^+ increases with radius). This initial condition may be overcome by allowing the frequency of the (+) RMF is decreased as it penetrates or by inducing a radial profile on the ion fluid by the application of the (-) RMF.

CHAPTER 5 PENETRATION OF THE RMFS AND ENTRAINMENT OF THE ELECTRON AND ION FLUIDS

In Chapter 3, it was demonstrated that there exist steady states where the electron and ion fluid rotate with small slips with respect to the (-) and (+) RMFs respectively. In Chapter 4, it was demonstrated that these steady states are possible for the entire plasma, where both the RMFs may penetrate much further than the classical skin depth. These "global" steady states are accessible by satisfying the conditions for entrainment layer by layer. It was also suggested that the accessibility of the steady states may be more easily achieved for the (-) RMF than for the (+) RMF, since the penetration of the (+) RMF is more sensitive to the initial conditions. We now present a numerical model of the Clemente scheme, analysing the accessibility of the steady states by simulation. Simulation results will be presented showing that the Clemente steady states are accessible, analysing the transient behaviour of the plasma, and outlining the initial conditions and RMF magnitudes required for accessibility of the steady states for both the (-) and (+) RMFs.

In this section the penetration and entrainment of the electron and ion fluids is considered for a model in which the radial motion is suppressed. The effect of radial motion is included in Chapter 6, where a preformed FRC model will be considered. Section 5.1 outlines the physical model and equations of motion, section 5.2 the numerical method employed, section 5.3 presents the initial conditions and in section 5.4 the boundary conditions are considered. Simulation results are presented in sections 5.5

and 5.6, for the penetration of the (-) RMF and the (+) RMF, respectively. Section 5.7 summarises the simulation results presented in this chapter.

5.1 Physical model and equations of motion

The physical model considered is that outlined in section 2.1. The *r*-component of the plasma velocity is a quantity of the first group, and hence it must vanish in the steady state. This is a result of the continuity equation (equation (6.17)) which shows that for the density to be constant requires that v_r vanishes if there are no sources or sinks. A complete analysis of the transient behaviour of the plasma should allow for the motion of the plasma in the *r*-direction and the consequent adjustment of the radial profile of the plasma pressure. These effects, however, are not essential for the study of the penetration of the RMF into the plasma and would introduce unnecessary complications. Hence the simulations presented here have the radial motion of the plasma suppressed. The motion of the plasma in the radial direction will be introduced in Chapter 6 in the study of the Clemente scheme applied to an FRC.

The equations of motion to be numerically modelled are those given as equations (2.60) to (2.66) in section 2.3.

$$\frac{\partial A_z^{\pm}}{\partial t} = \left(\frac{\eta^{*\pm}}{\mu_0} \nabla^2 A_z^{\pm} - i\omega^{\pm} A_z^{\pm} \right) \Bigg/ \left[\frac{1}{S_e^{\pm}} + \frac{m_e}{m_i} \left(\frac{1}{S_i^{\pm}} - 1 \right) \right] \tag{5.1}$$

$$\frac{\partial B_z}{\partial t} = \frac{\eta}{\mu_0} \nabla^2 B_z - \frac{1}{r} \frac{\partial}{\partial r} r \left(\left\langle v_{ez}^{-} B_r^{-} \right\rangle + \left\langle v_{ez}^{+} B_r^{+} \right\rangle \right) \tag{5.2}$$

$$\frac{\partial P_\theta}{\partial t} = \frac{1}{n} \left\langle J_z^{-} B_r^{-} + J_z^{+} B_r^{+} \right\rangle \tag{5.3}$$

$$v_{i\theta} = \frac{1}{(m_e + m_i) n} \left(P_\theta + \frac{m_e J_\theta}{e} \right) \tag{5.4}$$

$$v_{e\theta} = \frac{1}{(m_e + m_i) n} \left(P_\theta - \frac{m_i J_\theta}{ne} \right) \tag{5.5}$$

$$J_\theta = -\frac{1}{\mu_0} \frac{\partial B_z}{\partial r} \tag{5.6}$$

$$J_z^{\pm} = -\frac{1}{\mu_0}\nabla^2 A_z^{\pm} \tag{5.7}$$

$$\eta^{*\pm} \cong \eta\left(\frac{1}{S_e^{\pm}} + \frac{m_e}{m_i}\frac{1}{S_i^{\pm}} + i\frac{1}{\xi^{\pm}}\right) \tag{5.8}$$

5.2 Numerical Method

Equations (5.1) to (5.3) are solved numerically using a semi-implicit finite difference approximation with a variable time step. The divergence of equation (5.1), when

$$\frac{1}{S_e^{\pm}} + \frac{m_e}{m_i}\left(\frac{1}{S_i^{\pm}} - 1\right) \approx 0\,, \tag{5.9}$$

is overcome by decreasing the time step whenever this relation becomes small. This does not mean that the time derivative of the vector potential becomes large, but rather that $\frac{\eta^{*\pm}}{\mu_0}\nabla^2 A_z^{\pm} \approx i\omega A_z^{\pm}$ when the condition in equation (5.9) occurs.

The results are expressed in terms of the dimensionless parameters

$$\lambda^{\pm} = R\left(\frac{\omega^{\pm}\mu_0}{2\eta}\right) \text{ and } \gamma^{\pm} = \frac{B_{\omega}^{\pm}}{ne\eta}\,. \tag{5.10}$$

The driven current is presented as the dimensionless parameter α, the ratio of the driven current per unit length to the maximum possible steady state current, which is synchronous rotation with the RMFs.

$$\alpha = \frac{I}{I_{\max}} = \frac{\frac{1}{\mu_0}\left(B_z(R) - B_z(0)\right)}{\int ne\left(\omega^{+} - \omega^{-}\right)rdr} \tag{5.11}$$

Since the Clemente steady states correspond to small slips of the electron and ion fluid with respect to the (-) and (+) RMF respectively, for the Clemente steady states α will by slightly less than one.

Equations (5.1) to (5.3) are solved numerically using a finite difference scheme on a one-dimensional grid. The value of B_z at grid point i and time $t + \Delta t$ for example, (denoted $B_z(i, t + \Delta t)$) is approximated by

$$B_z(i,t+\Delta t) = B_z(i,t) + \frac{1}{2}\Delta t \frac{dB_z}{dt}(i,t) + \frac{1}{2}\Delta t \frac{dB_z}{dt}(i,t+\Delta t). \tag{5.12}$$

The derivatives at $t + \Delta t$ are to be evaluated in terms of the yet unknown values of the variables at $t + \Delta t$. The numerical scheme would be fully implicit if the resulting set of simultaneous equations could be solved for the updated values of the variables. This cannot be easily performed however, since the equations are nonlinear. We solve these equations approximately by simple iteration. Equations (5.1) to (5.8) are iterated until an error function is less than a given tolerance. The error function is determined by

$$\varepsilon = \left| \frac{\left(A_z - A_z'\right)^2}{A_z^{\,2}} \right| + \left| \frac{\left(B_z - B_z'\right)^2}{B_z^{\,2}} \right| \tag{5.13}$$

Where A_z' and B_z' are the values from the previous iteration. The iteration is found to converge to any desired accuracy provided that the time step Δt is not too large. Radial derivatives are calculated using a 3-point centred approximation at general points, except near the boundary where non-centred derivates are used.

5.3 Boundary Conditions

The boundary condition for the vector potential for this physical model (Hugrass & Grimm, 1981) is:

$$A_z^{\pm}(R) = 2A_{ext}^{\pm} - R\left.\frac{\partial A_z^{\pm}}{\partial r}\right|_{r=R} \tag{5.14}$$

where A_{ext} is the phasor of the externally applied RMF at $r = R$, and R is the radius of the plasma column.

In the presence of flux conserving rings the boundary condition for B_z is determined from the conservation of magnetic flux, with flux-preserving rings at radial distance b. At $t = 0$, there is a constant axial field $B_z(r, \theta, 0) = B_a$, giving an initial axial flux

$$\Phi_z(0) = \int_0^b B_a dA = \pi b^2 B_a . \tag{5.15}$$

After the RMF has been applied, the axial flux is given by

$$\Phi_z(t) = \int_0^b B_z(r,\theta,t) dA = \int_0^R r dr \int_0^{2\pi} d\theta\, B_z(r,\theta,t) + B_a \int_R^b dA . \tag{5.16}$$

Conservation of flux provides a boundary condition for B_z,

$$B_z(R,t) = \frac{b^2 B_a}{b^2 - R^2} - \frac{2}{b^2 - R^2} \int_0^R r B_z(r,t) dr . \tag{5.17}$$

Since B_z is an even function, and A_z an odd function with r,

$$\left.\frac{\partial B_z}{\partial r}\right|_0 = 0 \tag{5.18}$$

$$A_z^{\pm}(0) = 0 \tag{5.19}$$

The boundary values of A_z and B_z and their derivates are determined from three point non-centred difference on the uniform grid.

$$\left.\frac{\partial A_z^{\pm}}{\partial r}\right|_R = \frac{1}{2\Delta r}\left(3A_z^{\pm}(R) - 4A_z^{\pm}(R-\Delta r) + A_z^{\pm}(R-2\Delta r)\right) \tag{5.20}$$

$$\left.\frac{\partial B_z}{\partial r}\right|_R = \frac{1}{2\Delta r}\left(3B_z(R) - 4B_z(R-\Delta r) + B_z(R-2\Delta r)\right) \tag{5.21}$$

$$\left.\frac{\partial A_z^{\pm}}{\partial r}\right|_0 = \frac{1}{2\Delta r}\left(-3A_z^{\pm}(0) + 4A_z^{\pm}(\Delta r) - A_z^{\pm}(2\Delta r)\right) \tag{5.22}$$

$$B_z(0) = \frac{1}{3}\left(4B_z(\Delta r) - B_z(2\Delta r)\right) \tag{5.23}$$

$$A_z^{\pm}(R) = \frac{4A_{ext}^{\pm} + R\left(4A_z^{\pm}(R-\Delta r) - A_z^{\pm}(R-2\Delta r)\right)}{2\Delta r + 3R} \tag{5.24}$$

Outside plasma the current density is zero (no charge carriers) hence

$$\nabla \times B = 0 \qquad \text{and} \qquad \nabla^2 A_z = 0 \qquad r \geq R\,. \tag{5.25}$$

5.4 Initial conditions

The plasma is initially rotating before the RMFs are applied. The initial rotational velocities are chosen so that the initial rotational frequency of both electron and ion fluid are slightly larger than the RMF frequencies. As shown in Chapter 4, the initial condition of negative slip is essential for the (+) RMF, although not for the (-) RMF. Hence the initial current will be larger than the current for the Clemente steady states. The initial current therefore has α slightly larger than 1.

The (-) RMF is applied first to entrain the electron fluid. After a suitable time delay, t_D the (+) RMF is applied. The externally applied RMFs rise exponentially with rise times τ_r^- and τ_r^+ (determined by the source used to generate the RMFs) After both RMFs have fully penetrated the plasma (delay time t_d), the external magnitudes may be decreased. The standard results presented use the initial condition that the ions counter-rotate with the initial current evenly distributed between electron and ions, hence $\omega_e = -\omega_i$, and the rotation frequency is constant with radius for both the electron and ion fluids. We also choose the RMF frequencies to be equal in magnitude, $|\omega^+| = \omega^-$, for the majority of simulations presented in this chapter.

Typical plasma parameters are:

R = 10 cm

b = 15 cm

$n = n_e = n_i = 1 \times 10^{18}$ m^{-3}

$\omega_e = -\omega_i = 5.5$ MHz $(= 1.1\omega^-)$

$S_e^- = -0.1$

$S_i^+ = -0.1$

$\eta = 1 \times 10^{-4}\ \Omega\ m^{-1}$

$\nu_{ei} = 2.81 \times 10^6$ Hz

$m_e/m_i = 5.45 \times 10^{-4}$

Typical RMF parameters are

$\tau_r^- = \tau_r^+ = 1\ \mu s$

$t_D = 10\ \mu s$

$t_d = 100\ \mu s$

$\omega^- = -\omega^+ = 5$ MHz

$B_\omega^- = B_\omega^+ = 10$ G

$\lambda^- = \lambda^+ = 17.7$

$\xi^- = \xi^+ = 0.56$

$\gamma^- = \gamma^+ = 50$

The dimensionless parameter $\lambda^\pm$ is varied by changing the value of η, while keeping n constant. This is equivalent to changing the plasma temperature. The dimensionless parameter $\gamma^\pm$ is varied by changing the value of $B_\omega^\pm$. Typical values used for the numerical method are: $\Delta t = 1 \times 10^{-10}$ s, $\varepsilon = 1 \times 10^{-10}$.

5.5 Simulation Results – (-) RMF

We first consider the standard case where one RMF is applied. It is well known (Hugrass, 1985) that this RMF penetrates into the plasma when γ^- is larger than a certain critical value γ_c^- which depends on λ^-. If there is no applied RMF, the driven current decays with the electron relaxation time. If the (-) RMF is applied with $\gamma^- > \gamma_c^-$, the initial driven current decays during the transient phase as the (-) RMF penetrates the plasma. A quasi-steady state is then established where the electron fluid rotates synchronously with the (-) RMF. The driven current then decays approximately with the ion relaxation time. The time for the current to decay is also effected by the field

momentum relaxation. Figure 5.1 shows α against time for these two cases, for $\lambda^- = 17.7$, $\gamma^- = 50$.

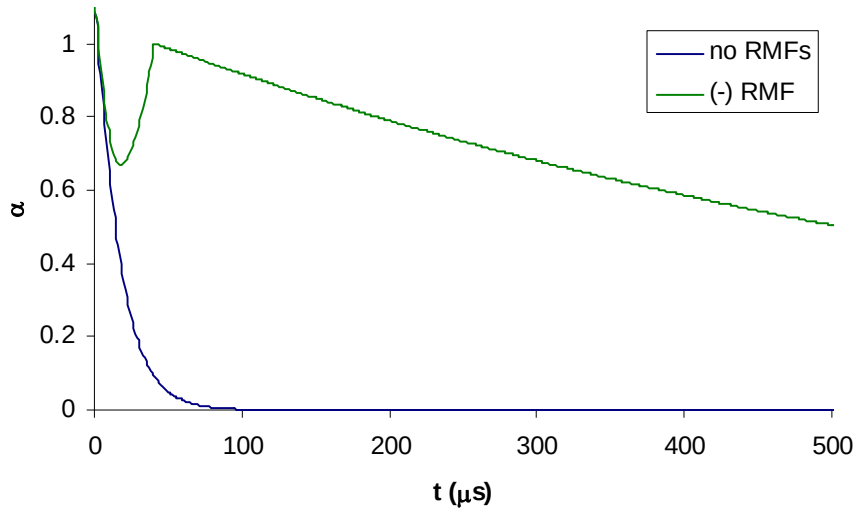

Figure 5.1. α against time for (i) no applied RMFs and (ii) (-) RMF applied with $\gamma > \gamma_c$.

Figure 5.2 shows a series of plots of B_z and J_θ against r/R at various time intervals where the (-) RMF is applied at $t = 0$, with $\lambda^- = 17.7$, $\gamma^- = 50$ ($B_\omega^- = 20$ G). At $t = 0$, the initial conditions are shown, where there is a driven current which in the absence of an applied RMF would decay through collisions. At $t = 10$ μs, the current has begun to decay, since the magnitude of the (-) RMF is not yet large enough to capture the inner layers of the electron fluid, the J_θ plot demonstrating that the driven current is mainly in the outer layers, which have been entrained by the (-) RMF. By $t = 50$ μs, the entire electron fluid is rotating synchronously with the (-) RMF, returning to a state similar to the initial conditions. The J_θ curve demonstrates that the driven current is through all layers. At $t = 0.1$ ms there is little change, and hence a quasi steady state has been achieved which is maintained over a time scale smaller than the ion relaxation time. At $t = 0.5$ ms there is a significant decay of the total driven current, with J_θ showing that the current decay is uniform throughout the plasma. By $t = 2$ ms, the driven current has completely decayed, with now both the electron and ion fluid rotating synchronously with the (-) RMF. This is the true steady state for a single applied RMF.

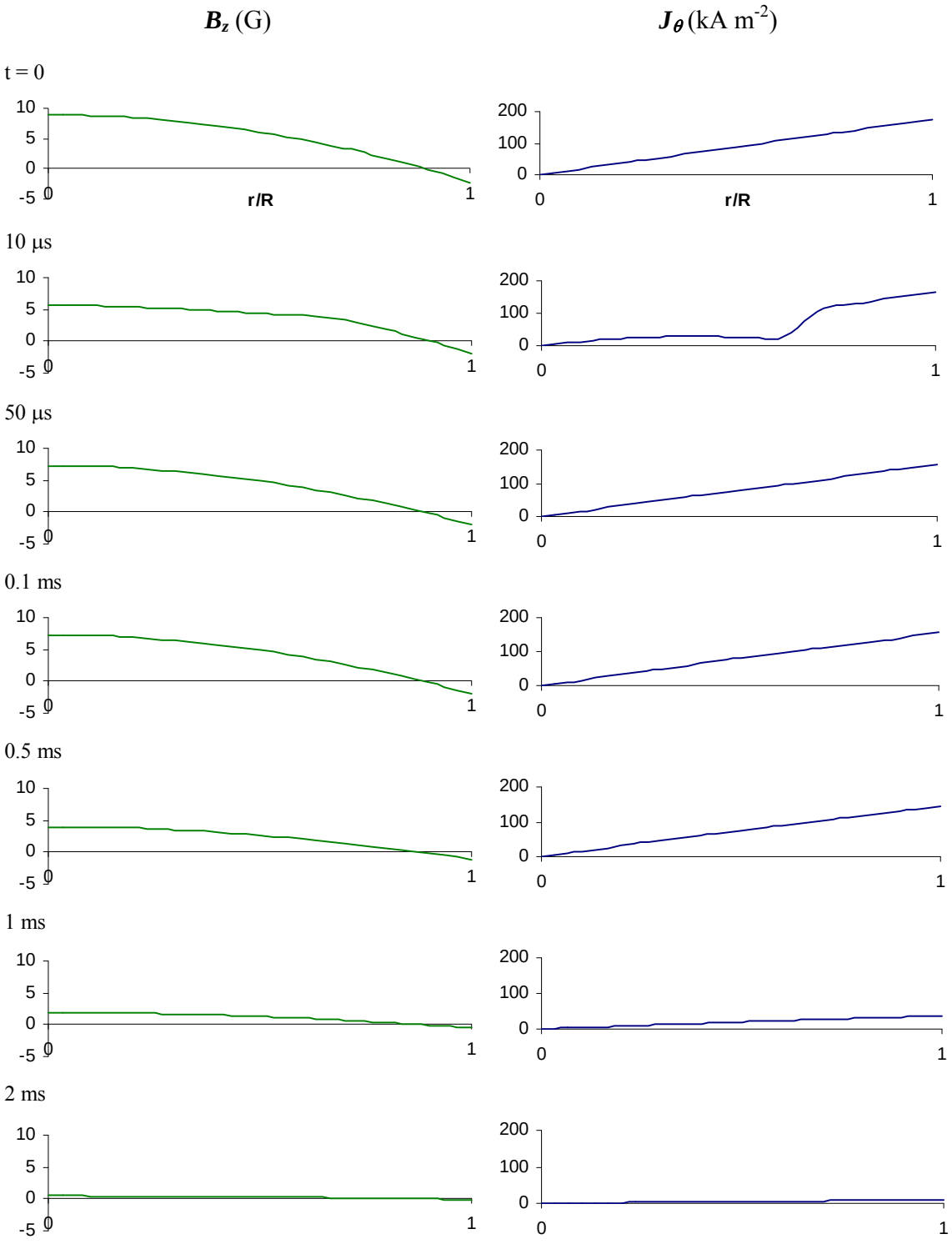

Figure 5.2. B_z and J_θ against r/R at selected time intervals for one applied RMF ($\lambda^- = 17.7$, $\gamma^- = 50$) where $\gamma^- > \gamma_c^-$.

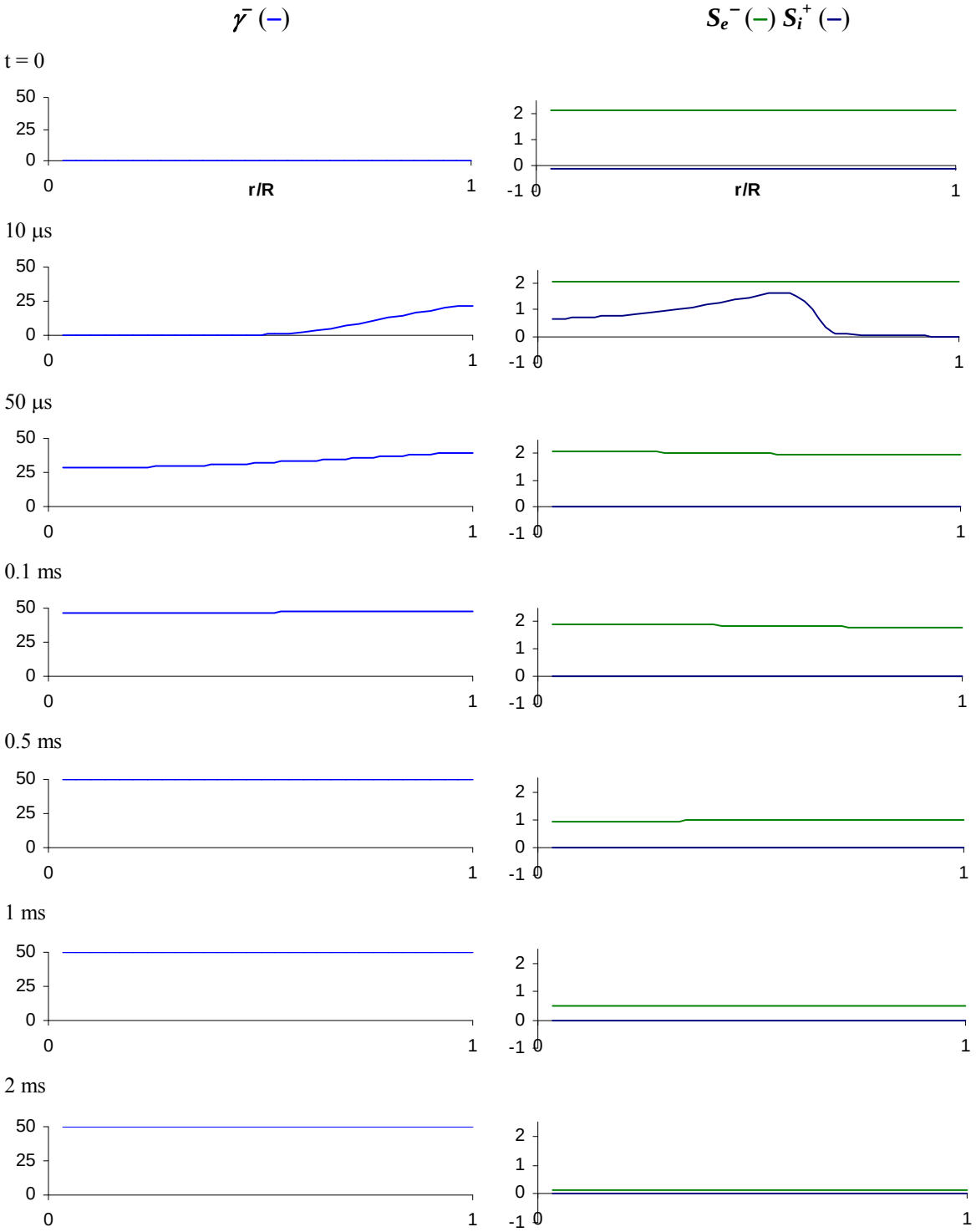

Figure 5.3. Local values of $\bar{\gamma}$, S_e^- and S_i^- against *r/R* at selected time intervals for one applied RMF ($\bar{\lambda}$ = 17.7, $\bar{\gamma}$ = 50) where $\bar{\gamma} > \gamma_c^-$.

Figure 5.3 shows plots of the local value of γ^-, and the slips of the electron and ion fluids (with respect to the (-) RMF) against *r/R* at various time intervals, for the same simulation as in Figure 5.2 ($\lambda^- = 17.7$, $\gamma^- = 50$, $B_\omega^- = 20$ G). At $t = 0$, the plots show the initial conditions, where the external value of B_ω^- is zero, and hence γ^- is everywhere zero. The electron and ion slips have initial values of $S_e^- = -0.1$, and $S_i^- = 2.1$. At $t = 10$ μs the penetration of the (-) RMF is limited to outer layers, and the electron fluid has relaxed at inner layers where the local value of γ^- is small. By $t = 50$ μs, the (-) RMF has fully penetrated, with the local value of γ^- approaching the maximum value everywhere. The entire electron fluid now rotates almost synchronously with the (-) RMF at all layers (with small slip), returning to a state similar to the initial conditions The $t = 0.1$ ms plots show little change apart from saturation of γ^-, and hence a quasi steady state has been achieved which is maintained over a time scale smaller than the ion relaxation time. The $t = 0.5$ ms shows that while the penetration of the (-) RMF is maintained, the ion fluid has relaxed significantly. By $t = 2$ ms the true steady state has been achieved, where both the electron and ion fluid now rotate almost synchronously with the (-) RMF.

The other case of interest for a single applied RMF is when the magnitude of the (-) RMF is not sufficient to entrain the electron fluid, where $\gamma^- < \gamma_c^-$. Figure 5.4 shows a series of plots of B_z and J_θ against *r/R* at various time intervals, where $\lambda^- = 17.7$, $\gamma^- = 25$ ($B_\omega^- = 10$ G). At $t = 0$, the plots show the initial conditions, where there is a driven current which in the absence of an applied RMF would decay through collisions. At $t =$ 10 μs, the current has begun to decay, since the penetration of the (-) RMF is not large enough to capture the inner layers of the electron fluid, the J_θ plot demonstrating that the driven current is only in the outer layers. By $t = 50$ μs, the driven current has almost completely decayed, with only a small driven current in outer layers. The steady state where the electrons rotate synchronously with the ion fluid has been achieved on a time scale of the electron relaxation time when $\gamma^- < \gamma_c^-$.

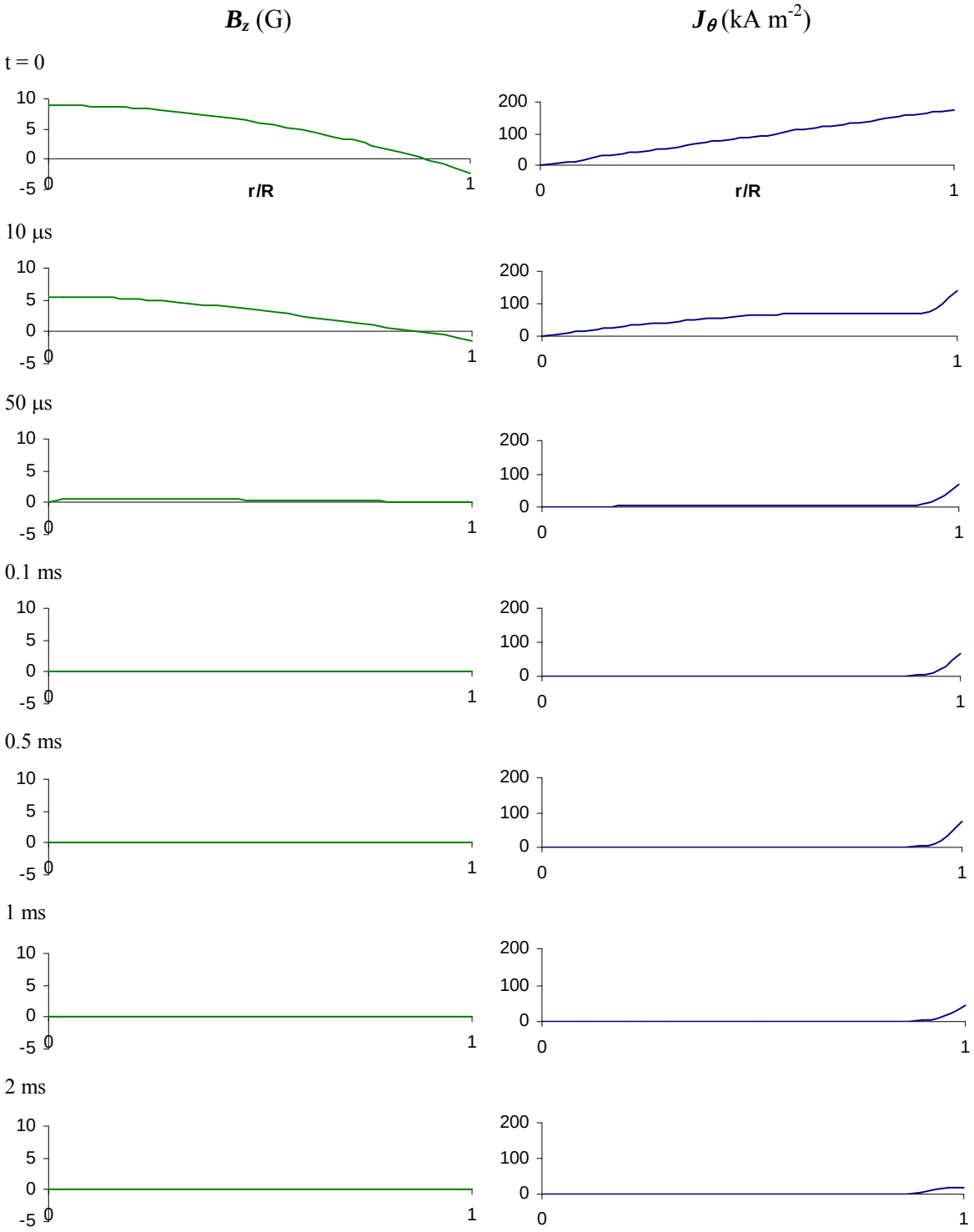

Figure 5.4. B_z and J_θ against r/R at selected time intervals for one applied RMF ($\lambda^- = 17.7$, $\gamma^- = 25$) where $\gamma^- < \gamma_c^-$.

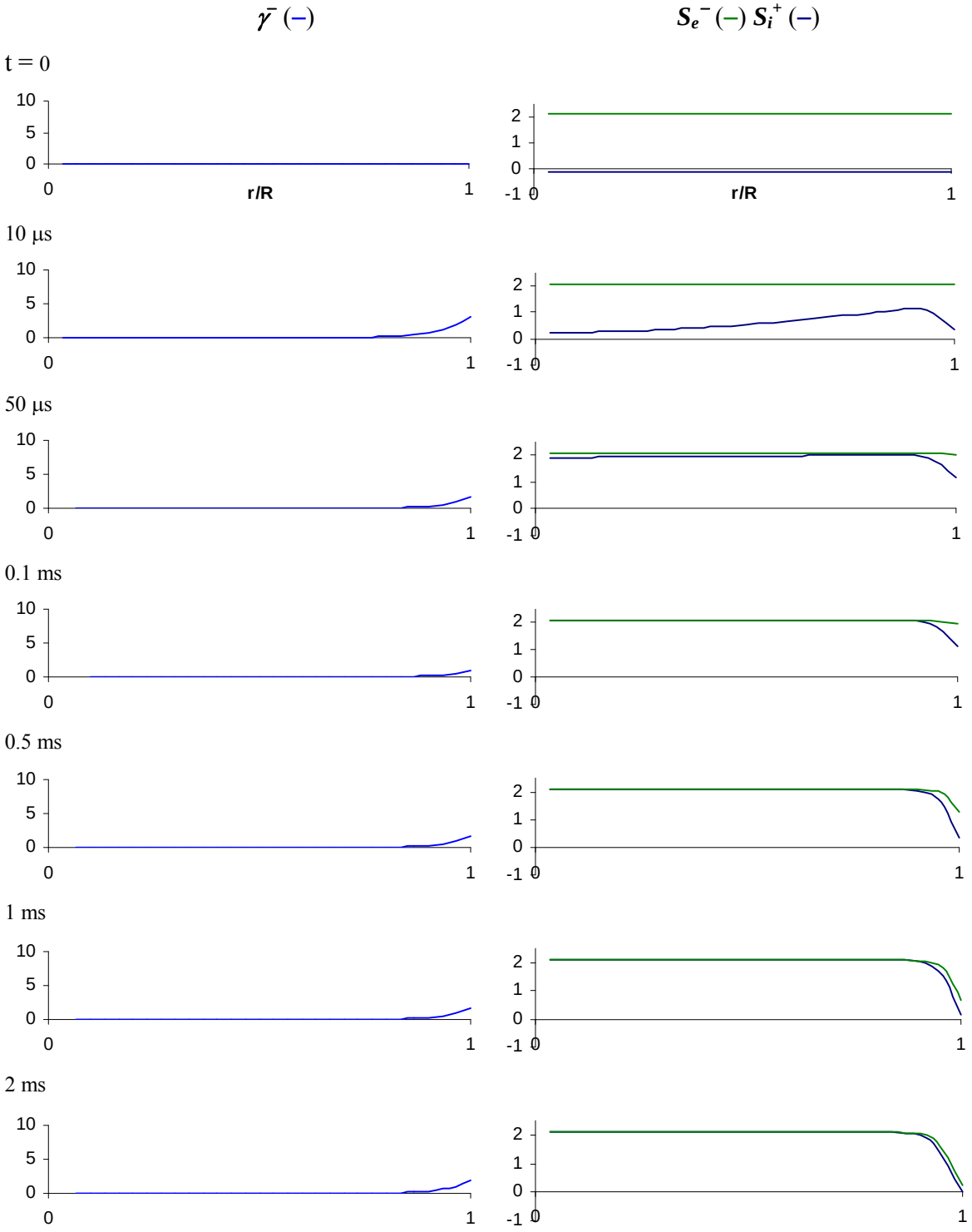

Figure 5.5. Local values of γ^-, S_e^- and S_i^- against *r/R* at selected time intervals for one applied RMF where $\gamma^- < \gamma_c^-$.

Figure 5.5 shows plots of the local value of γ^-, and the slips of the electron and ion fluids (with respect to the (-) RMF) against *r/R* at various time intervals, for $\lambda^- = 17.7$, $\gamma^- = 25$ ($B_\omega^- = 10$ G). At $t = 0$, the plots show the initial conditions, where the external value of B_ω^- is zero, and hence γ^- is everywhere zero. At $t = 10$ μs the penetration of the (-) RMF is limited to outer layers, and the electron fluid has relaxed at inner layers where the local value of is γ^- small. By $t = 50$ μs, the (-) RMF has failed to penetrate, with the local value of γ^- highly attenuated. The electron fluid now rotates almost synchronously with the ion fluid at all layers with $S_e^- \approx 2$, except in the very outer layers where it is affected by the (-) RMF. The penetration of the (-) RMF is highly attenuated and limited to outer layers and the electron fluid rotates synchronously with the ion fluid. The steady state has been achieved on a time scale of the electron relaxation time when $\gamma^- < \gamma_c^-$, except in the very outer layers, where the driven current decays with the ion relaxation time.

The above results demonstrate the existence of a critical value, γ_c^-, above which the electron fluid will be entrained by the (-) RMF. As demonstrated in section 4, this critical value required to entrain the electron fluid is dependant on λ^-, and also on the initial conditions for the ions, since the collisional force which the (-) RMF must oppose is proportional to $(\omega_i - \omega_e)$. As the Clemente scheme requires that the ions are initially in motion, the dependence of γ_c on initial ion slip should be considered when choosing a suitable value for the magnitude of the (-) RMF. For the initial condition considered here ($\omega_i = -\omega_e$) we expect that the critical value γ_c^- to be larger than that for the case when the ions are initially stationary for the same value of ω_e. The effect of the ion initial condition on the penetration of the (-) RMF is most easily seen if we constrain the ion motion by setting $m_i = \infty$.

Figure 5.6 shows the steady state value of the normalised current per unit length (α_{ss}) plotted against γ^- for two cases of the ion rotation (i) $S_i^- = 1.1$ (the ions have a rotation rate one tenth of the electron rotation rate) and (ii) $S_i^- = 2$ (the ions have a rotation rate equal in magnitude electron rotation rate) with $\lambda^- = 5.61$. For the initial condition $S_i^- = 1.1$, the observed value of $\gamma_c^- \approx 7$ is slightly larger than for earlier studies of the fixed-ion

model for the same value of λ^- (Milroy, 1999). For the ion fluid counter-rotating with the same frequency magnitude as the electron fluid, $\gamma_c^- \approx 10$ is significantly larger, as expected due to the larger ion drag on the electron fluid, which must be opposed by the (-) RMF.

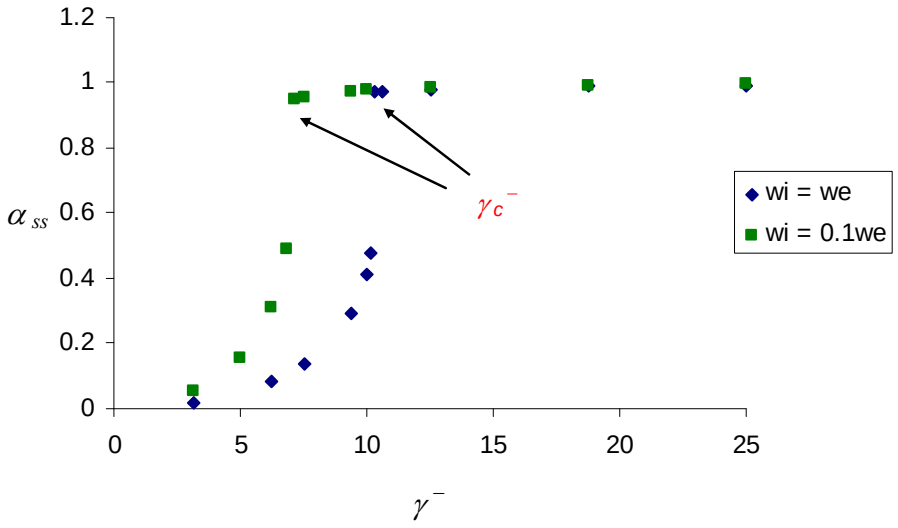

Figure 5.6. The steady state value of the normalised current per unit length α_{ss} plotted against γ^- for (i) $S_i^- = 1.1$ and (ii) $S_i^- = 2$ with $\lambda^- = 5.61$.

The critical value of γ^- is dependent on λ^-. For $\lambda^- > 6$, there are two critical values of γ^- (Hugrass, 1985). $\gamma_c^-(a)$ is the magnitude required to access the steady state, while $\gamma_c^-(b)$ is the magnitude required to maintain the steady state (hence $\gamma_c^-(b) \leq \gamma_c^-(a)$). The second critical value is found by decreasing the magnitude of the (-) RMF once it has completely penetrated the plasma. The RMF magnitude required to access the steady state is greater than that required to maintain the steady state. Figure 5.7 shows the steady state value of α, (α_{ss}) for two values of λ^- ($\lambda^- = 5.61$ and $\lambda^- = 12.5$) where $\omega_i = -\omega_e$ ($S_i^- = 2$) where the ions are fixed ($m_i = \infty$). For the case $\lambda^- = 5.61$, there is only one critical value, the (-) RMF cannot be reduced below $\gamma_c^-(a)$ once the RMF has fully penetrated. However, for $\lambda^- = 12.5$, there are two critical values, the magnitude of the (-) RMF may be significantly reduced once entrainment of the electron fluid is achieved.

These values are larger than that found by previous studies, for the case of no ion rotation.

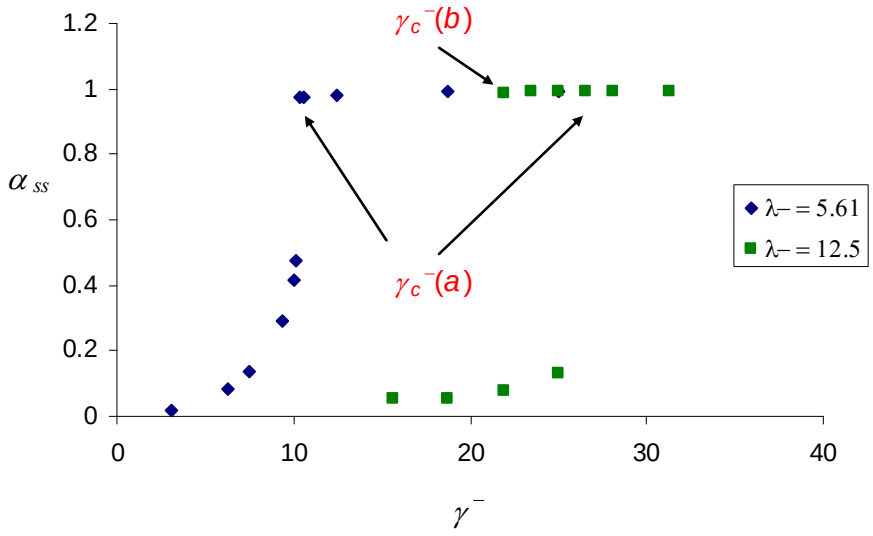

Figure 5.7. The steady state value of the normalised current per unit length α_{ss} plotted against γ^- for (i) $\lambda^- = 5.61$, and (ii) $\lambda^- = 12.5$.

Figure 5.8 shows the scaling of the two critical values of γ^- with λ^-, for the case $\omega_i = -\omega_e$ ($S_i^- = 2$) where the ions are fixed ($m_i = \infty$).. For low values of λ^-, the critical value required for field penetration is the same as that for expulsion. For $\lambda^- > 6$, the critical value required for field expulsion is greater than that for penetration. This demonstrates that the magnitude of the (-) RMF required to maintain the steady state becomes much less than that required to access the steady state. The study by Milroy (1999) found that $\gamma_c^-(b) = 1.12\lambda^-$ for expulsion when there is no ion motion, Figure 5.8 shows that the critical value is larger when the ions are initially counter-rotating. This is expected since the force due to collisions is proportional to ($\omega_e - \omega_i$), which the (-) RMF must overcome to access the steady state. For large values of λ^-, the magnitude of the (-) RMF may be significantly reduced once the electron fluid is entrained.

The effect of the initial conditions on the ion fluid is to increase both the critical value of γ^- required to access the steady state for the electron fluid, $\gamma_c^-(a)$, and the critical value

required to maintain the steady state, $\gamma_c^-(b)$. This is equivalent to rescaling the definition of λ^- in terms of $(\omega^- - \omega_i)$ rather than ω^-.

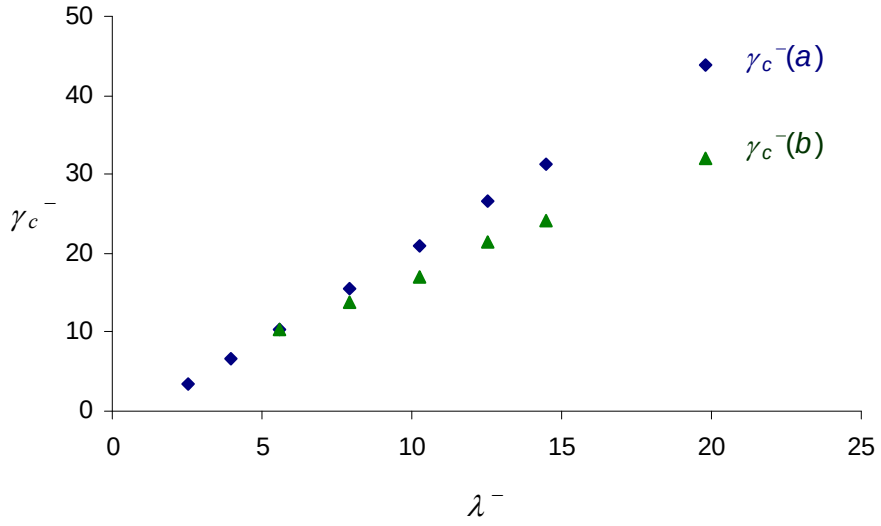

Figure 5.8. Critical values of γ_c^- for complete penetration, $\gamma_c^-(a)$ and expulsion, $\gamma_c^-(b)$ against λ^-.

5.6 Simulation Results – (+) RMF

Now we consider the case where the (+) RMF is applied. It has been demonstrated in Chapter 4 that there will be a critical value of γ^+ for entrainment of the ion fluid. Firstly we consider a case where the ions are initially rotating as a rigid rotor (i.e. the slip with respect to the (+) RMF is initially constant with radius). The (-) RMF is applied first to entrain the electron fluid. The (+) RMF is applied after a short time delay ($t_D = 50$ μs) during which time the outer layers of the electron fluid are entrained and the (-) RMF partially penetrates the plasma.

Figure 5.9 shows the driven current against time for three cases for $\lambda^- = \lambda^+ = 17.7$. Firstly, if there is no applied RMF, the current decays due to collisions in the electron relaxation time. The steady state achieved is the electron fluid rotating synchronously with the ion fluid. If the (-) RMF is applied only (with $\gamma^- > \gamma_c^-$), then the electron fluid

will be entrained by the (-) RMF. However the current now decays with the ion relaxation time, since the ion fluid relaxes due to collisions with the electron fluid and under the force due to the (-) RMF on the ion fluid. If both the (-) and (+) RMFs are applied (with $\gamma > \gamma_c$, for both RMFs) the current may be maintained indefinitely.

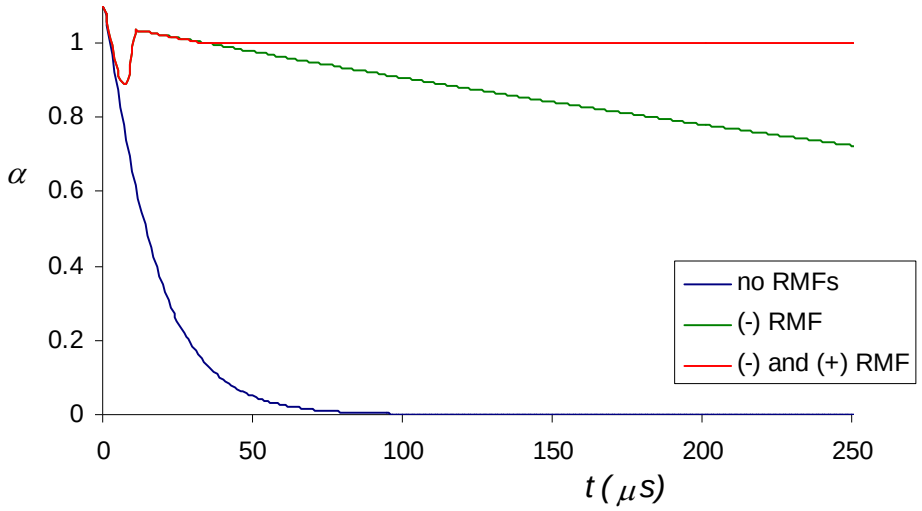

Figure 5.9. Normalised current, α against time for (i) no applied RMFs, (ii) (-) RMF applied with $\gamma > \gamma_c$ and (iii) 2 applied RMFs with $\gamma^{\pm} > \gamma_c^{\pm}$. ($\lambda^- = \lambda^+ = 17.7$, $\gamma^- = \gamma^+ = 312$).

Figure 5.10 shows a series of plots of B_z and J_θ against r/R at various time intervals, where $\lambda^+ = \lambda^- = 17.7$, $\gamma^+ = \gamma^- = 312$ ($B_\omega{}^+ = B_\omega{}^- = 50$ G). At $t = 0$, the initial conditions are shown, where there is a driven current which in the absence of an applied RMF would decay through collisions. At $t = 10$ μs, the (-) RMF has entrained the outer layers of the electron fluid, but has not yet captured the inner layers. By $t = 50$ μs, the entire electron fluid is rotating synchronously with the (-) RMF, returning to a state similar to the initial conditions. The J_θ curve demonstrates that the driven current is through all layers. At $t = 0.1$ ms there is little change, and hence a quasi steady state has been achieved which is maintained over a time scale smaller than the ion relaxation time. At $t = 0.5$ ms the total driven current has been maintained, since the (+) RMF has entrained the ion fluid. Subsequent plots show that a true steady state has been achieved, with the

driven current being maintained indefinitely. The Clemente steady states have been accessed since $\gamma^- > \gamma_c^-$ and $\gamma^+ > \gamma_c^+$.

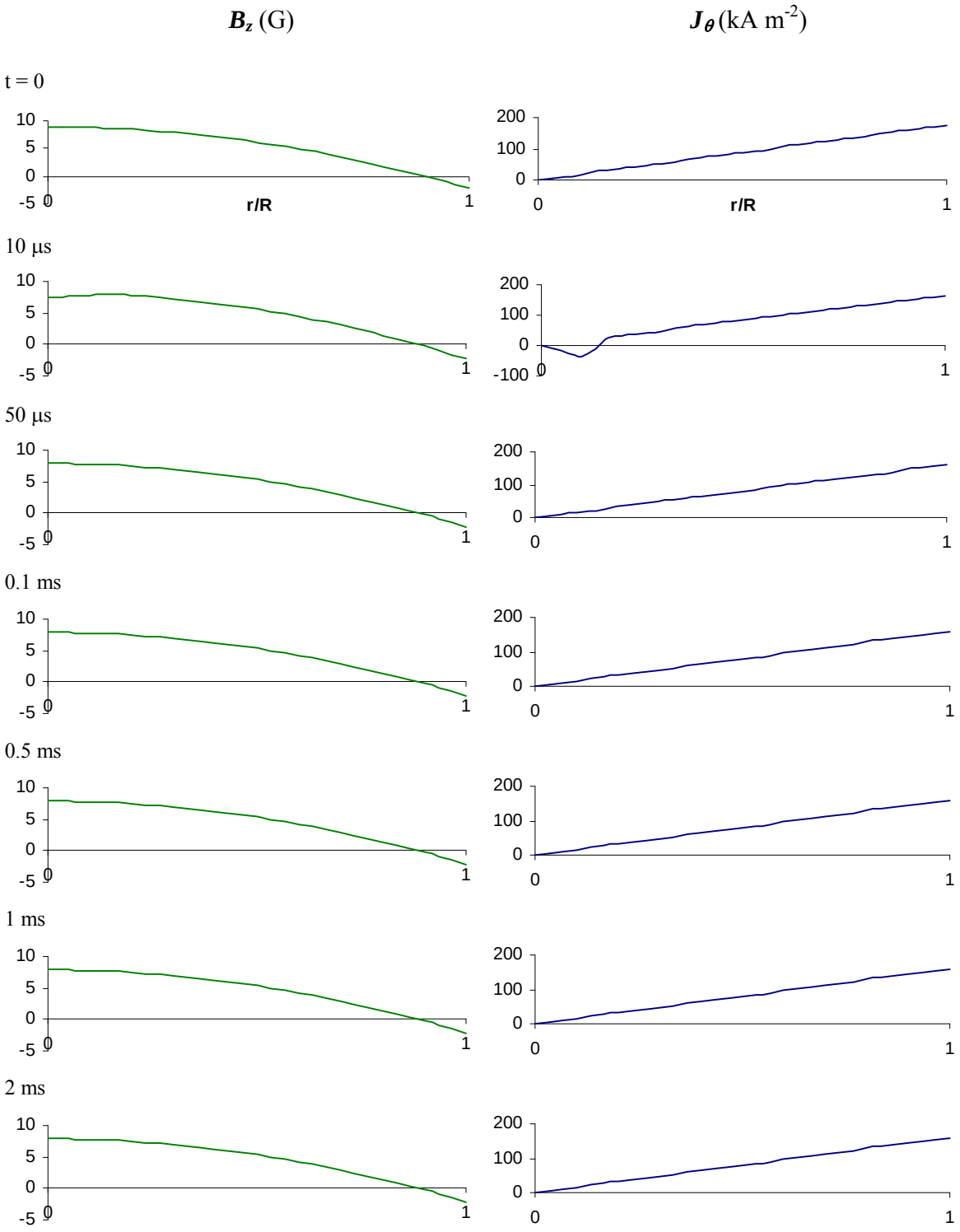

Figure 5.10. B_z and J_θ against r/R at selected time intervals for two applied RMFs ($\lambda^- = \lambda^+ = 17.7$, $\gamma^- = \gamma^+ = 312$) where $\gamma^+ > \gamma_c^+$.

Figure 5.11 shows plots of the local values of γ^- and γ^+, and the slips of the electron and ion fluids (with respect to the (-) RMF) against *r/R* at various time intervals, for $\lambda^+ = \lambda^- = 17.7$, $\gamma^+ = \gamma^- = 312$ ($B_\omega{}^+ = B_\omega{}^- = 50$ G). At $t = 0$, the plots show the initial conditions, where the external values of $B_\omega{}^-$ and $B_\omega{}^+$ are zero, and hence γ^- and γ^+ are everywhere zero. The electron and ion slips are have initial values of $S_e{}^- = -0.1$, and $S_i{}^- = 2.1$. At $t = 10$ μs the penetration of the (-) RMF is limited to outer layers, and the electron fluid has relaxed at inner layers where the local value of is γ^- small. By $t = 50$ μs, the (-) RMF has fully penetrated, with the local value of γ^- approaching the maximum value everywhere. The (+) RMF (which is applied at $t = 10$ μs) is approaching full penetration. The entire electron fluid now rotates almost synchronously with the (-) RMF at all layers (with small slip), returning to a state similar to the initial conditions The $t = 0.1$ ms plots show little change apart from saturation of γ^-, and γ^+ has also almost reached saturation at all layers, with the ion fluid entrained at all layers. The following plots show that a true steady state has been achieved with the electron fluid rotating almost synchronously with the (-) RMF and the ion fluid rotating almost synchronously with the (+) RMF. The electron motion is largely unaffected by the application of the (+) RMF, and the electrons continue to rotate synchronously with the (-) RMF. For $\gamma^- > \gamma_c{}^-$ and $\gamma^+ > \gamma_c{}^+$ the local value of γ for either RMF approaches the value defined by the external value of B_ω at all layers. Once accessed, this steady state can be maintained indefinitely.

For the (+) RMF to entrain the outer layers of the ion fluid, requires that these layers pass through the very small slip region where the force on the ion fluid due to the (+) RMF is large. The radial profile induced by the (-) RMF as it penetrates is vital to allow complete penetration of the (+) RMF. Since the outer layers of the electron fluid are entrained first, with the inner layers relaxing under collisions, the value of $(v_e - v_i)$ will be largest in the outer layers of the plasma, and smaller in the inner layers. Since the relaxation rate for the ions is proportional to $(v_e - v_i)$, the outer layers of the ion fluid will relax faster while the (-) RMF is penetrating. The effect of the penetration of the (-) RMF on the ion fluid is therefore to induce a small radial profile on the ion fluid, so that the inner layers are rotating slightly faster.

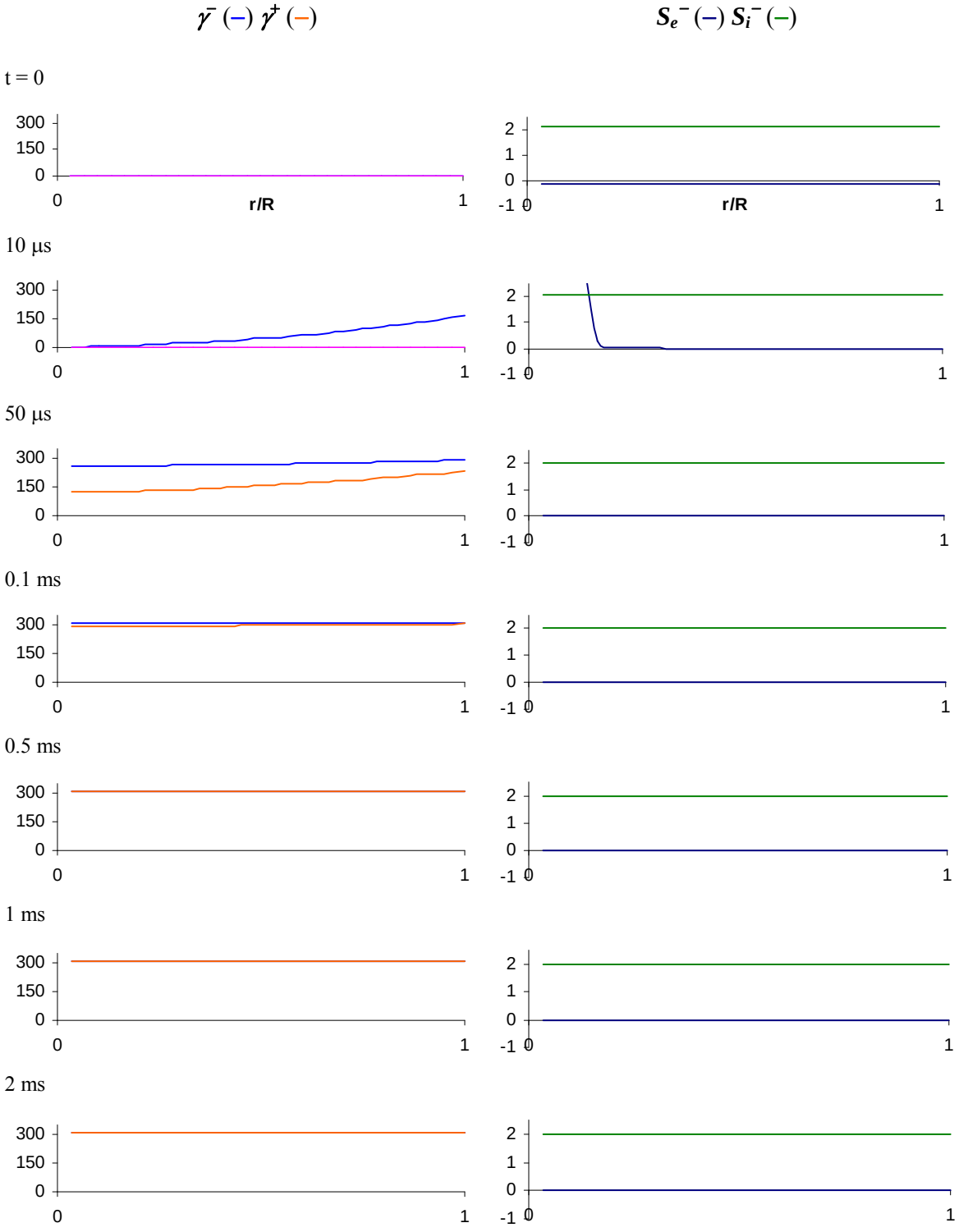

Figure 5.11. Local values of γ^-, γ^+, S_e^- and S_i^- against *r/R* at selected time intervals for two applied RMFs ($\lambda^- = \lambda^+ = 17.7$, $\gamma^- = \gamma^+ = 312$) where $\gamma > \gamma_c$ for both RMFs.

When the (+) RMF is applied, the layers of the ion fluid will pass the very small slip region required for enhanced penetration in sequence, allowing accessibility to the Clemente steady states for this initial condition. However, the magnitude of the (+) RMF required to access this steady state is very much larger than for the (-) RMF. The value of B_ω^+ may be significantly decreased once the ion fluid is fully entrained (as will be demonstrated in Figure 5.16, below).

The other case to consider for the (+) RMF is when $\gamma^- > \gamma_c^-$ but $\gamma^+ < \gamma_c^+$. Figure 5.12 shows a series of plots of B_z and J_θ against r/R at various time intervals, where $\lambda^+ = \lambda^- =$ 17.7, $\gamma^+ = \gamma^- = 62.5$ ($B_\omega^+ = B_\omega^- = 25$ G). At $t = 0$, the initial conditions are shown, where there is a driven current which in the absence of an applied RMF would decay through collisions. At $t = 10$ μs, the (-) RMF has entrained the outer layers of the electron fluid, but has not yet captured the inner layers. By $t = 50$ μs, the entire electron fluid is rotating synchronously with the (-) RMF, returning to a state similar to the initial conditions. The J_θ curve demonstrates that the driven current is through all layers. At t = 0.1 ms there is little change, and hence a quasi steady state has been achieved which is maintained over a time scale smaller than the ion relaxation time. By this time, the (+) RMF has partially penetrated, maintaining the driven current in outer layers, while the driven current at inner layers has begun to decrease. At $t = 0.5$ ms the total driven current has decreased considerably in the inner layers of the plasma, while being maintained in the outer layers, the (+) RMF failing to penetrate the plasma column fully. Subsequent plots show that a true steady state for these parameters is that the driven current in the outer layers will be maintained by the (+) RMF, but the current is zero in inner layers. The Clemente steady states have not been accessed for the entire plasma column since $\gamma^+ < \gamma_c^+$.

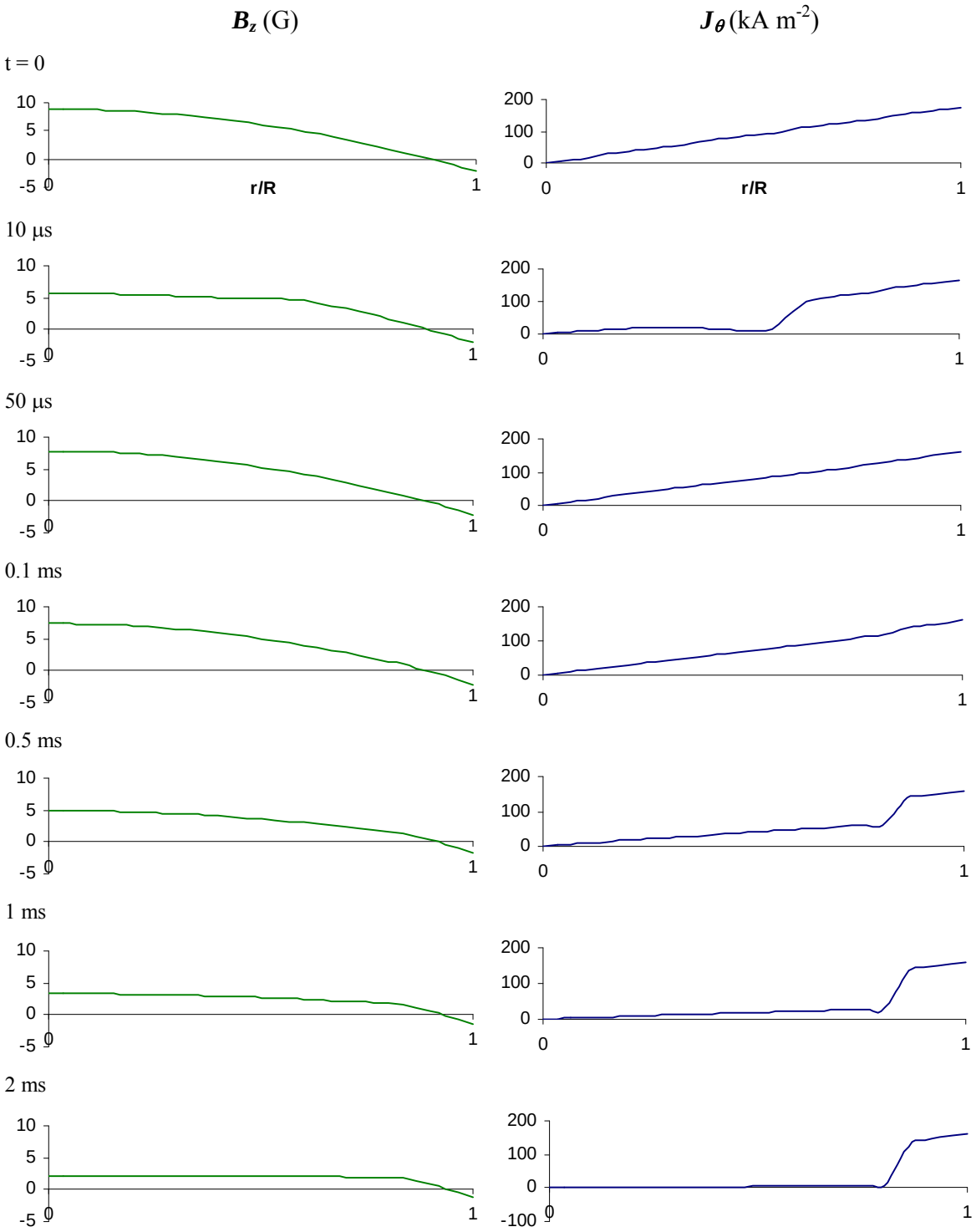

Figure 5.12. B_z and J_θ against r/R at selected time intervals for two applied RMFs ($\lambda^- = \lambda^+ = 17.7$, $\gamma^- = \gamma^+ = 62.5$) where $\gamma^+ < \gamma_c^+$.

Figure 5.13 shows plots of the local values of γ^- and γ^+, and the slips of the electron and ion fluids (with respect to the (-) RMF) against *r/R* at various time intervals, for $\lambda^+ = \lambda^- = 17.7$, $\gamma^+ = \gamma^- = 62.5$ ($B_\omega^+ = B_\omega^- = 50$ G). At $t = 0$, the plots show the initial conditions, where the external values of B_ω^- and B_ω^+ are zero, and hence γ^- and γ^+ are everywhere zero. The electron and ion slips are have initial values of $S_e^- = -0.1$, and $S_i^- = 2.1$. At $t = 10$ μs the penetration of the (-) RMF is limited to outer layers, and the electron fluid has relaxed at inner layers where the local value of is γ^- small. By $t = 50$ μs, the (-) RMF has fully penetrated, with the local value of γ^- approaching the maximum value everywhere. The (+) RMF (which is applied at $t = 10$ μs) is highly attenuated, and hence only has significant magnitude in the outer layers of the plasma. The entire electron fluid now rotates almost synchronously with the (-) RMF at all layers (with small slip), returning to a state similar to the initial conditions. The outer layers of the ion fluid have been entrained by the (+) RMF, but the inner layers have begun to decay through collisions. The $t = 0.1$ ms plots show saturation of γ^-, while γ^+ is still very small except in the outer layers. While the electron fluid remains entrained, the ion fluid is only entrained in the outer layers. The following plots show that a true steady state has not been achieved. While the electron fluid rotating almost synchronously with the (-) RMF, only the outer layers of the ion fluid rotate almost synchronously with the (+) RMF, with inner layers rotating synchronously with the (-) RMF by $t = 2$ ms. For $\gamma^- > \gamma_c^-$ and $\gamma^+ < \gamma_c^+$ the local value of γ^+ is highly attenuated, and the entrainment of the ion fluid by the (+) RMF limited to outer layers of the plasma.

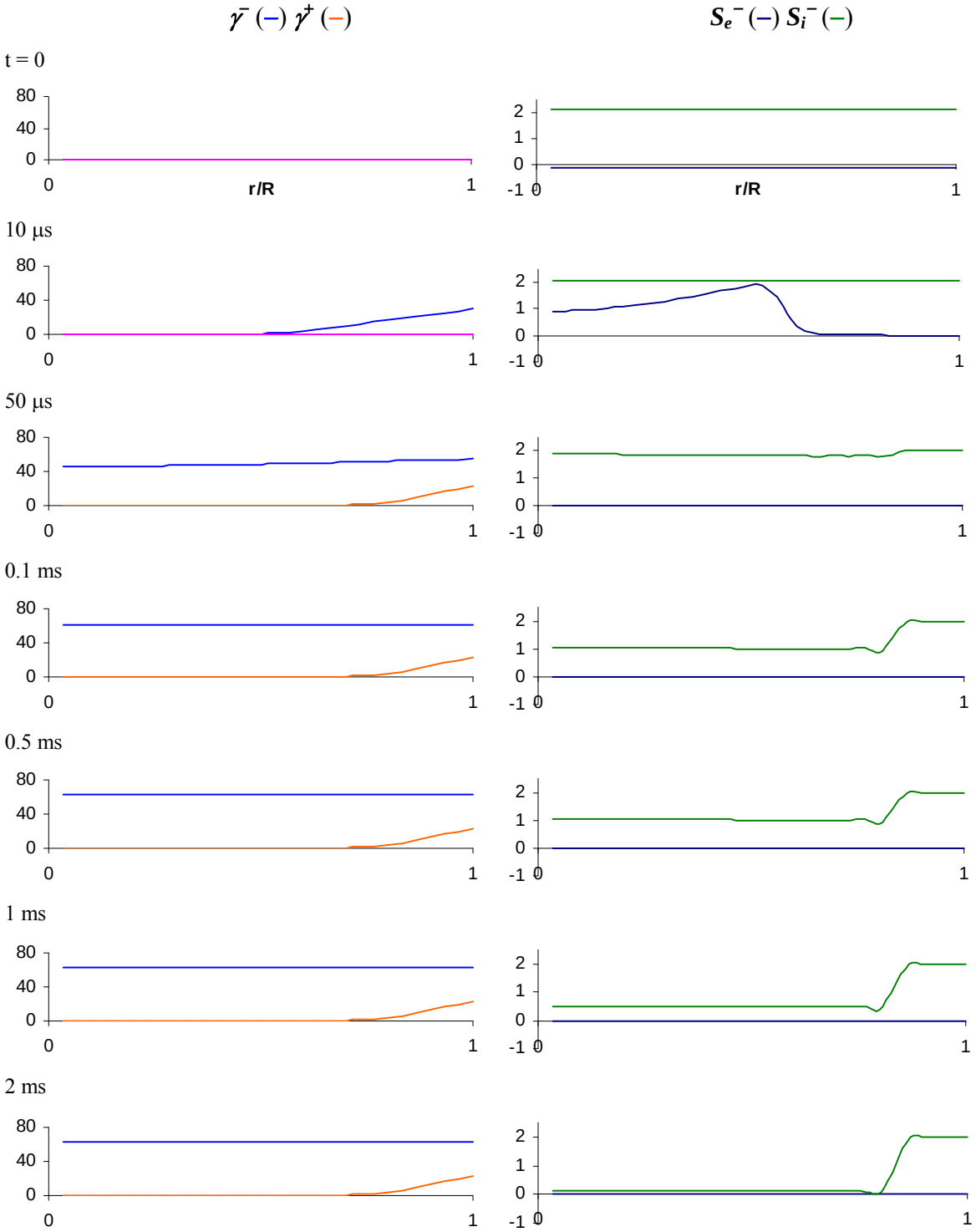

Figure 5.13. Local values of γ^-, γ^+, S_e^- and S_i^- against *r/R* at selected time intervals for two applied RMFs ($\lambda^- = \lambda^+ = 17.7$, $\gamma^- = \gamma^+ = 62.5$) where $\gamma^+ < \gamma_c^+$.

As for the (-) RMF, the (+) RMF may be decreased once the ion fluid has been entrained, maintaining the steady state. Figure 5.14 shows the steady state value of α, when two RMFs are applied (where $\gamma^- > \gamma_c^-(a)$ and $\omega_e = -\omega_i$), for $\lambda^+ = .17.7$ This figure demonstrates that there are two critical values of γ^+. $\gamma_c^+(a)$ is the magnitude required to access the steady state, while $\gamma_c^+(b)$ is the magnitude required to maintain the steady state. The second critical value is found by decreasing the magnitude of the (+) RMF once it has penetrated. The RMF magnitude required to access the steady state is greater than that required to maintain the steady state.

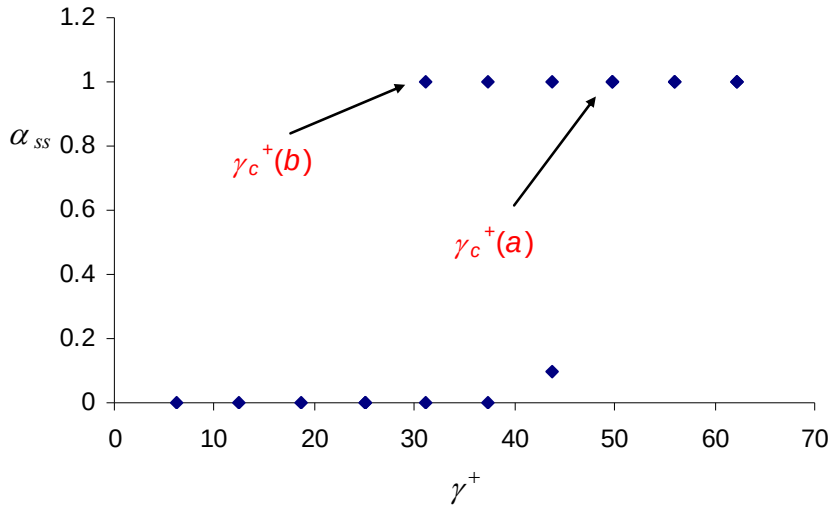

Figure 5.14. Steady state value of α plotted against γ^+ for $\lambda^+ = 17.7$.

While the Clemente steady states may be accessed from a rigid rotor initial condition for both fluids before either RMF is applied, the value of $\gamma_c^+(a)$ required is large in comparison to $\gamma_c^-(a)$. The small radial profile induced on the ion fluid by the transient phase of the application of the (-) RMF is only a small effect. The large value of γ_c^+ for this case suggests that the time taken for the relaxation of a layer past the critical region required for capture is not larger than the diffusion time of the (+) RMF. The value of $\gamma_c^+(a)$ required may be decreased by employing one of two techniques (1) having a significant radial profile on the ions as an initial condition before either RMF is applied, or (2) allowing the frequency of the (+) RMF to decrease as it penetrates.

Figure 5.15 compares the steady state driven current against γ^+ for (a) no radial profile and (b) an initial radial profile of $\omega_i = (1.3 - 0.2r/R)\omega^+$ for $\gamma^+ =$ (with $\gamma^- > \gamma_c^-(a)$ and $\omega_e = -\omega_i$) for $\lambda^+ = 12.5$.

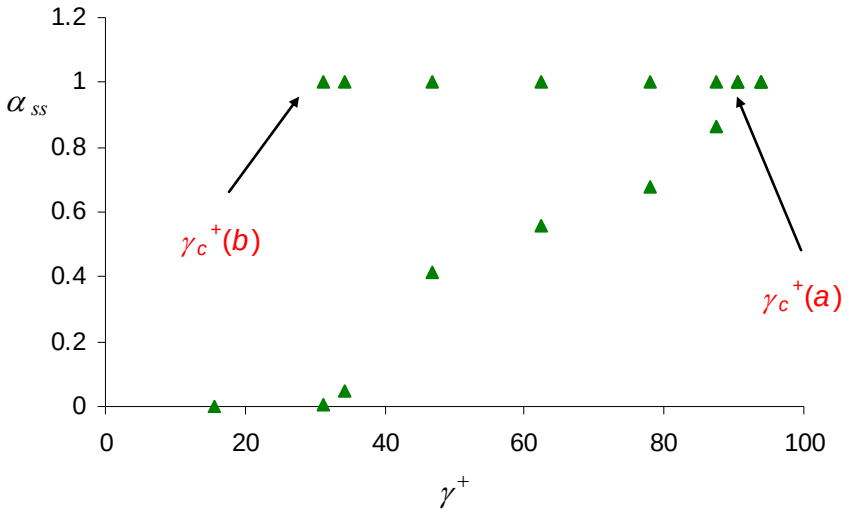

(a) $\omega_i(t=0) = 1.1\omega^+$

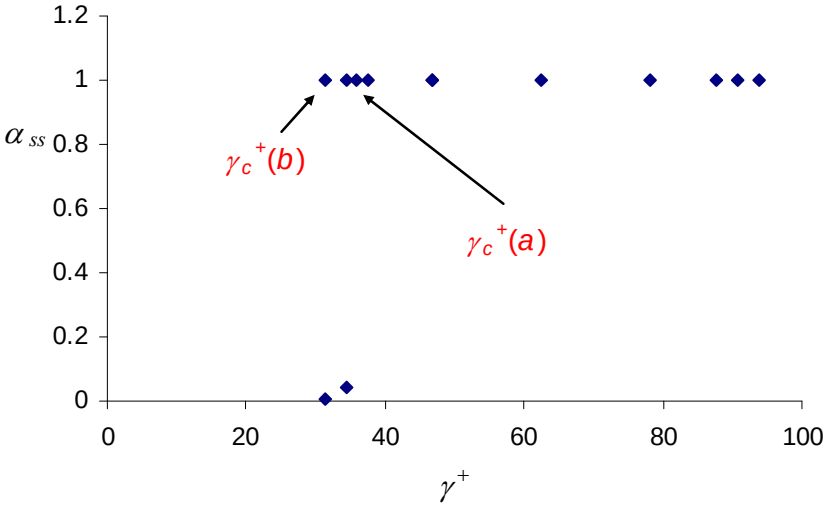

(b) $\omega_i(t=0) = (1.3 - 0.2r/R)\omega^+$

Figure 5.15. Steady state α against γ^+ for (a) no radial profile and (b) radial profile, for $\lambda^+ =$ 12.5.

The critical value of γ^+ required for entrainment of the ion fluid $\gamma_c^+(a)$, is significantly reduced when a radial profile is employed as an initial condition. The details of the small radial profile of the initial ion rotational velocity are not critical as long as the (+) RMF has sufficient time to diffuse to successively deeper layers before the rotational velocity at these layers decreases past the critical region $S_i^+ \cong (m_e / m_i)\xi^+$.

Consider the two cases presented in Figure 5.15 where $\gamma^+ = 50$. In both cases, the electrons are initially entrained by the (–) RMF. The (+) RMF penetration is not complete and is limited by the classical skin depth for case (a). The outer ions are caught by this field, as they satisfy the criterion $S_i^+ \cong (m_e / m_i)\xi^+$, but the inner ions slow down by collisions with the electrons before the (+) RMF diffuses in, and hence they fail to be entrained by the (+) RMF and do not allow further penetration. In the steady state, both the electron and the ion fluids rotate synchronously with the (–) RMF and hence the driven current vanishes and the plasma equilibrium is lost. The loss of the plasma equilibrium is not observed in our results because we do not consider the radial motion of the plasma. The (+) RMF does not exert appreciable force on the ions at any layer unless the slip (at this layer) becomes very small. The slip of the ions at inner layers would become too large to allow the (+) RMF to exert an appreciable force before it diffuses to these layers. For case (b), the (+) RMF penetrates into the plasma much farther than the classical skin depth. Successive layers of the ion fluid become entrained by the (+) RMF as they relax (by momentum-transfer collisions with the electrons) to the favourable value of the slip $S_i^+ \cong (m_e / m_i)\xi^+$. The electron motion is largely unaffected by the (+) RMF and the electrons continue to rotate synchronously with the (–) RMF.

It was reported in two previous papers (Visentin 2003) and (Visentin and Hugrass, 2003) that the steady states were not accessible from the rigid rotor initial condition. The results presented had $\gamma^+ < \gamma_c^+$ for the rigid rotor initial condition, but $\gamma^+ > \gamma_c^+$ for a radial profile, or use of the frequency modulation scheme. The magnitude of the (+) RMF was not large enough to entrain the ion fluid for the rigid rotor initial condition, and hence the accessibility of the steady states was not observed for the rigid rotor initial condition.

The Clemente steady states may be accessed for the rigid rotor initial condition for the parameters presented in these papers, but requires a much larger external magnitude of the (+) RMF than was attempted.

Since the penetration time of the (-) RMF is critical to the amount of radial profile induced in the ion fluid, we can most easily examine the critical values of γ^+ required for accessing and maintaining the Clemente steady states by using a radial profile initial condition. These results should be seen as the minimum value of $\gamma_c^+(a)$ while the value of $\gamma_c^+(b)$ is of course independent of the ion fluid initial conditions. Figure 5.16 shows a plot of the two critical values of γ^+ against λ^+ for the radial profile initial condition. The critical values of γ^+ are of the similar magnitude to the values of $\gamma_c^-(a)$ and $\gamma_c^-(b)$ found for the (-) RMF for the same value of λ.

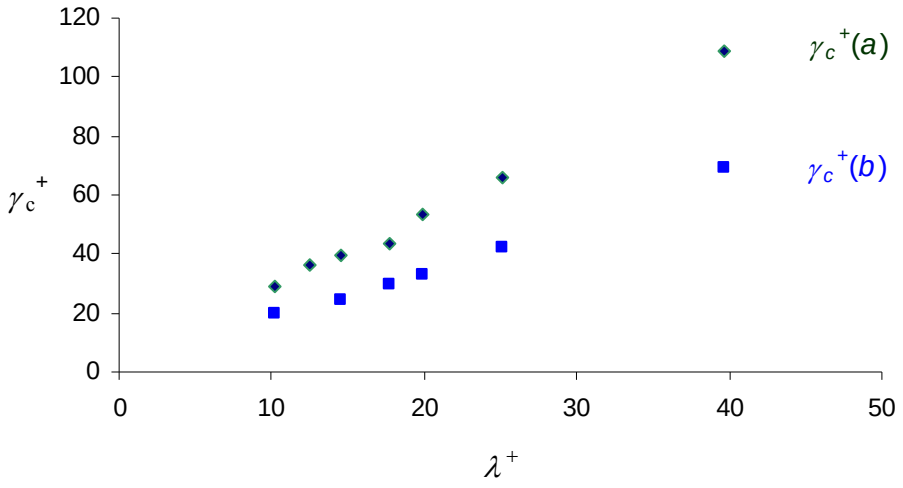

Figure 5.16. Critical values of γ_c^+ for complete penetration, $\gamma_c^+(a)$ and expulsion, $\gamma_c^+(b)$ against λ^+ for simulations using a radial profile on the ion fluid.

An alternative to inducing a radial profile on the ion fluid as an initial condition is to allow the frequency of the (+) RMF to decrease slightly with time. This frequency modulation of the (+) RMF will allow the favourable value of the slip to be re-established at each layer of the plasma as the (+) RMF penetrates.

The (-) RMF is applied at t = 0, the (+) RMF is applied at t = 3 μs, at which time the (-) RMF has partially penetrated the plasma and entrained the electron fluid. The initial slip of the ion fluid is constant with r, and has value S_i^+ = -0.1. After another time delay, the frequency of the (+) RMF is allowed to decrease linearly at t = 4 μs. A number of simulations were performed for $\lambda^+ = \lambda^- = 5.02$, $\gamma^+ = \gamma^- = 12.5$ ($B_\omega^+ = B_\omega^- = 20$ G), where the frequency of the (+) RMF decreases linearly from $\omega^+(t = 0) = 5$ MHz to $\omega^+ = 4.95$ MHz, with different rates of change of ω^+. A comparison of these frequency changes is shown in Figure 5.17. The total frequency change in each case is thus 1% of the initial value.

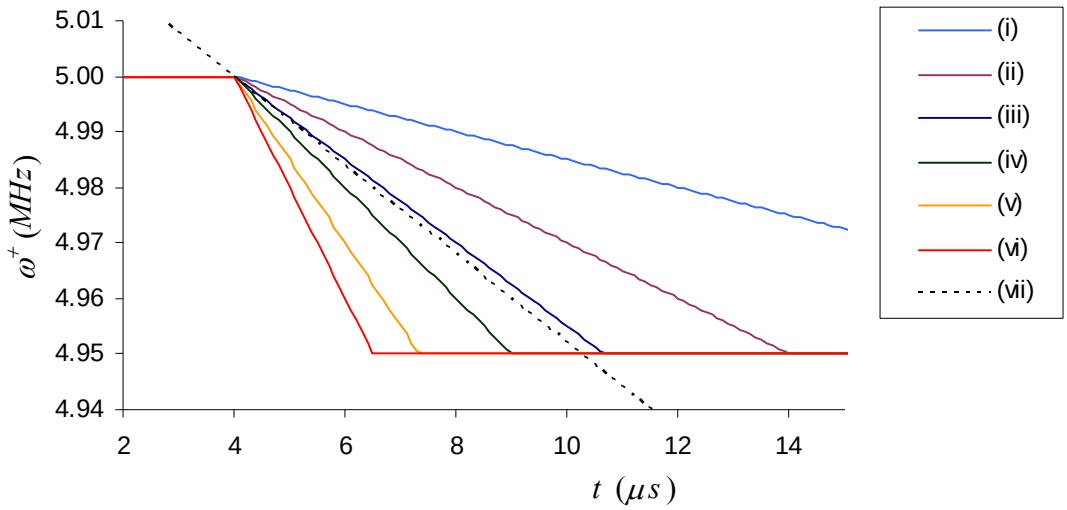

Figure 5.17. Time variation of frequency of the (+) RMF for 6 simulations (i) to (vi). (vii) Time variation of ion rotational frequency ω_i^+ under collisions with the electron fluid for the case S_e^+ - $S_i^+ = 2$.

Results for the profiles shown in Figure 5.17 fall into two groups. Where the frequency change is too slow (curves (iv) to (vi) in Figure 5.17), the penetration of the (+) RMF is limited by the classical skin depth. Only outer layers are initially captured by the (+) RMF, and in the steady state the ion fluid rotates synchronously with the (-) RMF. The layers initially captured are not maintained since the relaxation of the inner layers (which are eventually entrained by the (-) RMF) reduces the magnitude of the local value of γ^+ in the outer layers below that required for synchronous rotation of the ion

fluid. Where the frequency change is fast enough (curves (i) to (iii) in Figure 5.17), the (+) RMF fully penetrates the plasma, capturing the ion fluid, which rotates synchronously with the (+) RMF in the steady state. The critical value of the rate of change of ω^+ is determined by the relaxation rate of the ion rotational frequency due to collisions with the electron fluid, which is given by

$$\frac{\partial \omega_i}{\partial t} = \nu_{ie}\omega^+\left(S_i{}^+ - S_e{}^+\right). \tag{5.26}$$

Curve (vii) in Figure 5.17 shows this expression for the case where the electrons are rotating synchronously with the (-) RMF and the ions are rotating synchronously with the (+) RMF (i.e. $S_e^+ - S_i^+ = 2$).

In order to completely entrain the ion fluid, the rate of change of the frequency of the (+) RMF must be greater than the ion relaxation time, due to collisions with the electron fluid, expressed as curve (vii) in Figure 2. Results presented are for the case of a 1% variation in ω^+, however, the total change in ω^+ is not critical.

Results presented above are for the case of a rigid rotor initial condition on the ions, which is chosen arbitrarily as an example of the broadening of the class of initial conditions on the ion fluid. By allowing the frequency of the (+) RMF to vary linearly allows the access of the Clemente steady states for smaller values of γ^+. A linear frequency change also allows penetration of the (+) RMF and entrainment of the ion fluid, for cases where the ion fluid has a small initial radial profile, where S_i^+ either increases or decreases with radius. The frequency modulation method is thus not limited to the case of a constant initial value of S_i^+. The prescribed frequency variation would have to be determined for each case of initial radial profile of the ion slip.

5.7 Summary of Simulation Results

It was demonstrated in this section that:

(1) The penetration of the (-) RMF for this model is consistent with previous studies (Hugrass & Grimm, 1981 and Milroy, 1999). The critical value of γ^- required to

maintain the steady state is linear with λ^-. The critical value of γ^- required to access the steady state may be much larger than that required to maintain it. Hence the external magnitude of the (-) RMF may be decreased once full penetration has been achieved. This nonlinearity of the (-) RMF penetration increases with λ^-. The critical values of γ^- are dependant on the ion rotation. If the ions are counter-rotating, the critical values of γ^- are increased for a given value of λ^-, since the collisional force which must be opposed by the (-) RMF is larger for this case. This effect of ion rotation on the accessibility of the steady states has not previously been considered in theoretical work for the application of a single RMF to a preformed FRC.

(2) The steady states for the electron fluid are maintained when the (+) RMF is applied. If the (-) RMF is allowed to be at least partially entrained before the (+) RMF is applied, then the electron fluid continues to rotate almost synchronously with the (-) RMF.

(3) The penetration of the (+) RMF has a similar behaviour to the (-) RMF. There is a critical value of γ^+ required to maintain the steady state, which scales linearly with λ^+. The critical value of γ^+ required to access the steady state may be much larger than that required to maintain it. Hence the external magnitude of the (+) RMF may be decreased once full penetration has been achieved. This nonlinearity of the (+) RMF penetration increases with λ^+. The ion fluid steady states may only be accessed form the $S_i^+ < 0$ initial condition.

(4) The critical value of γ^+ required to access the steady state is dependant on the initial conditions for the ion fluid. It is required that the (+) RMF have a radial profile where S_i^+ increases with radius (and is everywhere negative). The penetration of the (-) RMF (which is applied first) induces a small radial profile on the ion fluid, which allows accessibility of the steady states. The (+) RMF may fully penetrate the plasma for smaller values of γ^+ when either (a) the ions have a radial profile as an initial condition, or (b) the frequency of the (+) RMF is allowed to decrease slowly with time.

CHAPTER 6 MAINTAINING A FIELD-REVERSED CONFIGURATION

In Chapter 5 the radial motion of the plasma has been suppressed, and the initial conditions were not representative of real equilibria. This chapter investigates the accessibility of the Clemente steady states for a preformed FRC. The radial motion of the plasma is included so that pressure balance is always maintained. The number density (and hence the collision frequency) is not uniform in an FRC. This makes it even more difficult to satisfy the stringent conditions required for the penetration of the (+) RMF at all layers. The numerical simulations demonstrate the accessibility of the Clemente steady states provided that: a) the preformed FRC equilibrium has the experimentally observed rotational motion (Tuszewski, 1988) b) the (+) RMF has sufficiently large magnitude and c) it is applied at a suitable time.

Section 5.1 outlines the physical model and derives equations of motion where radial motion of the plasma is considered. In section 5.2 the boundary and initial conditions corresponding to a preformed FRC are described. The numerical model is outlined in section 5.3, simulation results described in section 5.4 and section 5.5 provides discussion and conclusions.

6.1 Physical model and equations of motion

Two RMFs are applied to a preformed infinitely long FRC. The axial magnetic flux is maintained by means of flux preserving rings located at radius $b > R$, where R is the plasma radius. Thus the flux-conserving boundary required by the FRC equilibrium is

provided and the two RMFs can be generated by means of polyphase currents in an array of coils located outside the flux conserving surface. It is well known (Tuszewski, 1988) that FRCs are observed to rotate (in the direction of the ion diamagnetic current) and are eventually destroyed by the n =2 rotational instability, unless suitable quadrupole fields are applied. So in a preformed FRC the electron fluid rotates in one direction and the ion fluid rotates in the opposite direction. In the simulations presented in this chapter, the (-) RMF is applied to the preformed FRC with a short rise time to entrain the electron fluid. The (+) RMF is applied with a longer rise time to allow a suitable time delay for complete penetration of the (-) RMF and entrainment of the electron fluid before the magnitude of the (+) RMF becomes large. When the (+) RMF is applied, it does not prevent the electron fluid from rotating synchronously with the (-) RMF provided that certain conditions are satisfied.

In chapter 5 the radial motion of the plasma was neglected since we aimed at investigating the penetration of the RMFs in the plasma and assumed, without rigorous justification, that the radial motion would not influence this process. In this chapter the equation of motion in the radial direction is included, so that the pressure balance is maintained when J_θ and B_z change. The simulations presented justify the assumption that the radial motion does not influence the penetration of the RMF into the plasma. Satisfying the pressure balance equation however necessitates the variation of the plasma parameters with radius. This makes it more difficult to satisfy the conditions required for the penetration of the RMFs into the plasma at all layers.

We now present the derivation of equations of motion for the case where the plasma is allowed to move in the radial direction. Some of the equations presented in this section also appear in the same form in Chapter 2 for the case where the radial motion is suppressed, but are included here for convenience. As for the case of no radial motion, in the steady state, all the relevant physical quantities can be classified in two groups (Hugrass, 1982). Quantities of one group can be expanded as Fourier series with odd harmonics of (ωt - θ) and quantities of the second group can be expanded as Fourier series with even harmonics of (ωt - θ) where the effect of the second and higher harmonics is small and may be neglected (Milroy, 1999). Hence quantities of the

second group are functions of r only, and quantities of the first group can be conveniently represented by complex phasors and have derivatives,

$$\frac{\partial}{\partial t} = i\omega^{\pm} \qquad \frac{\partial}{\partial \theta} = -i \qquad \frac{\partial}{\partial z} = 0\,. \tag{6.1}$$

When we study time-varying configurations which change in time scales much larger than the period of the RMF, this classification is still valid, with quantities of the second group real functions of r and t, while the phasors for quantities of the first group are complex functions of r and t such that $\partial/\partial t << \omega$ and $v_r\,\partial/\partial r << \omega$. These relations also hold for the case where ω is allowed to vary slowly with time.

The equations of motion for the electron and ion fluids are

$$m_e n\left(\frac{\partial \mathbf{v_e}}{\partial \mathbf{t}} + \mathbf{v_e} \bullet \nabla \mathbf{v_e}\right) = -en\left(\mathbf{E} + \mathbf{v_e} \times \mathbf{B}\right) - \nabla P_e + m_e n \nu_{ei}\left(\mathbf{v_i} - \mathbf{v_e}\right), \tag{6.2}$$

$$m_i n\left(\frac{\partial \mathbf{v}_i}{\partial \mathbf{t}} + \mathbf{v}_i \bullet \nabla \mathbf{v}_i\right) = en\left(\mathbf{E} + \mathbf{v}_i \times \mathbf{B}\right) - \nabla P_i + m_e n \nu_{ei}\left(\mathbf{v}_e - \mathbf{v}_i\right). \tag{6.3}$$

Faraday's law and equation (6.1) provide the following expression for the phasor of the z-component of the electric field,

$$E_z^{\pm} = -i\omega A_z^{\pm} - \frac{\partial A_z^{\pm}}{\partial t} = \omega r B_r^{\pm} - \frac{\partial A_z^{\pm}}{\partial t}\,. \tag{6.4}$$

The derivation of the time-dependent equations is greatly simplified if we note as in section 2.2 that the phasor for the time derivative of v_{ez} (V'_{ez}) is approximately related to the phasor for v_{ez} (V_{ez}) by the equation

$$V'^{\pm}_{ez} = i\omega^{\pm}\, V_{ez}^{\pm} + \frac{\partial}{\partial t}\, V_{ez}^{\pm} \approx i\omega^{\pm}\, V_{ez}^{\pm}\,. \tag{6.5}$$

and similarly for the ion fluid

$$V'^{\pm}_{iz} \approx i\omega^{\pm}\, V_{iz}^{\pm}. \tag{6.6}$$

We will always neglect the partial derivatives of the phasors of quantities of the first group as we did in equations (6.5) and (6.6) except in situations when we want to evaluate such derivatives in order to update the values of these phasors in the finite difference equations. The derivatives of the phasor of the vector potentials are retained in equation (6.4) above for this reason.

Using equations (6.2) to (6.6) and assuming that $v_r \dfrac{\partial}{\partial r} \approx \dfrac{\partial}{\partial t} << \omega^{\pm}$, the z-components of the equations of motion can be written as:

$$i\omega m_e n S_e^{\pm} V_{ez}^{\pm} = -en\left(S_e^{\pm} E_z^{\pm} + \left(S_e^{\pm} - 1\right)\frac{\partial A_z^{\pm}}{\partial t} - v_r \frac{\partial A_z^{\pm}}{\partial r} \right) - m_e n \nu_{ei} \left(V_{ez}^{\pm} - V_{iz}^{\pm}\right) \tag{6.7}$$

$$i\omega m_e n S_e^{\pm} V_{ez}^{\pm} = -en\left(S_e^{\pm} E_z^{\pm} + \left(S_e^{\pm} - 1\right)\frac{\partial A_z^{\pm}}{\partial t} - v_r \frac{\partial A_z^{\pm}}{\partial r} \right) - m_e n \nu_{ei} \left(V_{ez}^{\pm} - V_{iz}^{\pm}\right) \tag{6.8}$$

Equations (6.7) and (6.8) can be used to derive a generalised Ohm's law for the z-component of the electric field

$$E_z^{\pm} = \eta^{*\pm} J_z^{\pm} - \left[1 - \frac{1}{S_e^{\pm}} + \frac{m_e}{m_i}\left(1 - \frac{1}{S_i^{\pm}}\right)\right]\frac{\partial A_z^{\pm}}{\partial t} + \left[\frac{1}{S_e^{\pm}} + \frac{m_e}{m_i}\frac{1}{S_i^{\pm}}\right] v_r \frac{\partial A_z^{\pm}}{\partial r} \tag{6.9}$$

The partial derivative of the vector potential with respect to time is a small quantity and could be neglected in equation (6.9), but it is retained because this equation is used to evaluate this derivative in order to update the value of the vector potential in the finite difference approximation of equation (6.10) below.

The time-dependent equation for A_z is obtained with the help of equations (6.4) and (6.9)

$$\begin{aligned} \frac{dA_z^{\pm}}{dt} &= \frac{\partial A_z^{\pm}}{\partial t} + v_r \frac{\partial A_z^{\pm}}{\partial r} \\ &= \left[\frac{\eta^{*\pm}}{\mu_0}\nabla^2 A_z^{\pm} - i\omega^{\pm} A_z^{\pm} - \frac{m_e}{m_i} v_r \frac{\partial A_z^{\pm}}{\partial r}\right] \Bigg/ \left[\frac{1}{S_e^{\pm}} + \frac{m_e}{m_i}\left(\frac{1}{S_i^{\pm}} - 1\right)\right] \end{aligned} \tag{6.10}$$

It is evident from equation (6.10) that the steady state solutions for $A_z^{\pm}$ satisfy the equation

$$\frac{\eta^{*\pm}}{\mu_0}\nabla^2 A_z^{\pm} - i\omega^{\pm} A_z^{\pm} = 0. \tag{6.11}$$

and thus, in the steady state, $A_z^{\pm}$ penetrate the plasma with enhanced skin depth. The penetration of A_z^{-} into the plasma is enhanced because $\eta^{*-} > \eta$ for $S_e^{-} < 1,$ and the penetration of A_z^{+} into the plasma is enhanced because $\eta^{*+} > \eta$ for $S_i^{+} < \frac{m_e}{m_i}$.

In order to derive an expression for the force density on both the electron and ion fluids we require an expression for the axial components of the fluid velocities. The phasors of the axial-components of the fluid velocities can be found from equations (6.7) to (6.9),

$$V_{ez}^{\pm} = \frac{ie}{m_e\omega^{\pm}}\left(1 - \frac{1}{S_e^{\pm}}\frac{\eta}{\eta^{*\pm}}\right)E_z^{\pm}, \tag{6.12}$$

$$V_{iz}^{\pm} = \frac{-ie}{m_i\omega^{\pm}}\left(1 - \frac{1}{S_i^{\pm}}\frac{\eta}{\eta^{*\pm}}\right)E_z^{\pm}. \tag{6.13}$$

The small partial derivatives of $A_z^{\pm}$ are neglected compared to $\omega^{\pm}A_z^{\pm}$. We only retain these derivatives if the equation is used to evaluate them for the purpose of updating the variables in the finite difference approximation.

The θ-component of the force densities on the electron and ion fluids then have steady parts

$$F_e^{\pm} = -\frac{en}{2}\mathrm{Re}\left\{V_{ez}^{\pm}B_r^{\pm}\right\} = \frac{e^2 nr\left|B_r^{\pm}\right|^2}{2m_e S_e^{\pm}\xi^{\pm}\left[\left(\frac{1}{S_e^{\pm}} + \frac{m_e}{m_i}\frac{1}{S_i^{\pm}}\right)^2 + \frac{1}{\xi^{\pm 2}}\right]}, \tag{6.14}$$

$$F_i^{\pm} = \frac{en}{2}\,\mathrm{Re}\left\{V_{iz}^{\pm} B_r^{\pm}\right\} = \frac{e^2 nr\left|B_r^{\pm}\right|^2}{2m_i S_i^{\pm}\xi^{\pm}\left[\left(\frac{1}{S_e^{\pm}} + \frac{m_e}{m_i}\frac{1}{S_i^{\pm}}\right)^2 + \frac{1}{\xi^{\pm 2}}\right]}. \tag{6.15}$$

A time dependent equation for B_z is obtained from the θ-component of the equation of motion of the electron fluid and Faraday's law.

$$\frac{\partial B_z}{\partial t} + v_r\frac{\partial B_z}{\partial r} = \frac{\eta}{\mu_0}\nabla^2 B_z - J_\theta\frac{\partial \eta}{\partial r} - \frac{1}{r}\frac{\partial}{\partial r}\frac{r}{en}\left(F_e^{-} + F_e^{+}\right) - \frac{B_z}{r}\frac{\partial\left(rv_r\right)}{\partial r}. \tag{6.16}$$

The first term in the right hand side of equation (6.16) is the normal resistive diffusion term. The second term is the effect of non-uniform resistivity on the diffusion process. The third term shows the effect of the RMF is to oppose the field diffusion and maintain the current. The fourth term shows that the magnetic field is frozen to the plasma and is carried with it.

The continuity equation for the number density is,

$$\frac{\partial n}{\partial t} + v_r\frac{\partial n}{\partial r} = -\frac{n}{r}\frac{\partial\left(rv_r\right)}{\partial r}. \tag{6.17}$$

The plasma temperature is assumed constant as it is observed in most experiments (Tuszewski, 1988) and we do not have a valid model for energy transport. We assume also that the plasma current varies in a time scale much longer than the radial Alfven time and hence radial pressure balance (quasi-equilibrium) is always maintained, hence

$$\frac{B_z^{\,2}}{2\mu_0} + n\left(T_e + T_i\right) = C\ . \tag{6.18}$$

Differentiating this expression gives

$$\frac{dn}{dt} = \frac{\partial n}{\partial t} + v_r\frac{\partial n}{\partial r} = -\frac{B_z}{\mu_0\left(T_e + T_i\right)}\frac{dB_z}{dt}. \tag{6.19}$$

Using equations (6.16), (6.17) and (6.19) we obtain

$$\frac{dB_z}{dt} = \frac{\partial B_z}{\partial t} + v_r \frac{\partial B_z}{\partial r} = \frac{\frac{\eta}{\mu_0}\nabla^2 B_z - J_\theta \frac{\partial \eta}{\partial r} - \frac{1}{r}\frac{\partial}{\partial r}\frac{r}{en}\left(F_e^- + F_e^+\right)}{1 + \frac{B_z^{\,2}}{\mu_0 n\left(T_e + T_i\right)}}. \tag{6.20}$$

The resistivity in equation (6.20) is the classical resistivity given by

$$\eta = 2.91 \mathrm{x} 10^{-12} \Lambda \frac{m_e}{e^2} T_e^{-3/2}. \tag{6.21}$$

The dependence of the Coulomb logarithm on n is neglected as usual and we choose Λ = 20. Since the temperature is constant, the resistivity is also constant and equation (6.20) becomes

$$\frac{dB_z}{dt} = \frac{\frac{\eta}{\mu_0}\nabla^2 B_z - \frac{1}{r}\frac{\partial}{\partial r}\frac{r}{en}\left(F_e^- + F_e^+\right)}{1 + \frac{B_z^{\,2}}{\mu_0 n\left(T_e + T_i\right)}}. \tag{6.22}$$

Equations (6.10), (6.22) and (6.26) (below) are solved numerically using a finite difference scheme on a moving one-dimensional grid. The grid points follow the radial motion of the plasma. The value of B_z at grid point i and time $t + \Delta t$ for example, (denoted $B_z(i, t + \Delta t)$) is approximated by

$$B_z\left(i, t + \Delta t\right) = B_z\left(i, t\right) + \frac{1}{2}\Delta t \frac{dB_z}{dt}\left(i, t\right) + \frac{1}{2}\Delta t \frac{dB_z}{dt}\left(i, t + \Delta t\right) \tag{6.23}$$

Note that the derivatives at $t + \Delta t$ are to be evaluated in terms of the yet unknown values of the variables at $t + \Delta t$. The numerical scheme would be fully implicit if the resulting set of simultaneous equations could be solved for the updated values of the variables. This cannot be easily performed however, since the equations are nonlinear. We solve these equations approximately by simple iteration. The iteration is found to converge to any desired accuracy provided that the time step Δt is not too large.

The radial velocity of the plasma (and the computational grid) is obtained from equations (6.17) and (6.19).

$$v_r = -\frac{1}{r}\int \frac{r}{n}\frac{dn}{dt}dr = \frac{1}{r}\int_0^r \frac{rB_z}{\mu_0 n(T_e + T_i)e}\frac{dB_z}{dt}. \tag{6.24}$$

The number density is determined from the pressure balance condition of equation (6.18)

$$n = \frac{C - \frac{B_z^{\,2}}{2\mu_0}}{e(T_e + T_i)}. \tag{6.25}$$

The azimuthal momentum density P_θ is obtained using the equation

$$\begin{aligned}\frac{dP_\theta}{dt} &= \left\langle J_z^{\,-} B_r^{\,-} + J_z^{\,+} B_r^{\,+} \right\rangle - v_r \frac{P_\theta}{r} \\ &= \frac{1}{2}\mathrm{Re}\left(\frac{\omega^- r \left|B_r^{\,-}\right|^2}{\eta^{*-}} + \frac{\omega^+ r \left|B_r^{\,+}\right|^2}{\eta^{*+}} \right) - v_r \frac{P_\theta}{r}.\end{aligned} \tag{6.26}$$

The azimuthal components of the fluid velocities are determined from the following equations.

$$v_{i\theta} = \frac{1}{(m_e + m_i)n}\left(P_\theta + \frac{m_e J_\theta}{e} \right), \tag{6.27}$$

$$v_{e\theta} = \frac{1}{(m_e + m_i)n}\left(P_\theta - \frac{m_i J_\theta}{e} \right). \tag{6.28}$$

The components of the current density are obtained from the z components of the magnetic field and vector potential using Ampere's law.

$$J_\theta = -\frac{1}{\mu_0}\frac{\partial B_z}{\partial r}, \tag{6.29}$$

$$J_z^{\,\pm} = -\frac{1}{\mu_0}\nabla^2 A_z^{\,\pm}. \tag{6.30}$$

6.2 Initial and Boundary Conditions

FRCs are known to spin up until an $n = 2$ rotational instability destroys the equilibrium (Tuszewski, 1998). Hence, in the simulations we consider, the RMFs are applied to a preformed FRC where the electrons and ions are initially counter-rotating. Assuming that the rotational velocity of the ion fluid is smaller than the ion thermal velocity, the centrifugal force can be ignored and the equilibrium satisfies the equation

$$\mathbf{J} \times \mathbf{B} = \nabla P . \tag{6.31}$$

We note that the plasma pressure P is a quantity of the second group. It consists of a slowly varying function of t and r as well as even harmonics in $(\omega t - \theta)$. As mentioned earlier, the effects of the second and higher harmonics can be neglected and hence P as well as grad P are slowly varying functions of t and r. Similarly the right hand side of equation (6.31) consists of a slowly varying part as well as the even harmonics terms which are neglected. The slowly varying part consists of $J_\theta B_z$ and the average part of $J_z B_\theta$. The average part of $J_z B_\theta$ is very small and can be neglected because J_z and B_θ are almost 90° out of phase. It follows that the plasma pressure can be evaluated using the steady axial magnetic field. The RMFs make no contribution to the plasma equilibrium. This assumption was first used by Storer (1981) to compute Rotamak equilibria. In a later paper Storer (1983) showed that these equilibria agreed well with the plasma pressure measurements made independently of the magnetic field measurements. Since the plasma equilibrium equation has no reference to the RMF, we can employ the standard terminology used to describe FRC configurations. The terms closed flux and separatrix are used in this sense and they refer to the steady component of the magnetic field. The fact that the lines of the total magnetic field (including the RMF) are not closed is irrelevant for our purpose.

We assume that initially the electron fluid rotates as a rigid rotor with angular frequency ω_e while the ion fluid rotates as a rigid rotor with angular frequency ω_i. Equation (6.31) can then be reduced to

$$-\frac{\mu_0 e^2(\omega_i-\omega_e)^2}{T_e+T_i}=\frac{1}{nr}\frac{\partial}{\partial r}\left[\frac{1}{nr}\frac{\partial n}{\partial r}\right]. \tag{6.32}$$

Equation (6.32) can be solved to obtain the initial distribution of the number density and axial component of the magnetic field

$$n(r)=n_0\operatorname{sech}^2 g\left(r^2-R_0{}^2\right), \tag{6.33}$$

$$B_z(r)=-\sqrt{2\mu_0 n_0(T_e+T_i)e}\tanh g\left(r^2-R_0{}^2\right). \tag{6.34}$$

where R_0 is the field null radius, $n_0=n(R_0)$ is the peak number density and

$$g^2=\frac{\mu_0 e^2 n_0(\omega_e-\omega_i)^2}{8(T_e+T_i)}. \tag{6.35}$$

For an FRC we impose the condition: $n(R) = n(0)$, where R is the radius of the separatrix, and hence the radius of the FRC is given by

$$R=\sqrt{2}R_0. \tag{6.36}$$

The ratio of the boundary density to the peak density $n(R)/n_0$, determines the value of the constant g.

$$g=\frac{2}{R^2}\operatorname{sech}^{-1}\sqrt{\frac{n(R)}{n_0}} \tag{6.37}$$

The boundary condition for B_z is determined from the conservation of magnetic flux, with flux-preserving rings at radial distance b.

$$B_z(R,t)=\frac{\left(b^2-R(0)^2\right)}{\left(b^2-R(t)^2\right)}B_z(R,0)+\frac{2}{\left(b^2-R(t)^2\right)}\left(\int_0^{R(0)}rB_z(r,0)-\int_0^{R(t)}rB_z(r,t)\right) \tag{6.38}$$

The boundary condition for A_z for this physical model is given by Hugrass & Grimm (1981).

$$A_z{}^{\pm}(R)=2A_{ext}{}^{\pm}-R\left.\frac{\partial A_z{}^{\pm}}{\partial r}\right|_{r=R} \tag{6.39}$$

where $A_{ext}^{\pm}$ is the phasor of the vector potential for each externally applied RMF at $r = R$.

Equations (6.10), (6.22) and (6.26) are solved numerically using a semi-implicit finite difference approximation with variable time step as in Chapter 5. The grid points now move with the radial motion of the plasma. Hence time-derivatives are determined by

$$\frac{d}{dt} = \frac{\partial}{\partial t} + v_r \frac{\partial}{\partial r}. \tag{6.40}$$

6.3 Results

The results presented are for numerical simulations with the following initial parameters for the FRC: $m_e/m_i = 5.45 \times 10^{-4}$, $R = 10$ cm, $T_e = 20$ eV, $T_i = 60$ eV, $n_0 = 2 \times 10^{18}$ m^{-3}, $n(R)/n_0 = 0.2$, and the flux conserver radius is $b = 1.5\,R(0) = 15$ cm.

The electrons and ions are initially counter-rotating. We present simulations with $|\omega^+| < \omega^-$ since the initial conditions have the electron fluid carrying the majority of the current $\omega_e(0) = 9.07$ MHz $|\omega_i(0)| = 0.89$ MHz. The applied RMFs have frequencies of $\omega^- = 8.16$ MHz and $\omega^+ = 0.58$ MHz and hence $\lambda^- = 21.1$, $\lambda^+ = 5.63$. FRC equilibria are observed to spin with increasing angular velocity until the $n = 2$ instability destroys this configuration (Tuszewski, 1988). When the (-) RMF is applied, the rotation of the FRC would slow down and eventually, in the absence of a (+) RMF, rotate with the (-) RMF. Hence the current diminishes and the configuration is destroyed. The initial conditions presented in this chapter conform to the initial stages of a preformed FRC.

Both the (-) and (+) RMFs are applied at $t = 0$. The rise time for the (-) RMF is smaller than for the (+) RMF. ($\tau_r^- = 1$ μs and $\tau_r^+ = 10$ μs). This is to satisfy the condition $\omega\tau > 1$ for both RMFs, and also allows the electron fluid to be partially entrained by the (-) RMF before the external magnitude of the (+) RMF becomes large. After the (-) RMF has penetrated into the plasma and entrained the electron fluid, it is possible to decrease the magnitude of the RMF to levels much lower than is required for penetration and the

(-) RMF maintains complete penetration into the plasma with the electron fluid entained by it (Hugrass, 1985). Our simulations show that the same is true for the (+) RMF. The results presented in this section have RMF magnitudes of 60 G (for both the (+) and (-) RMF) unless stated otherwise. The RMF magnitudes are decreased once both fluids are entrained, with time constant $\tau = 10\ \mu$s to a value of 10 G (for both the (+) and (-) RMF).

Figure 6.1 shows the variation of the driven current with time for: (i) no RMFs are applied, (ii) when the (-) RMF alone is applied, (iii) when both RMFs are applied. The driven current is shown as the dimensionless parameter α, defined as

$$\alpha = \frac{\frac{1}{\mu_0}\left(B(R) - B(0)\right)}{\int n(r,0)e\left(\omega^+ - \omega^-\right)rdr}, \tag{6.41}$$

where the bottom line of equation (6.41) is the current when both the electron and ion fluid rotate with the (-) and (+) RMF respectively.

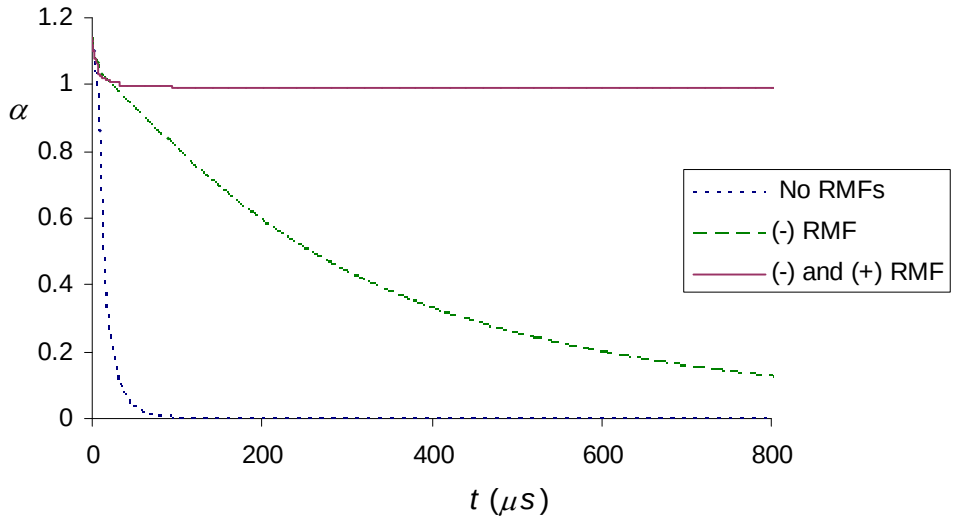

Figure 6.1. Driven current per unit length (as dimensionless parameter α) against time for (i) the (-) RMF applied only and (ii) Both (-) and (+) RMFs applied.

When there are no external RMFs, the current decays with the electron relaxation time, eventually reaching a steady state where the electron fluid rotates synchronously with the ion fluid. When only the (-) RMF is applied, the current decays with the ion relaxation time, eventually reaching a steady state where both electrons and ions rotate synchronously with the (-) RMF. When both RMFs are applied a true steady state is achieved, with the electrons and the ions rotating synchronously with the (-) and (+) RMFs respectively.

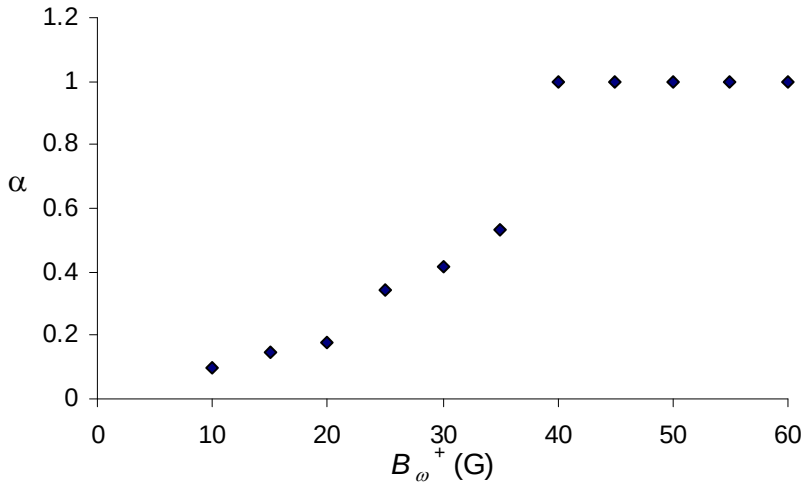

Figure 6.2. Driven current per unit length (as dimensionless parameter α) against the magnitude of the applied (+) RMF, B_{ω}^{+}.

The nonlinear nature of the penetration of the (-) RMF in the plasma is well known (Jones, 1999). The penetration of the (+) RMF is also strongly nonlinear as can be seen from Figure 2. For small values of B_{ω}^{+} the (+) RMF is restricted to the outer layers of the plasma due to the skin effect. The ions in these outer layers are entrained by the (+) RMF while the ions in the inner regions are eventually dragged by the electron fluid, which results in the observed reduction in the steady state current. For values of B_{ω}^{+} above a certain threshold value, the (+) RMF fully penetrates into the plasma and entrains the ion fluid. The magnitude of the (+) RMF required to access the steady state is much larger than that required to maintain the steady state. The magnitude of the (+) RMF (and the (-) RMF) may be decreased significantly below the threshold value required for penetration (in the results presented, to a value of 10 G).

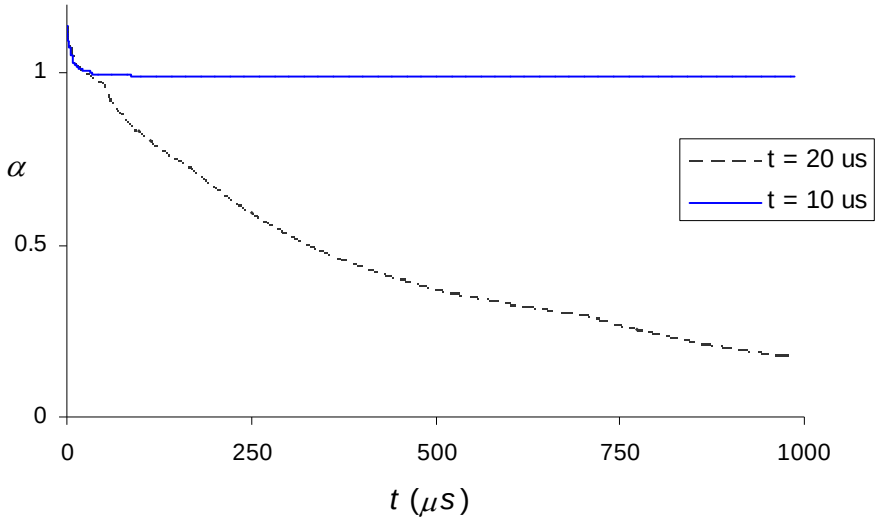

Figure 6.3. Driven current (as dimensionless parameter α) against time when both the (-) and (+) RMF are applied, for two different rise times of the (+) RMF (i) 10 μs, and (ii) 20 μs.

The penetration of the (+) RMF into the plasma also requires suitable timing for the application of the (+) RMF. In the simulations presented, both RMFs are applied at the same time, but the magnitude of the (+) RMF is kept small in initial stages of the simulation by having a longer rise time for the (+) RMF. If the magnitude of the (+) RMF is not large enough at the correct time (longer rise time of 20 μs shown in Figure 3), it may fail to penetrate into the plasma and entrain the ion fluid even though its magnitude is sufficiently large at later times. This phenomenon can be explained by examining equation (6.15) (the ion force as function of slip). The force applied by the (+) RMF on the ion fluid is very small except for a small range of values of the slip. This force is not sufficient to bring the motion of the ion fluid into synchronous rotation with the (+) RMF. The rotational velocity of the ion fluid must change under the influence of collisions until the slip of the ion fluid is such that the (+) RMF exerts sufficient force on the ion fluid and entrainment thus occurs. For the longer rise time of 20 μs shown in Figure 6.3, the ion fluid has already relaxed past the small range of slip values required for entrainment before the magnitude of the (+) RMF becomes large enough to allow the existence of a small slip operating point for the ion fluid. Similar results are produced if the application of the (+) RMF is significantly delayed. The

steady state achieved is hence determined by the plasma initial conditions, the timing and rise time of the (+) RMF, and its frequency.

Increasing the frequency of either the (-) or (+) RMF once both fluids are entrained also allows the total driven current and the closed flux to be increased. Figure 4(a) demonstrates the increase of the closed flux as the angular frequency of the (-) RMF is increased. The closed flux is given by

$$\phi = \int_0^{R_0} rB_z dr \tag{6.42}$$

where R_0 is the field null radius. The lines of the total magnetic field (including the RMF) are open, but the RMF does not contribute to the pressure balance equation. By closed flux, we mean the magnetic flux excluding the RMF. The closed flux is constant once the steady state has been achieved with the (-) RMF entraining the electron fluid and the (+) RMF entraining the ion fluid. When the (-) RMF frequency is increased, the closed flux increases. Figure 4(b) shows that there is a corresponding increase in the plasma radius and the total driven current (here α is defined with respect to the initial values of the RMF frequencies).

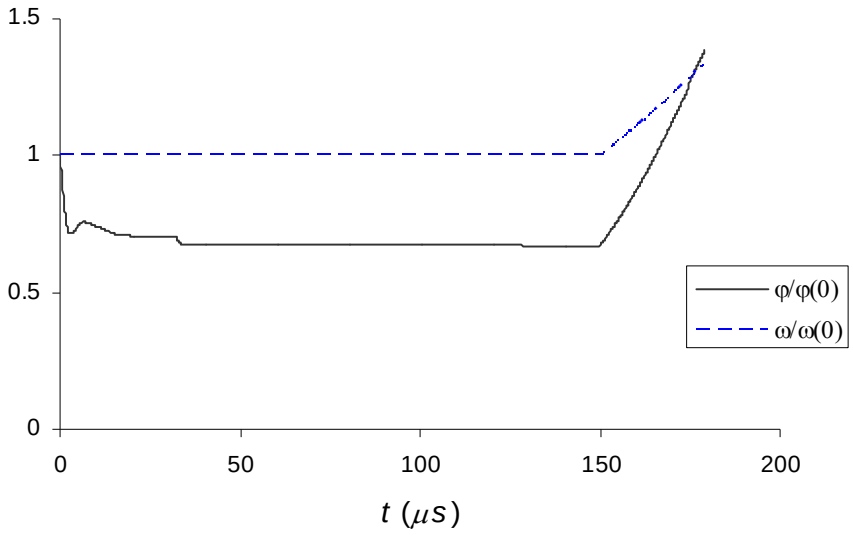

Figure 6.4. (i) Closed flux ϕ, and (ii) frequency of (-) RMF, ω^- (normalised to initial values) against time.

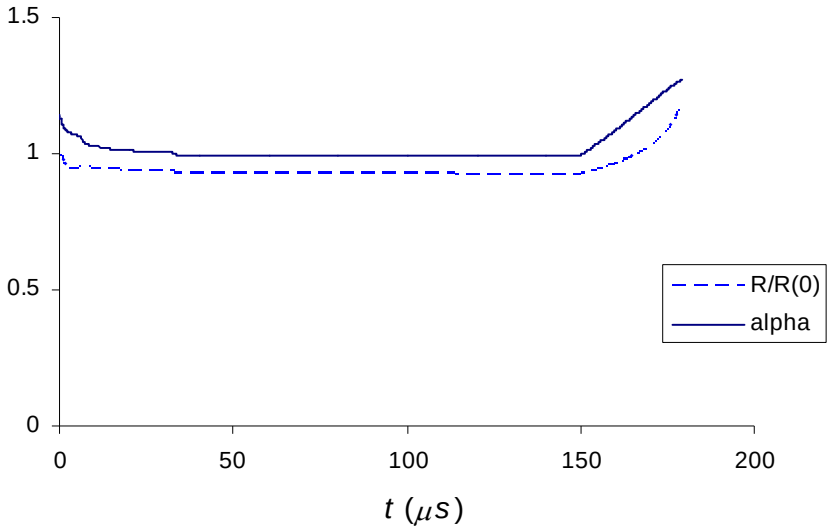

Figure 6.5. (i) Plasma radius R (normalised to initial value), and (ii) α against time.

6.4 Conclusions

It has been demonstrated that a preformed FRC can be sustained using two counter-rotating magnetic fields. The Clemente steady states, where the electron and ion fluids rotate synchronously with the (-) and (+) RMF, respectively, are accessible for the case where the electrons carry the majority of the current. The penetration of the (+) RMF is enhanced in this case due to a significant increase in the classical skin depth for the (+) RMF while the skin depth is decreased slightly for the (-) RMF. The conditions required for enhanced penetration of the (+) RMF are more restrictive than for the (-) RMF.

The conditions required for the (+) RMF to penetrate the plasma and entrain the ion fluid are very restrictive. One has to acknowledge that these conditions would not be easily achieved in the laboratory, although observations of ion rotation in FRCs demonstrate that the ion rotation is essentially a rigid rotor (Tuszewski, 1988), although the rotation may be smaller at inner layers (Hoffman, 2003). This type of ion rotation would provide the required initial condition for the Clemente scheme. The need to resort to such an elaborate scheme has not been established as the predicted spin-up of the ion fluid has not been observed so far. On the other hand, it is highly likely that the ion spin-up will

be the limiting factor for the use of the RMF technique to sustain reactor-grade FRC equilibria with large particle confinement time. The Clemente scheme would allow the FRC equilibria to be sustained indefinitely. It may also be possible to control the length and radius of the FRC as well as the closed flux by changing the frequency of the RMFs and the magnitude of the axial magnetic field. Obviously we have not investigated the possibility of controlling the length of the FRC, since the model we have presented is for an infinitely long plasma column.

In this chapter we presented simulations for the penetration of counter-rotating magnetic fields into infinitely long FRCs. Further work is required to investigate the penetration of the counter-rotating magnetic fields into preformed FRCs with finite length. Many of the simplifying assumptions utilised in this work would not be applicable for the case of finite-length FRCs and the analysis would be much more complex. The simulation would also require considerable computing resources.

CHAPTER 7 CONCLUSIONS AND FUTURE WORK

7.1 Conclusions

This thesis has demonstrated a simplified model for RMF current drive, and analysed the conditions required for the existence of local steady states for the Clemente scheme. This was then extended to the conditions required for the existence of a global steady state for the entire plasma, and the conditions required for the accessibility of the steady states analysed. A numerical model was produced which demonstrated the accessibility of the Clemente steady states, and the initial conditions and plasma parameters required to access them. Finally, it was demonstrated by simulation that a preformed FRC can be maintained indefinitely by the Clemente scheme.

The penetration of the (+) RMF has been shown to follow a similar process as for the (-) RMF. The steady states where the ion fluid rotates synchronously may be maintained when the external magnitude of the (+) RMF is sufficiently large. The critical value of γ^+ required to maintain the steady state scales with λ^+. As for the (-) RMF, the penetration of the (+) RMF is highly nonlinear, hence the critical value of γ^+ required to access the steady state may be larger than that required to maintain it.

The difference between the penetration of the (+) RMF and the (-) RMF is the initial conditions which lead to enhanced penetration. While the (-) RMF may fully penetrate the plasma column and entrain the electron fluid from any initial conditions if the external magnitude of the (-) RMF is sufficiently large, complete penetration of the (+) RMF and entrainment of the ion fluid is dependant on the initial conditions for the ion

fluid. The initial conditions for the ion fluid is that $S_i^+ < 0$ and that there is either a radial profile of the ion slip (S_i^+ increases with radius) or the frequency of the (+) RMF is decreased as it penetrates. This radial profile may be induced by the application of the (-) RMF. The requirement of special initial conditions for the ion fluid provides the most serious problem for the successful application of the Clemente scheme. Observations of ion rotation in FRCs demonstrate that the ion rotation is essentially a rigid rotor (Tuszewski, 1988), although the rotation may be smaller at inner layers (The TCS Program, 2003). This type of ion rotation would provide the required initial condition for the Clemente scheme.

The Clemente scheme may be used to indefinitely maintain a preformed FRC, with the steady states being accessible from initial conditions relevant to translation and confinement techniques. However, the accessibility requires correct timing of the application of the (+) RMF, and since the rotational motion of the ion fluid is not known to sufficient accuracy, the accessibility of the steady states may be very difficult to achieve in an experiment.

7.2 Future Work

In this thesis we presented simulations for the penetration of counter-rotating magnetic fields into infinitely long plasmas. Further work is required to investigate the penetration of the counter-rotating magnetic fields into preformed FRCs with finite length. Many of the simplifying assumptions utilised in this work would not be applicable for the case of finite-length FRCs and the analysis would be much more complex. The simulation would also require considerable computing resources.

Since the penetration of the (+) RMF is dependant on the ion fluid initial conditions when the (+) RMF is applied, successful application of the Clemente scheme requires knowledge of the ion rotation in FRCs. Before this scheme can be seriously considered, a more complete observation of the ion motion is required.

REFERENCES

Abramowitz, M. (1964). *Handbook of mathematical functions; with formulas, graphs and mathematical tables/edited by M. Abramowitz and I.A. Stegun.* Washington Government Press.

Blevin, H.A. & Thoneman, P.C. (1962). Plasma confinement using an alternating magnetic field. *Nuclear Fusion, 55-60.*

Clemente, R.A. (1998). On current drive in field-reversed configurations. *Journal of the Physical Society of Japan*, **67**, 3450-3.

Guo, H.Y., Hoffman, A.L., Brooks, R.D., Peter, A.M., Pietrzyk, Z.A., Tobin, S. J. & Votroubek, G.R. (2002). Formation and steady-state maintenance of field reversed configuration using rotating magnetic field current drive. *Physics of Plasmas,* **9,** 185-200.

Hoffman, A.L. (1995). Reactor prospects and present status of field-reversed configurations. *Fusion Technology,* **27**, 91-6.

Hoffman, A. L. The TCS Program. *Translation, confinement and sustainment of FRCs. Final Report.* Redmond Plasma Physics Laboratory, Seattle, 2003.

Hoffman, A.L., Guo, H.Y., Miller, K.E. & Milroy, R. D. (2005). Long pulse FRC sustainment with enhanced edge driven rotating magnetic field current drive. *Nuclear Fusion,* **45,** 176-183.

Hoffman, A.L., Guo, H.Y., Miller, K.E. & Milroy, R.D. (2006). Principal physics of rotating magnetic-field current drive of field reversed configurations. *Physics of Plasmas,* **13**, 12507-1-16.

Hoffman, A.L., Guo, H.Y., Slough, J.T., Tobin, S.J., Schrank, L.S., Reass, W.A. & Wurden, G.A. (2002). The TCS rotating magnetic field FRC current-drive experiment. *Fusion Science and Technology,* **41,** 92-106.

Hugrass, W.N. (1982). Cylindrical plasma equilibria maintained by means of a rotating magnetic field. *Journal of Plasma Physics,* **28,** 369-378.

Hugrass, W.N. (1984). Power and momentum relations in rotating magnetic field current drive. *Australian Journal of Physics*, **37**, 509-19.

Hugrass, W.N. (1985). The existence of non-unique steady state solutions to the RMF current drive equations. *Australian Journal of Physics,* 38, 157-69.

Hugrass, W.N. (1998). Effect of the motion of ions on the penetration of a rotating magnetic field into a plasma cylinder. *Australian Journal of Physics*, **51**, 859-864.

Hugrass, W. N. (2000). Control of the motion of the ions in rotating magnetic field current drive: 1. Steady-state analysis. *Plasma Physics and Controlled Fusion*, **42**, 1219-1225.

Hugrass, W.N., Jones, I.R. & Phillips, M.G.R. (1981). An experimental investigation of current production by means of rotating magnetic fields. *Journal of Plasma Physics,* **26**, 465-8880.

Hugrass, W.N. & Grimm, R.C. (1981). A numerical study of the generation of an azimuthal current in a plasma cylinder using a transverse rotating magnetic field. *Journal of Plasma Physics*, **26**, 455-64.

Jackson, J.D. (1999). *Classical Electrodynamics 3rd Ed.* New York: Wiley.

Jones, I.R. (1986). *Review of Rotamak Research.* Proceedings of the IAEA Committee Meeting on advances in compact torus research, Sydney IAEA – TECDOC – 369 p.117.

Jones, I.R. (1986). Current drive by means of $\left\langle \tilde{\mathbf{j}} \times \tilde{\mathbf{B}} \right\rangle$. *Comments on Plasma Physics and Controlled Fusion*, **10**, 115-28.

Jones, I.R. *The Rotamak Concept*. Flinders University Report # FUPH-R-151, 1979.

Jones, I.R. *On the possibility of generating and/or sustaining the reverse field pinch configuration by means of a transverse rotating magnetic field*. Flinders University Report # FUPH-R-153, 1979.

Jones, I.R. (1999). A review of rotating magnetic field current drive and the operation of the rotamak as a field-reversed configuration (Rotamak-FRC) and a spherical tokamak (Rotamak-ST). *Physics of Plasmas,* **6**, 1950-7.

Jones, I.R. & Hugrass, W.N. (1981). Steady-state solutions for the penetration of a rotating magnetic field into a plasma column. *Journal of Plasma Physics,* **26**, 441-53.

Jones, I.R. & Knight, A. (1985). *A field reversed configuration generated by means of a rotating magnetic field*. Twelfth European Conference on Controlled Fusion and Plasma Physics, Budapest.

Knight, A.J., & Jones, I.R. (1990). A quantitative investigation of rotating magnetic field current drive in a field-reversed configuration. *Plasma Physics and Controlled Fusion*, **32**, 575-604.

Milroy, R.D. (1999). Numerical study of rotating magnetic fields as a current drive for field reversed configurations. *Physics of Plasmas*, **6**, 2771-2780.

Milroy, R.D. (2000). A magnetohydrodynamic model of rotating magnetic field current drive in a field-reversed configuration. *Physics of Plasmas,* **7**, 4135-42.

Ohnishi, M. & Ishida, A. (1996). Effects of radial flow on current drive in a field reversed configuration by a rotating magnetic field. *Nuclear Fusion,* **36**, 232-6.

Ono, Y., Inomoto, M., Okazaki, T. & Ueda, Y. (1997). Experimental investigation of three-component magnetic reconnection by use of merging spheromaks and tokamaks. *Physics of Plasmas,* **4,** 111953-63.

Slough, J.T. & Hoffman, A.L. (1990). Experimental study of the formation of field-reversed configurations employing high-order multipole fields. *Physics of Fluids B (Plasma Physics)*, **2**, 797-808.

Steinhauer, L.C. (1996). FRC 2001: a white paper on FRC development in the next five years. *Fusion Technology,* **30**, 116-127.

Storer, R.G. (1982). Pressure balance equilibria in the Rotamak. *Plasma Physics*, **24**, 543-54.

Storer, R.G. (1983). Compact torus equilibria set up in the Rotamak by rotating magnetic fields. *Nuclear Instruments and Methods in Physics Research,* **207,** 135-8.

Tuszewski, M. (1988). Field reversed configurations. *Nuclear Fusion,* **28**, 2033-92.

Visentin, D.C. (2003). Ion motion control in RMF current drive by means of a frequency modulated counter-RMF. *Plasma Physics and Controlled Fusion,* **45,** 1027-35.

Visentin, D.C., & Hugrass, W.N. (2003). Control of the motion of the ions in rotating magnetic field current drive. 2. Transient analysis. *Plasma Physics and Controlled Fusion,* **45** 209-19.